Characterising turf grass adaptation to drought and heat and assessing its potential cooling effect

Combined report on turf grass field experiments

Work package 1: Climate and drought
Work package 2: Climate and temperature

Ayodeji O. Deolu-Ajayi[1], Adrie van der Werf[1] and Leon Mossink[2]

1 Agrosystems, Wageningen Plant Research, Wageningen University & Research, 6700 AH Wageningen, the Netherlands
2 Centre for Crop System Analysis, Wageningen University Department of Plant Sciences, Wageningen University & Research, 6700 AH Wageningen, the Netherlands

Report WPR-OT 1083

WAGENINGEN
UNIVERSITY & RESEARCH

Characterising turf grass adaptation to drought and heat and assessing its potential cooling effect

Combined report on turf grass field experiments

Work package 1: Climate and drought

Work package 2: Climate and temperature

Ayodeji O. Deolu-Ajayi[1], Adrie van der Werf[1] and Leon Mossink[2]

1 Agrosystems, Wageningen Plant Research, Wageningen University & Research, 6700 AH Wageningen, the Netherlands

2 Centre for Crop System Analysis, Wageningen University Department of Plant Sciences, Wageningen University & Research, 6700 AH Wageningen, the Netherlands

This study was carried out by the Wageningen University and Research (WUR) and was commissioned and financed by Ministry of Agriculture, Nature and Food quality (LNV) through the Top Sector Agri & Food and Horticulture & Production Materials (project number BO-60-003-002. The work is a collaboration as Public-Private Partnership (PPP) with a consortium of various parties from the grass seed breeding industry (Plantum and its members DLF, DSV seeds Nederland BV, Barenbrug and Limagrain), the Sports and Cultural Technology Trade Association and the Royal Dutch Golf Federation.

Wageningen, January 2024

Deolu-Ajayi, A. O., van der Werf, A., and Mossink, L., 2024. *Characterising turf grass adaptation to drought and heat and assessing its potential cooling effect; Combined report on turf grass field experiment Work package 1: Climate and drought, Work package 2: Climate and temperature.* Wageningen Research, Report WPR-OT 1083. 80 pp.

Keywords: turf grass, drought, hyperspectral imaging, soil moisture content, soil temperature

This report can be downloaded for free at https://doi.org/10.18174/652111

Report WPR-OT 1083

Cover photo: Leon Mossink

Summary

Work Package 1: Climate and drought

Multiple experiments performed in late spring or summer 2022 and 2023 in an established turf grass field was used to characterise variation among species based on their response to drought (combined drought and heat stress in some cases, due to the weather conditions at the time of experimentation). The turf grass field used for experimentation is open air and therefore, exposed to variable weather conditions, especially rainfall. The experiments were performed on selected turf grass genotypes, consisting of monocultures (single species) and mixtures, growing under dry (irrigation paused during a dry and sometimes hot period, replicating drought only, or combined drought and heat stress) or irrigated (control) conditions. Here, we quantified drought and heat-related indices via hyperspectral imaging and linked this to real-time field measurements (soil temperature and soil moisture content sensors) and complex gene expression (via whole genome RNA sequencing), to determine to what extent drought stress can be detected on a turf grass field using the indirect technique i.e., hyperspectral imaging.

Hyperspectral imaging was used to indirectly estimate turf grass response to drought. Two imaging techniques: a drone with a hyperspectral camera attached, and a hand-held hyperspectral camera were used. Results indicated little to no difference in hyperspectral imaging techniques, therefore either drone or hand-held techniques can be used for estimating drought stress in turf grass, depending on customer preferences.

Hyperspectral indices showed varied response of the turf grasses under dry and irrigated conditions. Photochemical reflectance index 512 (PRI512), Carter index 2, normalised difference vegetation index, chlorophyll red-edge and water band index were the main indices explaining variation within our dataset. Differences in spectral indices among turf grass genotypes gave first indications on potential genotypes that are drought resilient or sensitive. Most of the genotypes analysed showed consistent differences between the dry (stress) and irrigated (control) samples. Most notable was *Festuca rubra* (roodzwenkgras) and sport mixture (a combination of 50% *Lolium perenne* diploid and 50% *Poa pratensis*) that significantly differed while *Festuca arundinacea* (rietzwenkgras) and park mixture (composed of 35% *Lolium perenne* diploid, 50% *Poa pratensis* and 15% *Festuca rubra trichophylla*) showed little to no significant differences between their dry and irrigated conditions. Thus, indicating *F. rubra* and sport mixture as drought sensitive genotypes while *F. arundinacea* and park mixture are resilient genotypes. This specific conclusion on species should be taken with caution until multiple common varieties of the species have been assessed under similar conditions.

The most notable index was PRI512 which also had significant positive or negative correlation with most of the other estimated indices, as well as on-ground field measurements of soil moisture content. The varied response (in index values) of the genotypes can be linked to induction of specific stress-induced genes. For example, the upregulation and downregulation of several heat shock proteins in *F. arundinacea*, *F. rubra* and *L. perenne* (Engels raaigras tetraploid). Additionally, an upregulation of multiple dehydrins was observed in *F. rubra* only. Overall, these results are promising thus, indicating hyperspectral imaging with either a hand-held camera or camera attached to as drone, has potential use to estimate drought and heat stress under field conditions.

Work Package 2: Climate and temperature

Little detailed information is available in literature on the cooling effect of grass vegetation under different management in Western Europe. Research in China and the USA has explored the cooling effect of turf grass under various management, including irrigation (Amani-Beni, 2018). Studies based on remote sensing and field measurements reveal that trees have a greater cooling effect, and the cooling effect extends further (60 m) beyond the green area into the surrounding built up area than for grasses (10m) (Grilo, 2020). Turf grass can however have a significant cooling effect on urban areas (e.g. Lee, 2016; Armson, 2012; Connors, 2012; Shashua-Bar, 2009).

Paved surfaces generally have similar surface temperatures in the morning as (well-watered) turfgrass surfaces. From around noon, the surface temperature of turf grass during various measuring days often remained roughly 5 degrees above the air temperature, while the temperature of paved surfaces continued to rise. In the late afternoon, concrete, tiles and pavers can easily be 20-30 degrees warmer than the grass, while artificial grass became 40 degrees warmer than irrigated grass during a measurement day and around 30 degrees warmer than dry grass. Concrete showed that it remained 20 degrees warmer than the grass during the evening and much of the night. Grass could often cool down to well below the air temperature (5-15 degrees cooler than air temperature) during the evening and night hours. Further research on different types of artificial turfgrass such as hybrid turfgrass and paved surfaces such as grass tiles is recommended. Methodologically, more use can be made of remote sensing, as was also evident in the joint measurements with work package 1.

Field Measurements of Grass under Different Management: mowing height did not seem to have impact surface temperature, irrigation however showed (significant) influence on the surface temperature of (turf)grass in several occasions. The difference increased as the colour difference between the irrigated and dry (also referred to as non-irrigated) treatment increased due to a long-term soil moisture percentage of around 5% as the air temperature increased. Dry turf grass could be between 5 and 25°C warmer than irrigated grass. *Festuca arundinacea* and sometimes also *Lolium perenne* tetraploid showed significantly cooler surface temperatures than ‘sport mixture’ composed of 50% *L. perenne* diploid and 50% *Poa pratensis* and ‘park mixture’ composed of 20% *L. perenne* diploid, 20% *P. pratensis*, 30% *F. rubra* and 30% *F. rubra* trichophylla. This could amount to a difference of 10 degrees in surface temperature. In the evening and night, both dry and irrigated grass was often (5-15°C) cooler than the air temperature. Within the irrigated treatments, tall fescue was in some cases cooler than other grass surfaces. For follow-up research, it is highly advisable to look at different varieties within species, as drought and heat tolerance are properties for which further selection is and can be made. Perhaps the contribution to the cooling effect can be increased by using the same species, but with the most climate-resistant varieties. Remote sensing can also contribute to this research. A very useful addition for measuring the cooling effect of grass under different management would also be measuring current evaporation.

In general, the monocultures of *F. rubra*, *P. pratensis* and mixtures with *F. rubra* and *P. pratensis* appeared to be the most sensitive to persistent dry and warm periods in terms of DGCI and Canopy Cover %. Monocultures of *F. arundinacea* had on average the highest DGCI and Cover %. Mixtures with *F. arundinacea* and *L. perenne* were also greener on average and had a relatively high Cover % in non-irrigated treatments.

Although a high-resolution thermal camera can clearly see which individual species, vegetation compositions and vegetation states (parched or green) are cool or warm, it is difficult to make statements about an entire plot of biodiverse turf grasses because the variation within a plot can be very large. The variation within plots also appears

to be extra-large in the transition from sufficient soil moisture to low soil moisture contents. This may be due to the wide variety of species, some of which can root (very) deeply and others not at all or less, so that the water that a plant needs to evaporate remains available for a long time for some species and not for others. Further research into drought tolerance/cooling effect in relation to rooting depth in different species but also within species could provide very useful data. To take surface temperature measurements on biodiverse grasslands, it is advisable to measure from a greater distance above the 'surface' than +/- 1 meter above ground level as is currently done. This is because there are height differences in vegetation within biodiverse grasslands and the canopy can move even with small amounts of wind, so measurements are not always the average of the same parts of leaf area within a plot. This makes time-series measurements over a day with multiple measurements at fixed points more difficult to compare. Remote sensing / drone imaging can overcome some beforementioned issues.

Root research showed that there was a difference in root biomass (total) between irrigated and non-irrigated for *F. arundinacea* and *L. perenne* tetraploid. There is less biomass when the turf grass is irrigated, both in *F. arundinacea* and *L. perenne* tetraploid. There is less biomass in the deeper layers 5 - 10 cm and 10 - 20 cm than in the top layer 0 - 5 cm, both in irrigated and non-irrigated plots and for both species. *L. perenne* tetraploid has slightly less root mass than tall fescue on average over all treatments and over all depths, but almost the same, and has slightly more root biomass than *F. arundinacea* when it is not irrigated. Both *L. perenne* tetraploid and *F. arundinacea* have more root biomass in the layers 5 – 10 cm and 10 – 20 cm when they are not irrigated compared to when they are irrigated. Investing less in root mass with a continuous sufficient supply of soil moisture logically can be related to trade-offs (there is simply less need to invest in roots because there is enough water available for the plant to function, even with fewer roots). However, less root mass can also mean that when there is suddenly less soil moisture available, the grass with less root mass becomes more vulnerable to drought.

Samenvatting

Werkpakket 1: Klimaat en droogte

In de late lente en zomer van 2022 en 2023 zijn veldexperimenten uitgevoerd om met behulp van hyperspectrale camera analyses na te gaan welke grasveldsoorten dan wel specifieke grasmengsels resistent zijn tegen droogte dan wel hoge temperaturen. Hyperspectrale camera's meten zowel de inkomende straling als de gereflecteerde straling door het belichte object. Uit de literatuur is bekend dat deze objecten (gebouwen, gewassen, enz.) ieder hun specifieke reflectiepatroon hebben in afhankelijk van de structuur en samenstelling van het object. De centrale vraag was of deze hyperspectrale reflectietechniek gebruikt kan worden voor (vroegtijdige) detectie van droogte. Hiertoe werden specifieke droogte- en hitte gerelateerde indexen, bekend uit de literatuur, gekoppeld aan real-time veldwaarnemingen (bodemtemperatuur en bodemvochtgehalte) en aan genexpressie data (via RNA-sequencing).

De hyperspectrale reflectiemetingen werden op twee verschillende manieren uitgevoerd: 1) met behulp van een camera bediend door de mens en 2) met behulp van een camera gekoppeld aan een drone. Er werden geen tot zeer kleine verschillen tussen beide manieren van meten gevonden en beide kunnen dus toegepast worden afhankelijk van de wensen/ mogelijkheden van de gebruiker.

Een aantal indexen bekend uit de literatuur lieten een duidelijk verschil zien tussen de droge en geïrrigeerde behandelingen, en geven dus mogelijkerwijs een eerste indicatie welke genotypen d.w.z., monoculturen of mengsels, droogte resistent zijn. Zo bleek dus *Festuca rubra* (roodzwenkgras) en het sporten mengsel bestaande uit 50% *Lolium perenne* diploid en 50% *Poa pratensis* gevoelig te zijn voor droogte, terwijl *Festuca arundinacea* (rietzwenkgras) en het parken mengsel, bestaande uit 35% *Lolium perenne* diploid, 50% *Poa pratensis* en 15% *Festuca rubra trichophylla,* juist ongevoelig bleek te zijn. Deze conclusie moet met de nodige voorzichtigheid worden geïnterpreteerd aangezien het een variëteit binnen een soort betrof.

De index PRI512 correleerde sterk met andere indexen welke en tevens met bodemvochtgehalte. Daarnaast correleerde PRI512 ook met de inductie van specifieke stress gerelateerde genen. Bijvoorbeeld, in *F. arundinacea*, *F. rubra* en *L. perenne* (Engels raaigras tetraploid) werden diverse heat shock eiwitten "upregulated" dan wel "downregulated". Daarnaast werden in *F. rubra* diverse dehydrines "upregulated". Al met al laten deze eerste resultaten zien dat hyperspectrale reflectiemetingen gebruikt kunnen worden om droogte in grasvelden (vroegtijdig) te meten.

Werkpakket 2: Klimaat en temperatuur

Er is weinig gedetailleerde informatie beschikbaar over het verkoelende effect van grasvegetatie onder verschillend beheer in West-Europa. Onderzoek betreffende verkoelend effect van gras onder verschillend beheer, waaronder irrigatie heeft met name betrekking op China en de VS (o.a. Amani-Beni, 2018). Studies op basis van remote sensing en veldmetingen laten zien dat bomen een groter verkoelend effect hebben dan gras, en dat het verkoelende effect verder (60m) buiten het groengebied reikt tot in de omliggende bebouwde kom dan voor grassen (10m) (Grilo, 2020). Gras kan echter een aanzienlijk verkoelend effect hebben op stedelijke gebieden (o.a. Lee, 2016; Armson, 2012; Connors, 2012; Shashua-Bar, 2009).

Verharde oppervlakken hebben 's ochtends over het algemeen vergelijkbare oppervlaktetemperaturen als (goed bewaterde) grasvelden. Vanaf ongeveer het middaguur bleef de oppervlaktetemperatuur van graszoden tijdens verschillende meetdagen vaak zo'n 5 graden boven de luchttemperatuur, terwijl de oppervlaktetemperatuur op verharde oppervlakken bleef stijgen. In de late namiddag kunnen beton, tegels en klinkers gemakkelijk 20-30 graden warmer zijn dan het gras, terwijl kunstgras tijdens een meetdag 40 graden warmer werd dan geïrrigeerd gras en ongeveer 30 graden warmer dan droog gras. Beton bleef 's avonds en een groot deel van de nacht 20 graden warmer bleef dan het gras. Gras kan 's avonds en 's nachts vaak afkoelen tot ver onder de luchttemperatuur (5-15 graden koeler dan de luchttemperatuur). Verder onderzoek naar verschillende soorten kunstgras zoals hybride grasvelden en verharde oppervlakken zoals grastegels is aan te bevelen. Methodologisch kan er meer gebruik worden gemaakt van remote sensing, zoals ook bleek uit de gezamenlijke metingen met werkpakket 1.

De maaihoogte leek geen invloed te hebben op de oppervlaktetemperatuur, maar irrigatie bleek in verschillende gevallen een (significante) invloed op de oppervlaktetemperatuur van gras. Het verschil nam toe naarmate het kleurverschil tussen de geïrrigeerde en droge (ook wel niet-geïrrigeerde) behandeling toenam als gevolg van een langdurig bodemvochtpercentage van ongeveer 5% naarmate de luchttemperatuur steeg. Droog gras kan tussen de 5 en 25 graden warmer zijn dan geïrrigeerd gras. Festuca arundinacea en soms ook Lolium perenne tetraploïde vertoonden significant koelere oppervlaktetemperaturen dan 'Sportmenging' bestaande uit 50% Lolium perenne diploïde en 50% Poa pratensis en 'Parkmengsel' bestaande uit 20% Lolium perenne diploïde, 20% Poa pratensis, 30% Festuca rubra en 30% Festuca rubra trichophylla. Dit kan oplopen tot een verschil van 10 graden in oppervlaktetemperatuur. 's Avonds en 's nachts was zowel droog als geïrrigeerd gras vaak (5-15 graden) koeler dan de luchttemperatuur. Binnen de geïrrigeerde behandelingen was rietzwenkgras in sommige gevallen koeler dan andere grasvelden. Voor vervolgonderzoek is het zeer aan te raden om te kijken naar verschillende rassen binnen soorten, aangezien droogte en hittetolerantie eigenschappen zijn waarop verder geselecteerd wordt en kan worden. Wellicht kan de bijdrage aan het verkoelende effect worden vergroot door dezelfde soort te gebruiken, maar met de meest klimaatbestendige rassen. Ook remote sensing kan een bijdrage leveren aan dit onderzoek. Een zeer nuttige toevoeging voor het meten van het koeleffect van gras onder verschillend beheer zou ook het meten van de huidige verdamping zijn.

Over het algemeen bleken de monoculturen van Festuca rubra, Poa pratensis en mengsels met Festuca rubra en Poa pratensis het meest gevoelig voor aanhoudende droge en warme periodes in termen van DGCI en Canopy Cover %. Monoculturen van Festuca arundinacea hadden gemiddeld de hoogste DGCI en Cover %. Mengsels met Festuca arundinacea en Lolium perenne waren gemiddeld ook groener en hadden een relatief hoog canopy cover % in niet-geïrrigeerde behandelingen.

Hoewel een thermische camera met hoge resolutie duidelijk kan zien welke individuele soorten, vegetatiesamenstellingen en vegetatietoestanden (uitgedroogd of groen) koel of warm zijn, is het moeilijk om uitspraken te doen over een hele plot omdat de variatie binnen een plot erg groot kan zijn wanneer het gaat om biodiverse grassen. Ook blijkt de variatie binnen plots extra groot te zijn in de overgang van voldoende bodemvocht naar een laag bodemvochtgehalte. Dit kan te maken hebben met de grote verscheidenheid aan soorten, waarvan sommige (zeer) diep kunnen wortelen en andere niet of minder, waardoor het water dat een plant nodig heeft om te verdampen voor sommige soorten lang beschikbaar blijft en voor andere niet. Verder onderzoek naar droogtetolerantie/verkoelend effect in relatie tot worteldiepte bij verschillende soorten maar ook binnen soorten zou zeer nuttige gegevens kunnen opleveren. Voor het meten van de oppervlaktetemperatuur op biodiverse graslanden is het raadzaam om vanaf een grotere afstand boven het 'oppervlak' dan +/- 1 meter boven het maaiveld te meten, zoals nu wordt gedaan. Dit komt omdat er hoogteverschillen zijn in vegetatie binnen biodiverse graslanden en de canopy zelfs bij kleine hoeveelheden wind kan bewegen, waardoor de metingen niet altijd het gemiddelde zijn van dezelfde delen van de canopy binnen een plot. Dit maakt tijdreeksmetingen over een dag met meerdere metingen op vaste punten moeilijker te vergelijken. Remote sensing / drone-imaging kan een aantal bovengenoemde problemen oplossen.

Wortelonderzoek liet zien dat er een verschil was in wortelbiomassa (totaal) tussen geïrrigeerd en niet-geïrrigeerd voor Festuca arundinacea en Lolium perenne tetraploïde. Er is minder biomassa wanneer het graszoden worden geïrrigeerd, zowel bij Festuca arundinacea als bij Lolium perenne tetraploïde Er is minder biomassa in de diepere lagen 5 - 10 cm en 10 - 20 cm dan in de bovenste laag 0 - 5 cm, zowel in geïrrigeerde als niet-geïrrigeerde percelen en voor beide soorten. Lolium perenne tetraploïde heeft gemiddeld iets minder wortelmassa dan rietzwenkgras over alle behandelingen en over alle dieptes, maar bijna hetzelfde, en heeft iets meer wortelbiomassa dan Festuca arundinacea wanneer het niet wordt geïrrigeerd. Zowel Lolium perenne tetraploïde als Festuca arundinacea hebben meer wortelbiomassa in de lagen 5 – 10 cm en 10 – 20 cm wanneer ze niet worden geïrrigeerd in vergelijking met wanneer ze worden geïrrigeerd. Minder investeren in wortelmassa met een continue toevoer van bodemvocht kan logischerwijs te maken hebben met compromissen (er is simpelweg minder noodzaak om te investeren in wortels omdat er voldoende water beschikbaar is om de plant te laten functioneren, zelfs met minder wortels). Minder wortelmassa kan echter ook betekenen dat wanneer er ineens minder bodemvocht beschikbaar is, het gras met minder wortelmassa kwetsbaarder wordt voor droogte.

Work Package 1: Climate and drought

Ayodeji O. Deolu-Ajayi and Adrie van der Werf

Contribution Statement and Acknowledgement

Work Package 1 was supported by several people from Wageningen University and Research. Bert Meurs, Willem de Visser and Annelies Beniers of Agrosystems Research performed hyperspectral imaging with the handheld Tec5 camera. Magdalena Smigaj of Laboratory of Geo-information Science and Remote Sensing performed the hyperspectral drone measurements. Ingrid van der Meer and Elio Schijlen of Bioscience managed all aspects of the mRNA sequencing, including writing up mRNA methodology. Jan Rinze van der Schoot of Open Teelten and Leon Mossink of Centre for Crop Systems Analysis managed the Nergena field where measurements were taken. Ayodeji O. Deolu-Ajayi and Adrie van der Werf of Agrosystems research were involved in all aspects of the project, including report writing and reviewing.

1. Introduction

Due to climate change, drought events are becoming more common, prolonged and extreme, negatively impacting plant, including turf grass biomass and quality (Fahad et al. 2017). In early stages of drought, only leaf discoloration and reduced growth that are still reversible upon irrigation, may occur but during prolonged drought periods, total loss of cover crops and turf grass may happen (Alhaithloul 2019). To combat these disastrous effects, frequency of irrigation during dry periods are increased. However, use of freshwater for turf grass irrigation e.g., on sport fields and parks especially during dry seasons, is facing more and more tight restrictions. Several solutions may facilitate mitigating the negative situation caused by drought stress. A top priority is detecting drought stress in turf grass genotypes as early as possible. This involves detection before the naked eyes can see the drought damages and when the negative effect of the stress is already irreversible. Additionally, selection of turf grass monocultures (single species) and mixtures that are drought resilient is needed. A third solution may focus on determining optimal timing for irrigation to ensure efficient water usage without compromising turf growth and quality. Thus, the aim of our study is to characterise early detection of drought stress in turf grass. This is further summarised in three research questions.

1. Can we indirectly detect or estimate drought (and heat) stress in turf grass using hyperspectral imaging?
2. What turf grass monocultures and mixtures are drought (and heat) sensitive, and which are resilient?
3. And in combination with point two above, what genes are induced due to drought (and heat) stress in the genotypes, that may be used for validation of the imaging techniques, as well as molecular markers for breeding?

For our study, we used a combination of hyperspectral imaging techniques, soil sensor measurements, and gene expression analysis via RNA sequencing, to decipher the research questions. Hyperspectral imaging is an established method that is used to estimate plant biomass, structure, photosynthetic activity and biochemical properties (Hermanns et al. 2021; Théau et al. 2021; Zhang et al. 2021), and therefore has potential use in our studies. Here, we defined drought resilience in the genotypes as monocultures and mixtures that maintain optimal growth during periods of water depravation and additionally, recover quickly from drought (and heat) stress after rainfall or irrigation (and lowering of temperature) occur.

2. Methodology

2.1 Field composition and experimental setup

All experiments were performed at a turf grass field located in UNIFARM, Nergena experimental fields of Wageningen University and Research (address: Bornsesteeg 10, Building 112, 6721 NG Bennekom). The turf grass field contains eight different monocultures and eight turf grass mixtures (see Annex 1 for map of the turf grass field). In the turf grass field, there is only a single variety per monoculture and mixture (Annex 1). Half of the field was barely irrigated allowing soil moisture content to drop to ~5% and denoted as stress (in this case, drought (and sometimes heat stress) or dry conditions, while the other half was irrigated to maintain a soil moisture content of at least 15% thus, denoted as control or irrigated conditions. Each half of the field was further divided into two, consisting of strips with either a 3 cm turf grass cutting height or a 6 cm cutting height. Only the small 2m x 2m plots were assessed in our experiments.

Eight genotypes and all monocultures: *Festuca arundinacea* (rietzwenkgras), *Lolium perenne* diploid (Engels raaigras diploid), *Lolium perenne* tetraploid (Engels raaigras tetraploid), *Poa pratensis* (veldbeemdgras), *Festuca rubra* (gewoon roodzwenkgras), *Festuca rubra trichophylla* (roodzwenkgras met fijne uitlopers), *Festuca rubra rubra* (roodzwenkgras met forse uitlopers), and *Festuca brevipila* (hardzwenkgras) were evaluated in 2022. The 3 cm cutting height plots only were measured at three technical replicates per genotype (monocultures) per condition (dry or irrigated).

Experiments in 2023 measured four monocultures and two mixtures i.e., a total of six genotypes. The monocultures were *Festuca arundinacea* (rietzwenkgras), *Lolium perenne* tetraploid (Engels raaigras tetraploid), *Poa pratensis* (veldbeemdgras) and *Festuca rubra* (gewoon roodzwenkgras); while the mixtures were 'park' composed of 35% *Lolium perenne* diploid: 50% *Poa pratensis*: 15% *Festuca rubra trichophylla*, and 'sport' consisting of 50% *Lolium perenne* diploid: 50% *Poa pratensis*. Both the 3 cm and 6 cm cutting height plots were assessed in the 2023 experiments at three technical replicates per genotype (monocultures and mixtures) per condition (dry vs. irrigated) per grass height (3 cm vs. 6 cm). The first three monocultures were selected due to contrasting results in the 2022 experiments, and these genotypes were used for RNA sequencing. The fourth monoculture *Poa pratensis*, is a common turf grass extensively used in urban green spaces, parks and sport fields worldwide and is drought sensitive (Shariatipour et al. 2022). Therefore, it serves as a good control species for the experiments. Both mixtures contain proportions of a fifth monoculture *Lolium perenne*, which is an important fast-growing turf grass that is also widely cultivated.

2.2 Field measurements

The turf grass field is maintained with a regular irrigation regimen of watering and mowing twice weekly. The dry part of the field is irrigated with less (at least half) amount of water than is given to the irrigated part of the field,

for maintenance. Volume of water used for irrigation is adjusted weekly based on the predicted weather conditions. The method used for the experiments is summarised below. For the duration of each experiment, the turf grass field was not mowed to facilitate sample collection.

a) During a drought period (approximately a few days to a week plus without rain, based on weather forecast) in late spring to summer, the measurements i.e., hyperspectral imaging, and on-ground sensor detection of soil moisture content and temperature, are scheduled.
b) Measurements were taken either at a single timepoint (2022 experiments) or daily in a work week (2023 experiments).
c) For the 2023 experiments only, daily measurements continued until a lower soil moisture content (~ 5%) is observed on the dry plots. After a day of lowered soil moisture levels, irrigation is resumed and recovery rate of the turf grasses were measured, in terms of changing hyperspectral indices.

2.3 Hyperspectral imaging

Two hyperspectral imaging measurements were performed in 2022 while three occurred in 2023. The 2022 experiments were single timepoint imaging while the 2023 experiments were multiple, daily timepoints within a work week. Hyperspectral imaging was performed remotely with a UAV (Unmanned aerial vehicle), and/ or a handheld device. For remote sensing, a Headwall Nano-Hyperspec VNIR camera (serial number: nHS337, 14mm lens) was mounted on a DJI M300 RTK UAV denoted in this report as 'hyperspectral camera attached to a drone'. Additionally, a handheld hyperspectral sensor system called HandySpec field (company: Tec5 Technology for Spectroscopy, serial number: 0067) denoted in this report as 'handheld Tec5 device', was used for imaging.

The first 2022 turf grass analysis was performed on 18 August (~3 days dry period pre-imaging) between 11 a.m. and 3 p.m., while the second took place on 30 August (~8 days dry period pre-imaging) between 10 a.m. and 2 p.m. First, the drone took flight imaging the whole field based on a pre-loaded flight path (Fig. 2.1A, B). Followed by imaging the selected plots with a hand-held Tec5 device (Fig. 2.1C) and lastly, collection of samples from the plots for mRNA sequencing. The handheld Tec5 device images a 72.3 cm diameter surface area only on each of the selected plots. In this report, we ensured the drone hyperspectral data is identical to the 72.3 cm diameter surface area imaged by the hand-held device, and this was determined from geographical coordinates of each individual plot, taken on the same day of imaging.

Imaging in the 2023 experiments was performed with the hand-held Tec5 device only that measures a 72.3 cm diameter surface area. Daily measurements were usually taken around 10.30 a.m., except when specified (Table 2.1). The first experiments took place between June 19 and 23, the second experiment occurred between 21 and 25 August, and the third experiment took place from 7 to 15 September.

Table 2.1: 2023 experimental schedule for hyperspectral imaging.

	# of dry days pre-imaging	**Monday**	**Tuesday**	**Wednesday**	**Thursday**	**Friday**
Exp 1	~ 7 days	19 June: Measurements	20 June: Measurements	21 June: Scheduled irrigation	22 June: Three timepoint measurements at 8:30, 11:15 and 14:20. **Note:** There was unprecedented rainfall at the last timepoint of 14:20.	23 June: Measurements
Exp 2	~ 5 days	21 August: Measurements	22 August: Measurements	23 August: Measurements	24 August: Measurements	25 August: Measurements
Exp 3	~ 5 days. **Note:** 3 days (Thursday 7 September) prior to the start of the third experiment, measurements were also taken.	11 September: Measurements	12 September: Two timepoint measurements at 10:30 and 14:30.	13 September: Measurements	14 September: Scheduled irrigation	15 September: Measurements

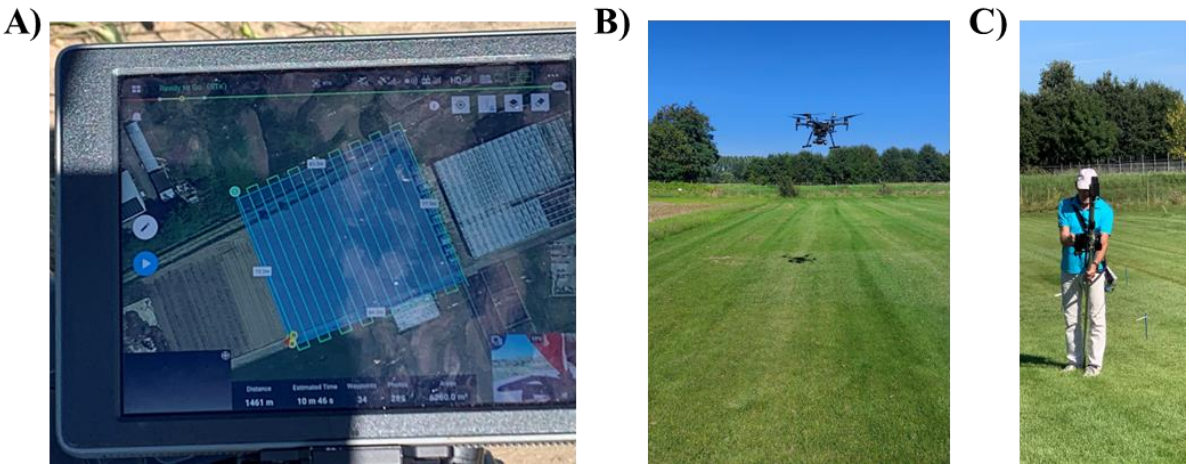

Figure 2.1: Hyperspectral imaging measurements. Flight path of the drone for the whole turf grass field (A), imaging of the field with a camera attached to a drone (B), and field imaging with a handheld Tec5 camera (C). It should be noted that picture B is for demonstrative purposes only because the drone flies at a much higher distance ~30 to 40 m above the field.

2.4 Data Analysis

Analysis of the reflectance dataset obtained from the hyperspectral imaging was performed with R statistical tools. Specific indices that indicate drought (and heat stress), soil water content, and status of turf grass health such as estimated photochemical reflectance index 512 (PRI512), Carter index 2 (CTR2), chlorophyll red-edge, carotenoid red-edge, normalised difference vegetation index (NDVI), normalised difference vegetation red-edge index (NDVI red-edge), normalised difference red-edge (NDRE), blue normalised difference vegetation index (BNDVI), green normalised difference vegetation index (GNDVI), optimised soil-adjusted vegetation index (OSAVI), and water band index (WBI) were analysed. Although all listed indices were assessed, we show results of only the five most interesting indices i.e., PRI512, CTR2, NDVI red-edge, chlorophyll red-edge and WBI, as well as results from the correlation analysis and principal component analysis (PCA) of the dataset as main figures. The indices consist of reflectance values at specified wavelengths in a formula.

PRI512 correlates with both short-term light use efficiency (LUE) changes caused by variation in carotenoid content and stomatal conductance, and long-term LUE shifts due to changes in chlorophyll-carotenoid ratio and seasonal variations in net CO_2 uptake (Hermanns et al. 2021). Therefore, it is an indicator of short- or long-term drought and heat stress. Optimal irrigated conditions due to rainfall or irrigation generally have a higher PRI512 value than measurements on dry plots created due to the drought and heat stress.

CTR2 combines a chlorophyll-sensitive red edge band and a near infra-red band making it an effective ratio index for stress detection (Hermanns et al. 2021). Irrigated conditions have a lower CTR2 value than dry conditions i.e., the higher the CTR2 value, the more stressed a turf grass is.

NDVI indices, including NDVI, NDVI red-edge, NDRE, BNDVI, GNDVI and OSAVI, denote the health of a plant. NDVI values of 0.6 to 1 are considered high and correspond to dense healthy vegetation, values between 0.3 to 0.5 are moderate and correspond to sparse healthy vegetation, including turf grasses, while values lower than 0.3 are considered low corresponding to unhealthy plants.

Chlorophyll red-edge and carotenoid red-edge are indices also indicating the health status of plants where higher estimated chlorophyll and carotenoid are synonymous with healthier turf grass. WBI is used to estimate changes in relative water content (Hermanns et al. 2021). This soil water content estimation by hyperspectral imaging is dependent on the number of dry days pre-measurement, and evaporation rate from the soil.

2.5 mRNA sequencing

In the 2022 experiments, turf grass samples (individual technical replicates per plot) were collected at both timepoints from all imaged plots for further analysis. The 2022 results facilitated genotype selection for follow-up mRNA sequencing analysis. Samples of *F. arundinacea* (rietzwenkgras), *L. perenne* tetraploid (Engels raaigras tetraploid) and *F. rubra* (gewoon roodzwenkgras) were sequenced.

All harvested turf grass samples were flash frozen in liquid nitrogen and stored at -80ºC. Frozen samples were ground in liquid nitrogen and approximately 200 mg per sample were used for RNA extraction using the Monarch Total RNA Miniprep method (New England Biolabs). Resulting RNA was treated with DNAse I, followed by final processing with the Monarch RNA purification kit (New England Biolabs). Total RNA was quantified using

Qubit (Life Technologies) and RNA integrity was analysed using Bioanalyzer total RNA Pico chip (Agilent Technologies). Approximately 1 µg total RNA was used for RNA library preparation using TruSeq stranded mRNA sample prep kit (Illumina). To summarise, after polyA based mRNA selection, RNA was further processed including fragmentation, first and second strand cDNA synthesis, adapter ligation and library amplification resulting in RNA sequencing libraries with unique dual indexes (IDT), all following manufacturer's protocol. Final libraries were eluted in 25 µl elution buffer followed by library quality assessment using a Bioanalyzer DNA 1000 assay (Agilent Technologies) and quantified by Qubit fluorescence measurements (Invitrogen, Life Technologies). Prepared libraries were pooled equimolar and combined with other indexed libraries for sequencing on an Illumina NovaSeq 6000 system. Final sequencing was done using a S1 type flow cell, and settings specific for 2x150 nt paired end reads plus dual IDT reads. All steps for sequencing were carried out according to manufacturer's recommendations. Demultiplexing of reads per sample by corresponding IDT was done using bcl2fastq v2.20 (Illumina Inc, San Diego CA, USA).

All sequencing data was imported into CLC Genomics Workbench (v 22.0.1, Qiagen) for further analysis. Data processing started with adapter trimming followed by de-novo transcriptome assembly of all RNA sequencing data per genotype. Full sequences of all assembled transcriptome contigs were used for BLASTn analysis against the NCBI database. For each contig sequence query, the first BLAST hit result was used as annotation of each corresponding 'transcript'. For all genotypes, this resulting whole transcriptome assembly was used as reference sequence for downstream expression analysis. For individual samples, all RNA sequencing reads were mapped to its corresponding assembled reference transcriptome to create gene expression (GE) tracks. Per genotype, all GE tracks were used to perform PCA and subsequent differential gene expression (DE) analysis. Differential expression analysis was done using settings to test DE due to condition per experimental timepoint, and comparison of all group pairs. For *F. arundinacea* results of differentially expressed genes identified were further filtered based on fold decrease ≤ -2 or fold increase ≥ 2 and a false discovery rate (FDR) p-value of ≤ 0.01. For *L. perenne* tetraploid and *F. rubra*, results of differentially expressed genes identified were further filtered based on fold decrease ≤ -2 or fold increase ≥ 2 and FDR p-value of ≤ 0.05.

3. Results

3.1 Reflectance output is similar independent of hyperspectral imaging method used for measurements

First, we compared results from the first and second turf grass experiments of 2022 to determine whether there were significant differences in reflectance data obtained from either hyperspectral imaging methods i.e., using the drone camera vs. using the handheld Tec5 camera. An initial analysis showed strong correlation between the turf grass dataset obtained from both hyperspectral imaging techniques (Fig. 3.1). This observation holds true for both absolute reflectance values of the measured individual grass plots (Fig. 3.1), as well as estimated indices of the grass plots where similar trends in genotype response were also observed (Fig 3.2, 3.4, 3.6, 3.8 and 3.10).
Overall, the hyperspectral imaging method is not a main factor impacting the measured dataset. Thus, methods can be used for imaging since they would yield similar results.

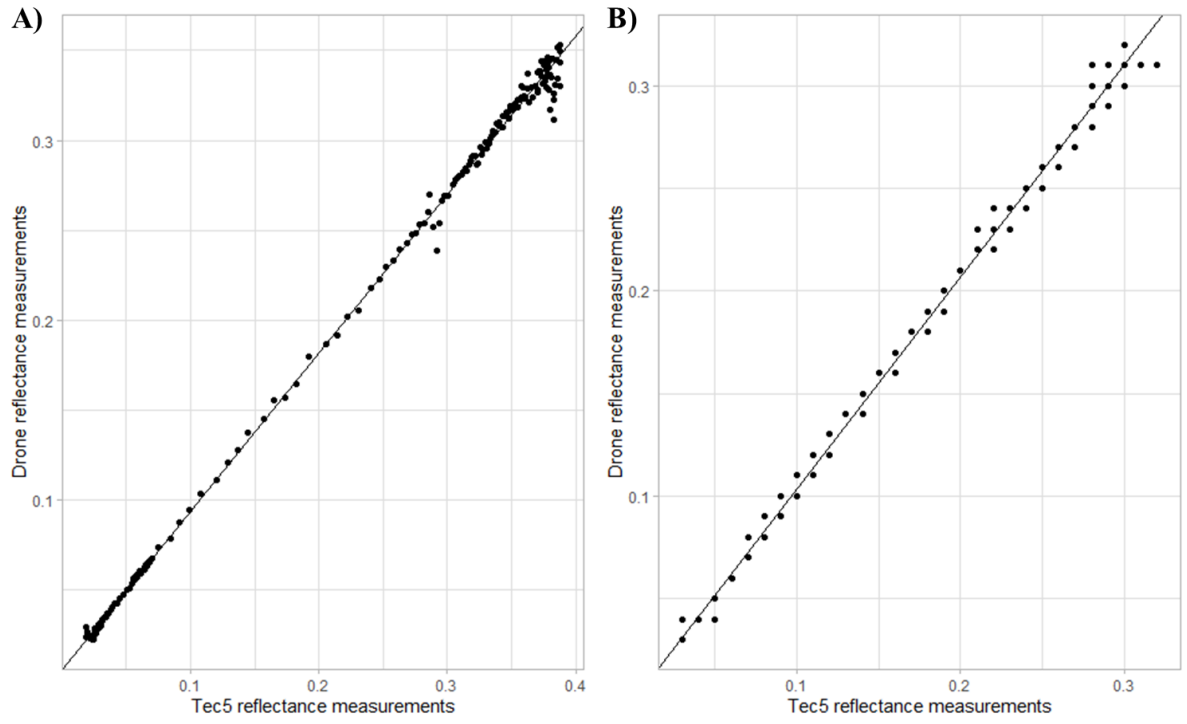

Figure 3.1: Correlation between hyperspectral reflectance measurements performed in 2022 with the drone camera and hand-held Tec 5 camera in experiment 1 (A) and experiment 2 (B). The first experiment occurred on 18 August 2022 while measurements for the second experiment took place on 30 August 2023. Each point represents reflectance values over the wavelength of 380 nm to 1050 nm, that is equal to a72.3 cm diameter surface area in individual plots imaged by both the drone and hand-held devices.

Next, we show the difference between dry and irrigated plots of selected genotypes in two 2022 experiments, and three 2023 experiments (Fig. 3.2-3.11). Since there was strong correlation between hyperspectral measurements from the handheld and drone cameras (Fig 3.1), experiments in 2023 were only imaged with the handheld device.

3.2 Drought stressed genotypes had a significantly lower PRI512 value

In the first 2022 experiment, there were significant PRI512 differences between dry and irrigated plots of *L. perenne* tetraploid, *P. pratensis*, *F. rubra* and *F. rubra rubra* independent of the camera used for the measurements (Fig. 3.2A, B). The drone measurements additionally indicated a significant difference for *L. perenne* diploid. For the second 2022 experiment, all genotypes showed significant difference between their dry and irrigated plots, except *F. arundinacea*, with the drone imaging only (Fig. 3.2C, D). Overall, the results suggest *F. arundinacea* as a drought and heat resilient genotype since they had no significant reduction in estimated PRI512 values in dry conditions relative to its response under optimal irrigated conditions, while *F. rubra trichophylla* and *F. brevipila* are slightly resilient since they only showed no significant differences in the first experiment. On the other hand, *L. perenne* diploid, *L. perenne* tetraploid, *P. pratensis*, *F. rubra* and *F. rubra rubra* are sensitive genotypes because they had the opposite phenotype; showing significant PRI512 differences between their dry and irrigated conditions. The observations in the second experiment can be linked to a higher number of dry days with drought (and heat) stress occurring prior to that timepoint measurement. Therefore, most genotypes including slightly resilient genotypes, showed significant differences between their dry and irrigated plots.

In the first 2023 experiment on 3 cm cutting height dry plots, *F. arundinacea* showed no reduction in PRI512 in a 72 hour-dry period and quickly recovered, seen as higher PRI512 values, when irrigation or rainfall occurred (Fig 3.3A). Interestingly, *F. rubra* had a similar response as *F. arundinacea*, although to a smaller extent, indicating that this species is very sensitive to changes in the environment, including recovery from stress. For *L. perenne* tetraploid and park mixture, a slight reduction in PRI512 during the initial 72 hour-dry spell was observed but these genotypes also quickly recovered after irrigation or rainfall. On the other hand, sport mixture and *P. pratensis* showed the opposite effect: large PRI512 reductions during the dry spell combined with a slower recovery after irrigation or rainfall. Irrigated 3 cm plots of the genotypes always had much higher PRI512 values than the dry plots at the specified timepoints (Fig. 3.3A, B). In the 6 cm cutting height plots, park mixture, *F. arundinacea*, *F. rubra* and sport mixture response were similar to observations on their 3 cm plots, but this was not the case for *L. perenne* tetraploid which instead had a much steeper reduction in PRI512 (Fig. 3.2G). On the other hand, *P. pratensis* that performed poorly at 3 cm grass height instead showed a similar response as park mixture and *F. arundinacea* (Fig. 3.3A, G). Responses under 6 cm irrigated conditions were like that observed in 3 cm except for *P. pratensis* that significantly differed with a much lower PRI512 (Fig 3.3B, H).

In the second 2023 experiments, all genotypes had similar responses in dry conditions as in irrigated conditions independent of the turf grass cutting height (Fig 3.3C, D, I, J). Again, in the third 2023 experiment, all genotypes had similar responses except *F. rubra* that had significantly higher PRI512 under dry conditions relative to its irrigated condition at the 3 cm cutting height only (Fig. 3.3C-F, I-L). Thus, indicating that drought stress did not occur for the duration of the second and third 2023 experiments. Even though there was no rainfall i.e., a dry period) of ~5 days prior to the start of imaging in both cases, the genotypes were not experiencing drought stress during the timepoint measurements linked to a combination of extended periods of rainfall in previous weeks, moderate temperatures (average of 21°C daily) and poor water evaporation from the turf grass field.

Overall, the observed PRI512 indices from both years of measurements suggest that *F. rubra* and sport mixture are drought (and heat) sensitive genotypes while *F. arundinacea* and park mixture are drought (and heat) resilient. Monocultures *L. perenne* tetraploid and *P. pratensis* give contradictory and inconsistent responses among the 2022 and 2023 experiments, therefore making conclusions on either monoculture difficult.

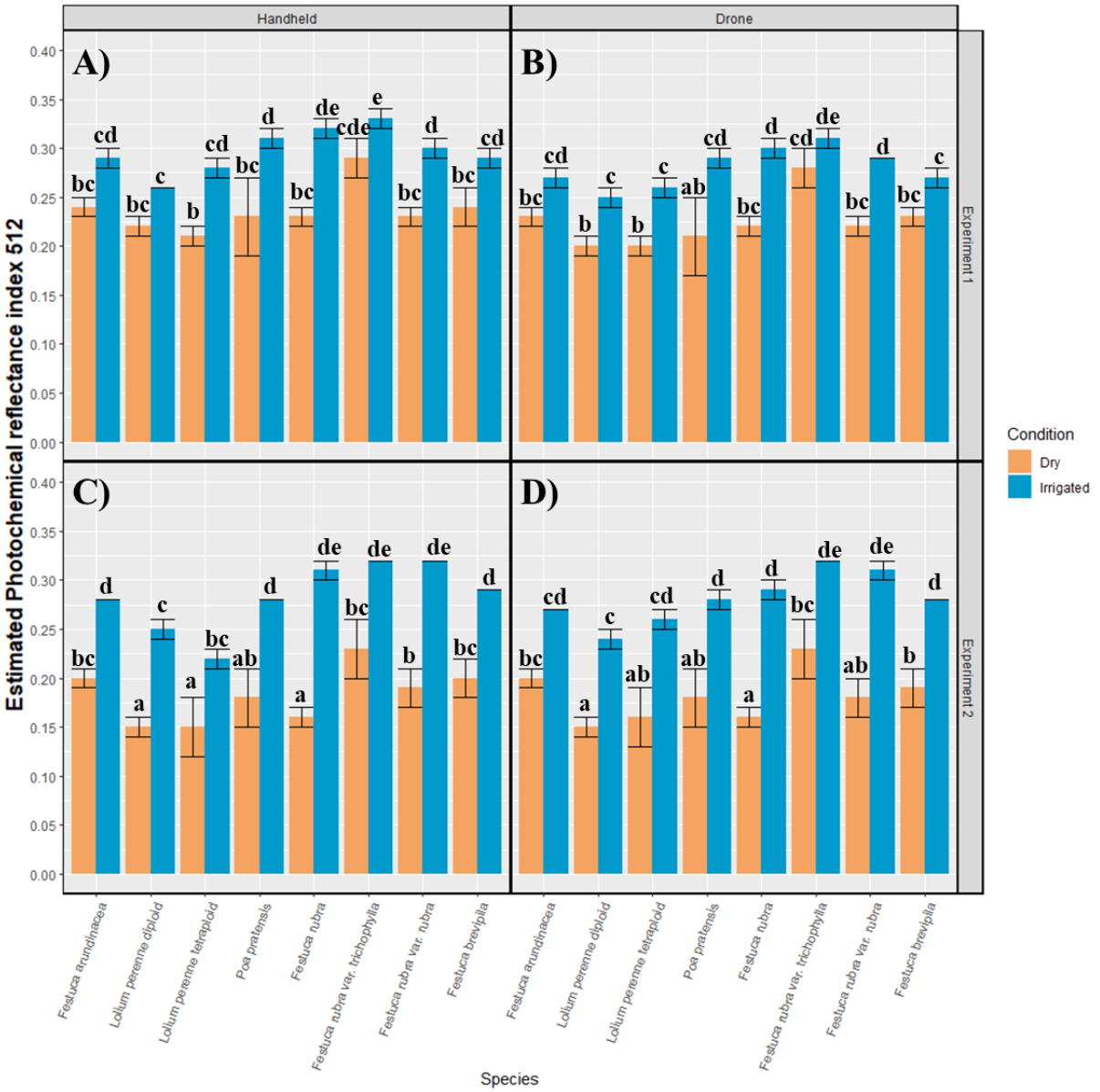

Figure 3.2: Estimated photochemical reflectance index 512 of grass genotypes' dry (A, C) and irrigated (B, D) plots in two different 2022 experiments. Both the first experiment (A, B) and second (C, D) were scheduled in August 2022. Grass plots of 3 cm cutting height were imaged with either hand-held Tec5 camera or a hyperspectral camera attached to a drone, and denoted a diameter of 72.3 cm. The bars are averages and standard errors of 3 replicates/ genotype/ condition. PRI512 was calculated as $(R_{532} - R_{512}) / (R_{532} + R_{512})$ where R refers to reflectance at specified wavelengths. Statistics was by two-way ANOVA with Tukey post-hoc where p-values of ≤ 0.05 are denoted by different alphabets. The genotypes were *Festuca arundinacea* (rietzwenkgras), *Lolium perenne* diploid (Engels raaigras diploid), *Lolium perenne* tetraploid (Engels raaigras tetraploid), *Poa pratensis* (veldbeemdgras), *Festuca rubra* (gewoon roodzwenkgras), *Festuca rubra trichophylla* (roodzwenkgras met fijne uitlopers), *Festuca rubra rubra* (roodzwenkgras met forse uitlopers), and *Festuca brevipila* (hardzwenkgras).

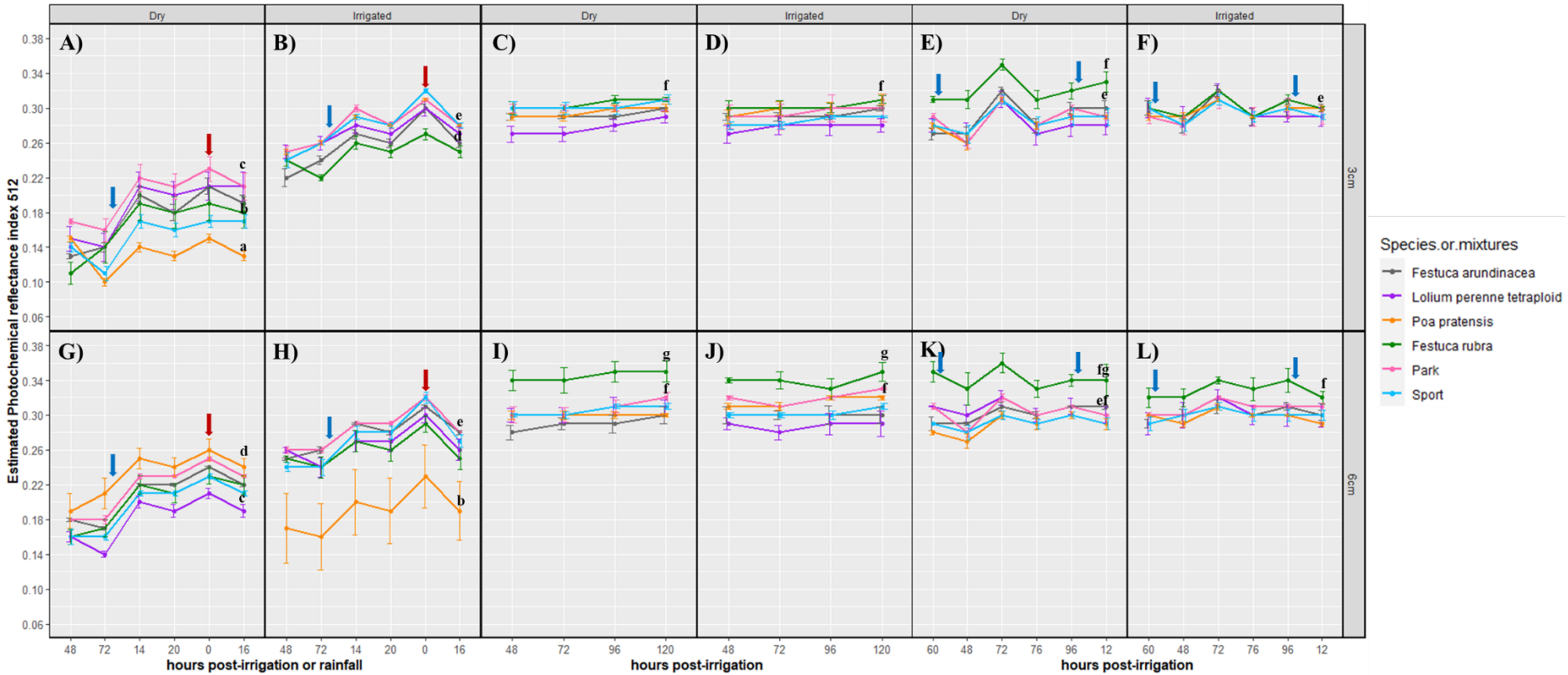

Figure 3.3: Estimated photochemical reflectance index 512 of selected grass genotypes' dry (A, C, E, G, I, K) and irrigated (B, D, F, H, J, L) plots at definite timepoints in 2023. The first experiment (A, B, G, H), second (C, D, I, J) and third (E, F, K, L) were scheduled in June, August and September 2023 respectively. Scheduled irrigation, denoted as blue arrows, took place 72 hours after a dry spell in the first experiment, and after 60 hours and 96 hours post-dry spell measurements in the third experiment. Unprecedented rainfall, denoted with red arrows, also occurred during one timepoint measurement in experiment 1. Grass plots were imaged with a hand-held Tec5 camera and denoted a diameter of 72.3 cm. The points are averages and standard errors of 3 replicates/ genotype/ condition/ cutting height at the timepoints post-irrigation or rainfall in the x-axis. PRI512 was calculated as $(R_{532} - R_{512}) / (R_{532 +} R_{512})$ where R refers to reflectance at specified wavelengths. Statistics was by two-way ANOVA with Tukey post-hoc where p-values of ≤ 0.05 are denoted by different alphabets. The genotypes were *Festuca arundinacea* (rietzwenkgras), *Lolium perenne* tetraploid (Engels raaigras tetraploid), *Poa pratensis* (veldbeemdgras), *Festuca rubra* (gewoon roodzwenkgras), park mixture composed of 35% *Lolium perenne* diploid: 50% *Poa pratensis*: 15% *Festuca rubra trichophylla*, and sport mixture consisting of 50% *Lolium perenne* diploid: 50% *Poa pratensis*.

3.3 Drought stressed genotypes displayed a significantly higher CTR2 value

Only *F. rubra* exhibited significant difference at both 2022 timepoints and independent of the device used (Fig. 3.4). Additionally, *L. perenne* diploid, *L. perenne* tetraploid, *P. pratensis* and *F. rubra rubra* had significantly higher CTR2 on dry plots, relative to their irrigated plots in the second 2022 timepoint only (Fig. 3.4C, D). The other three genotypes, *F. arundinacea*, *F. rubra trichophylla* and *F. brevipila* displayed no significant CTR2 differences between their dry and irrigated plots with *F. arundinacea* showing the smallest differences in all cases (Fig. 3.4).

For the first 2023 experiments at 3 cm grass height, park mixture showed the best response with the lowest CTR2 values on the dry plots. This was followed by *L. perenne* tetraploid and *F. arundinacea* (Fig. 3.5A). The genotypes *P. pratensis* and sport mixture had consistently higher CTR2 values for the duration of the experiments indicating poor response of these genotypes to drought stress. Although *F. rubra* also had higher CTR2 at the initial 72 hour-dry spell, its CTR2 values were lowered post-irrigation or rainfall indicating quick recovery of the species. Again, consistent with the narrative that this genotype is very sensitive to both conditions of stress and recovery. All genotypes under irrigated conditions had much lower CTR2 values than in dry conditions at all timepoints (Fig. 3.5A, B). At the 6 cm grass height, *P. pratensis*, followed by park mixture and *F. arundinacea* showed the best response in the dry condition while all genotypes had similar responses under irrigated conditions, except *P. pratensis* with significantly higher CTR2 value (Fig. 3.5G, H). The second and third 2023 experiments displayed no significant differences between dry and irrigated conditions (Fig. 3.5C-F, I-L). Moreover, all genotypes had low CTR2 independent of the condition. Thus, fitting the narrative of no drought and/ or heat stress in the second and third 2023 experiemnts.

Overall and consistent with the observations of the PRI512 results (Fig. 3.2, 3.3), *F. rubra* and sport mixture are drought (and heat) sensitive genotypes while *F. arundinacea* and park mixture are drought (and heat) resilient. Additionally, *F. rubra* remains a sensitive species that also quickly recovers from drought stress after rainfall or irrigation.

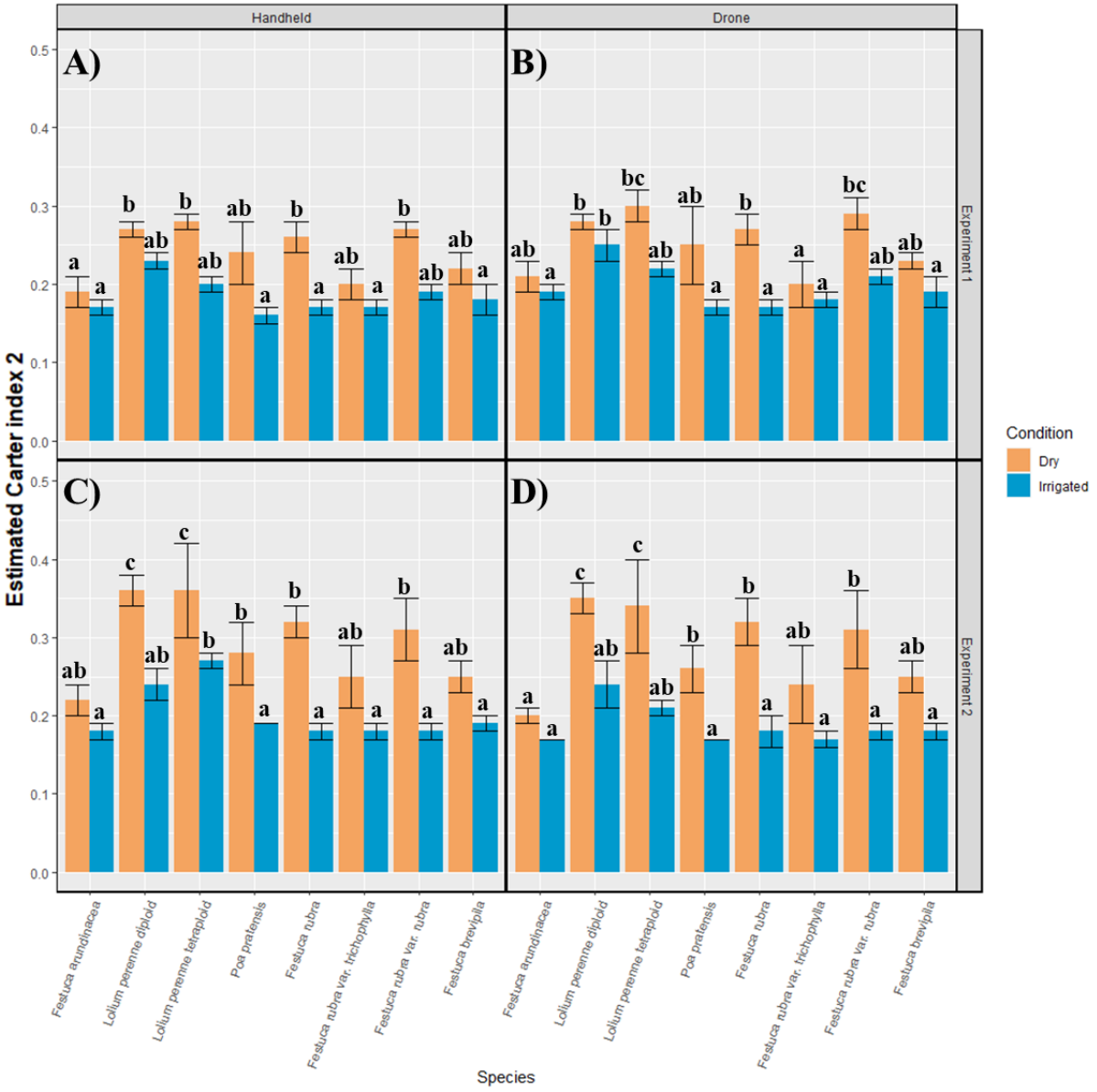

Figure 3.4: Estimated Carter index 2 of grass genotypes' dry (A, C) and irrigated (B, D) plots in two different 2022 experiments. Both the first experiment (A, B) and second (C, D) were scheduled in August 2022. Grass plots of 3 cm cutting height were imaged with either hand-held Tec5 camera or a hyperspectral camera attached to a drone, and denoted a diameter of 72.3 cm. The bars are averages and standard errors of 3 replicates/ genotype/ condition. CTR2 was calculated as R_{695} / R_{762} where R refers to reflectance at specified wavelengths. Statistics was by two-way ANOVA with Tukey post-hoc where p-values of ≤ 0.05 are denoted by different alphabets. The genotypes were *Festuca arundinacea* (rietzwenkgras), *Lolium perenne* diploid (Engels raaigras diploid), *Lolium perenne* tetraploid (Engels raaigras tetraploid), *Poa pratensis* (veldbeemdgras), *Festuca rubra* (gewoon roodzwenkgras), *Festuca rubra trichophylla* (roodzwenkgras met fijne uitlopers), *Festuca rubra rubra* (roodzwenkgras met forse uitlopers), and *Festuca brevipila* (hardzwenkgras).

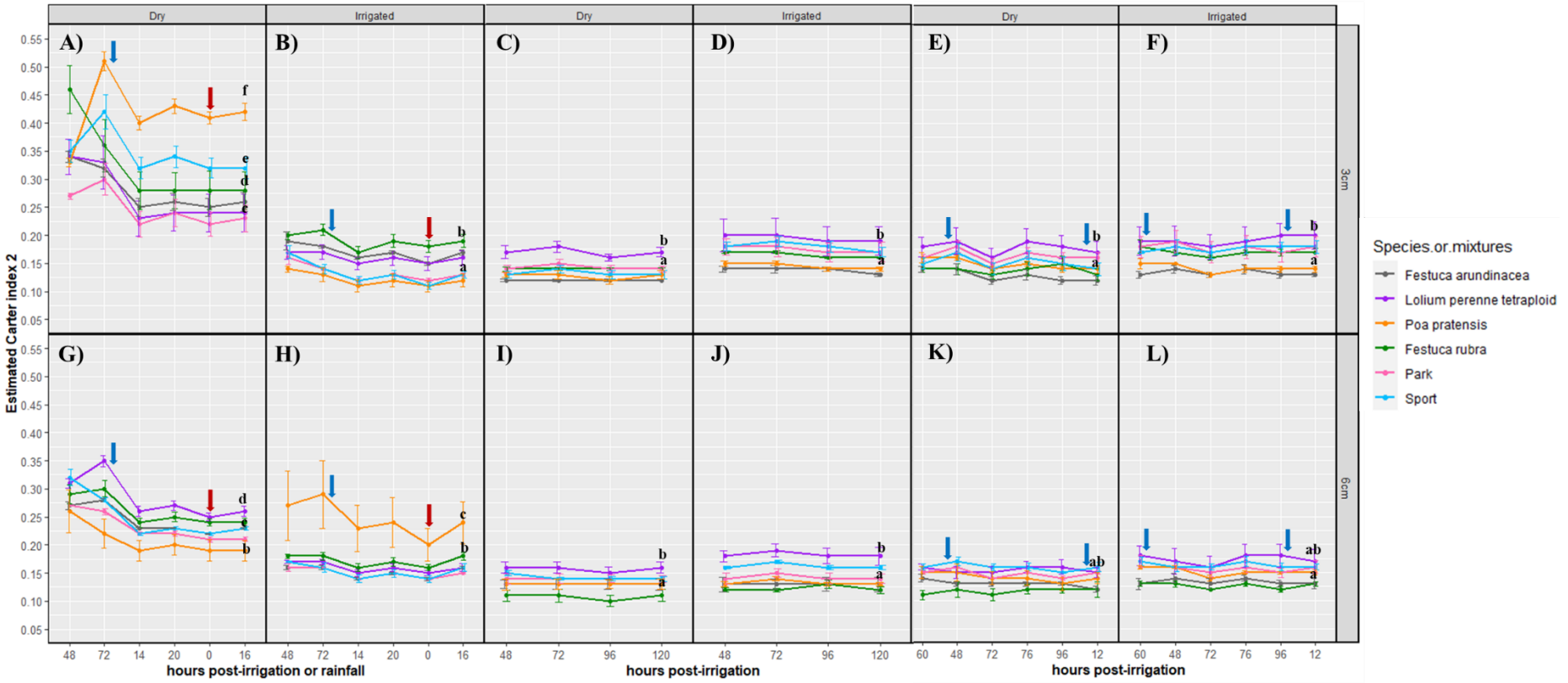

Figure 3.5: Estimated Carter index 2 of selected grass genotypes' dry (A, C, E, G, I, K) and irrigated (B, D, F, H, J, L) plots at definite timepoints in 2023. The first experiment (A, B, G, H), second (C, D, I, J) and third (E, F, K, L) were scheduled in June, August and September 2023 respectively. Scheduled irrigation, denoted as blue arrows, took place 72 hours after a dry spell in the first experiment, and after 60 hours and 96 hours post-dry spell measurements in the third experiment. Unprecedented rainfall, denoted with red arrows, also occurred during one timepoint measurement in experiment 1. Grass plots were imaged with a hand-held Tec5 device and denoted a diameter of 72.3 cm. The points are averages and standard errors of 3 replicates/ genotype/ condition/ cutting height at the timepoints post-irrigation or rainfall in the x-axis. CTR2 was calculated as R_{695} / R_{762} where R refers to reflectance at specified wavelengths. Statistics was by two-way ANOVA with Tukey post-hoc where p-values of ≤ 0.05 are denoted by different alphabets. The genotypes were *Festuca arundinacea* (rietzwenkgras), *Lolium perenne* tetraploid (Engels raaigras tetraploid), *Poa pratensis* (veldbeemdgras), *Festuca rubra* (gewoon roodzwenkgras), park mixture composed of 35% *Lolium perenne* diploid: 50% *Poa pratensis*: 15% *Festuca rubra trichophylla*, and sport mixture consisting of 50% *Lolium perenne* diploid: 50% *Poa pratensis*.

3.4 Most genotypes remained moderately healthy even after exposure to a drought (and heat) period

Only *F. rubra* had significant NDVI differences between their dry and irrigated plots in all 2022 experiments (Fig. 3.6). Additionally, *L. perenne* diploid, *L. perenne* tetraploid (drone measurements only), *P. pratensis*, *F. rubra trichophylla*, *F. rubra rubra*, and *F. brevipila* (drone only) had significant differences in the second 2022 experiment only. Thus, indicating that all genotypes, except *F. arundinacea*, in dry conditions experienced stress, although they remained moderately healthy since their average NDVI values were > 0.3. The first 2023 experiment showed significant difference in genotype response under dry and irrigated conditions at the 3 cm cutting height with the biggest reduction in NDVI seen in *P. pratensis*, *F. rubra* and sport mixture (Fig. 3.7A, B). At the 6 cm cutting height, *L. perenne* tetraploid, *F. rubra* and sport mixture had the lowest NDVI values especially during the 72 hour-dry spell while the other three genotypes are relatively higher NDVI in the dry conditions. There were no significant differences among the genotypes in irrigated conditions except for *P. pratensis* that had a significantly lower NDVI (Fig. 3.7G, H). Although the genotype responses varied in the second and third 2023 experiments, there was no significant differences between dry and irrigated conditions, regardless of the grass height (Fig. 3.7C-F, I-J). Moreover, all genotypes in both conditions had a relatively high NDVI value of 4.5 or higher. Thus, consistently suggesting that there was no stress during the second and third experiments.

Estimated chlorophyll only significantly differed (dry vs. irrigated conditions) for *F. rubra* in all 2022 experiments and additionally, for *L. perenne* diploid and *P. pratensis* in the second 2022 experiment only (Fig. 3.8). Significant differential variation among genotypes only occurred in the first 2023 experiment and in the 3 cm cutting height only (Fig. 3.9). Like observations in the NDVI red-edge graph, *P. pratensis*, *F. rubra* and sport mixture had the lowest estimated chlorophyll in the dry conditions that significantly differed (except F. rubra) from observations in irrigated conditions (Fig. 3.7A-B, 3.9A-B).

In all cases, significant WBI differences in the dry vs irrigated condition were observed for *F. rubra* and *F. rubra rubra* in the 2022 experiments (Fig. 3.10). At the second timepoint, *L. perenne* tetraploid also had significant WBI differences. Again, no significant differences were observed in the 2023 experiments except in the first experiment (Fig. 3.11). Two genotypes, *P. pratensis* and sport mixture, significantly differed in dry conditions relative to its corresponding irrigated condition at the 3 cm cutting height, but additionally, this significant difference was repeated for *P. pratensis* at 6 cm cutting height (Fig. 3.11A, B, G, H).

Overall, most genotypes maintained a relatively moderate NDVI value, chlorophyll content and WBI value. Therefore, suggesting that although drought and heat stress occurred in the 2022 experiments and first 2023 experiment, the genotypes were still not in the irreversible poor health zone, in the short term. This allows reversal of negative effects of drought stress by irrigating turf grass fields to again facilitate optimal growth. Therefore, parameters such as PRI512 and CTR2 are efficient indices to determine (early) drought and/ or heat stress in plants and thereby circumvent deleterious stress effects.

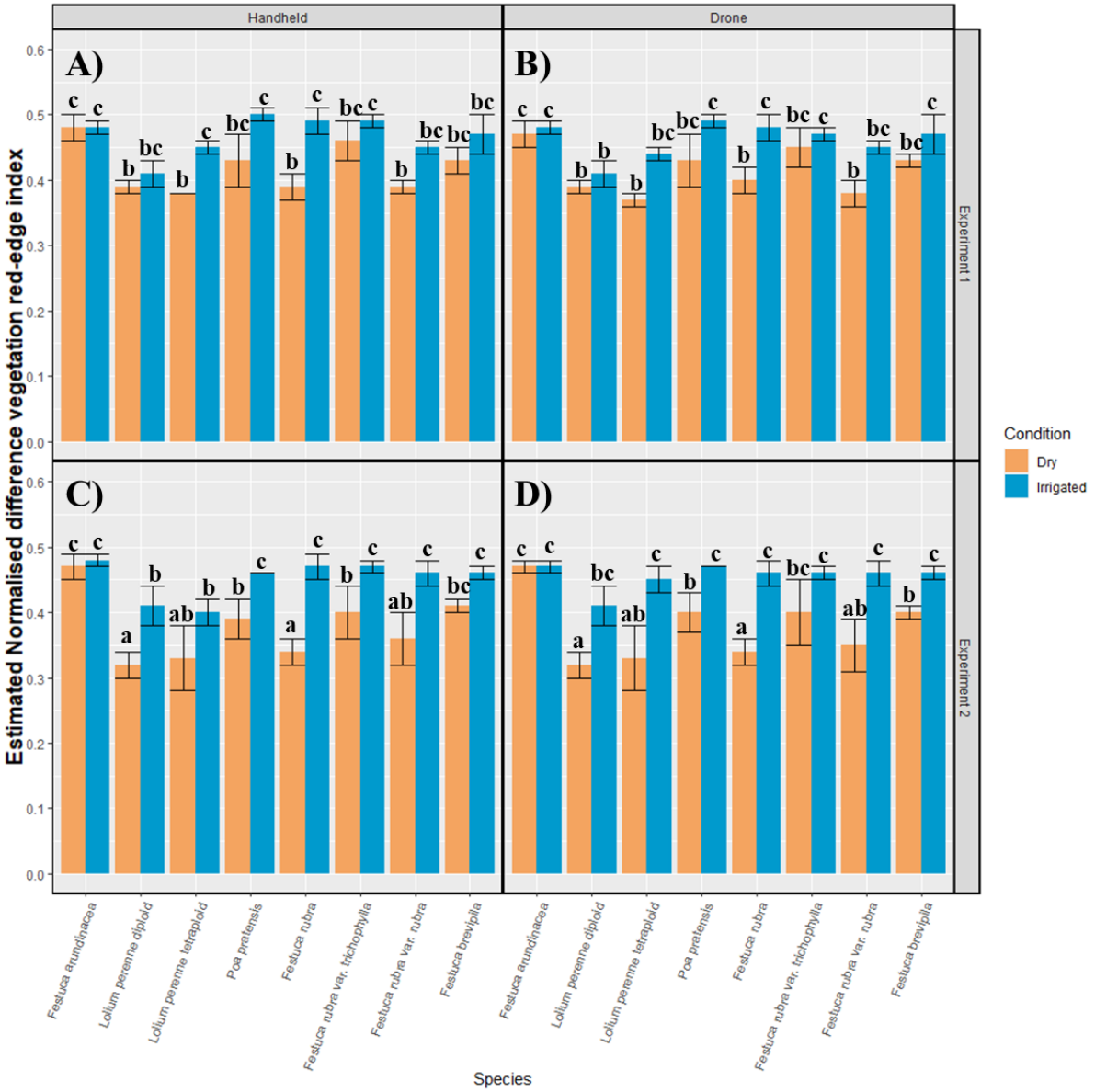

Figure 3.6: Estimated normalized difference vegetation red-edge index of grass genotypes' dry (A, C) and irrigated (B, D) plots in two different 2022 experiments. Both the first experiment (A, B) and second (C, D) were scheduled in August 2022. Grass plots of 3 cm cutting height were imaged with either hand-held Tec5 camera or a hyperspectral camera attached to a drone, and denoted a diameter of 72.3 cm. The bars are averages and standard errors of 3 replicates/ genotype/ condition. NDVI red-edge was calculated as $(R_{750} - R_{706}) / (R_{750} + R_{706})$ where R refers to reflectance at specified wavelengths. Statistics was by two-way ANOVA with Tukey post-hoc where p-values of ≤ 0.05 are denoted by different alphabets. The genotypes were *Festuca arundinacea* (rietzwenkgras), *Lolium perenne* diploid (Engels raaigras diploid), *Lolium perenne* tetraploid (Engels raaigras tetraploid), *Poa pratensis* (veldbeemdgras), *Festuca rubra* (gewoon roodzwenkgras), *Festuca rubra trichophylla* (roodzwenkgras met fijne uitlopers), *Festuca rubra rubra* (roodzwenkgras met forse uitlopers), and *Festuca brevipila* (hardzwenkgras).

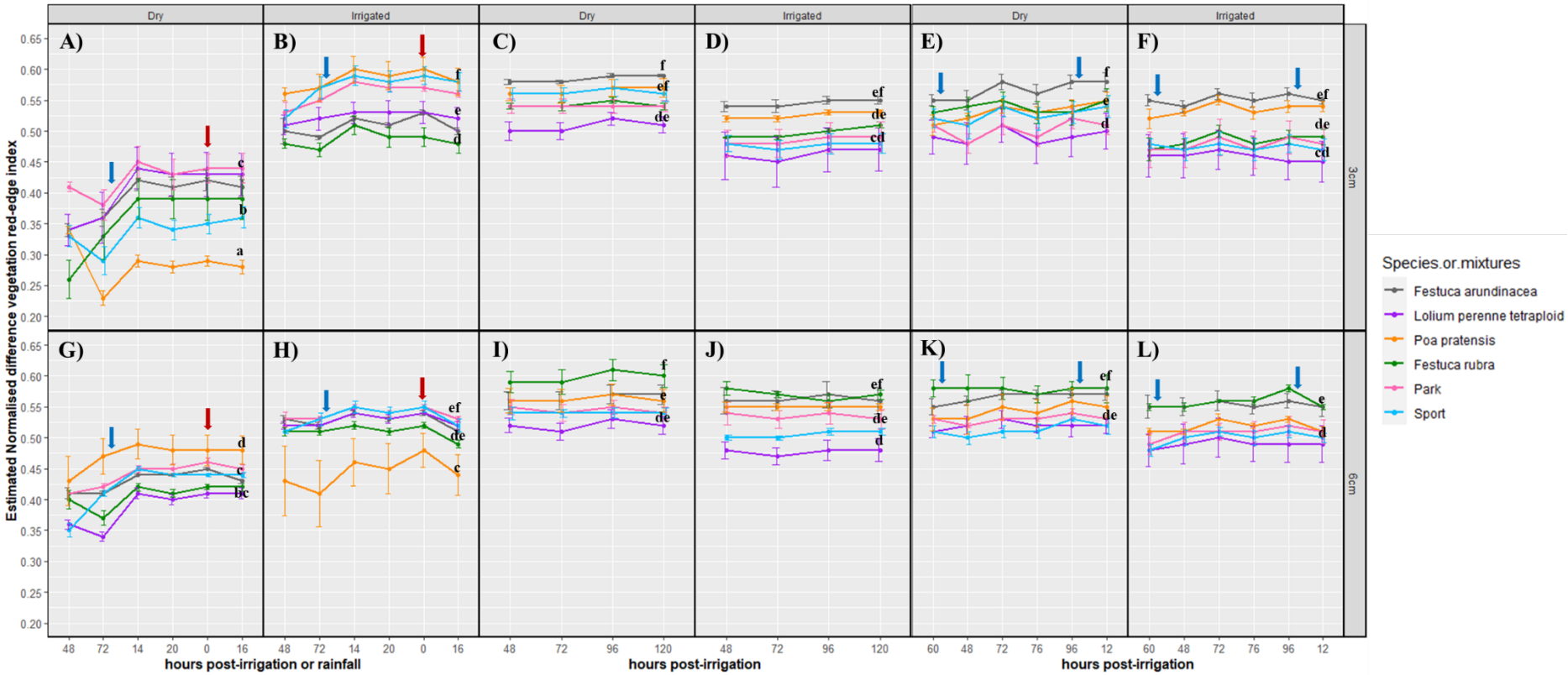

Figure 3.7: Estimated normalized difference vegetation red-edge index of selected grass genotypes' dry (A, C, E, G, I, K) and irrigated (B, D, F, H, J, L) plots at definite timepoints in 2023. The first experiment (A, B, G, H), second (C, D, I, J) and third (E, F, K, L) were scheduled in June, August and September 2023 respectively. Scheduled irrigation, denoted as blue arrows, took place 72 hours after a dry spell in the first experiment, and after 60 hours and 96 hours post-dry spell measurements in the third experiment. Unprecedented rainfall, denoted with red arrows, also occurred during one timepoint measurement in experiment 1. Grass plots were imaged with a hand-held Tec5 device and denoted a diameter of 72.3 cm. The points are averages and standard errors of 3 replicates/ genotype/ condition/ cutting height at the timepoints post-irrigation or rainfall in the x-axis. NDVI red-edge was calculated as $(R_{750} - R_{706}) / (R_{750} + R_{706})$ where R refers to reflectance at specified wavelengths. Statistics was by two-way ANOVA with Tukey post-hoc where p-values of ≤ 0.05 are denoted by different alphabets. The genotypes were *Festuca arundinacea* (rietzwenkgras), *Lolium perenne* tetraploid (Engels raaigras tetraploid), *Poa pratensis* (veldbeemdgras), *Festuca rubra* (gewoon roodzwenkgras), park mixture composed of 35% *Lolium perenne* diploid: 50% *Poa pratensis*: 15% *Festuca rubra trichophylla*, and sport mixture consisting of 50% *Lolium perenne* diploid: 50% *Poa pratensis*.

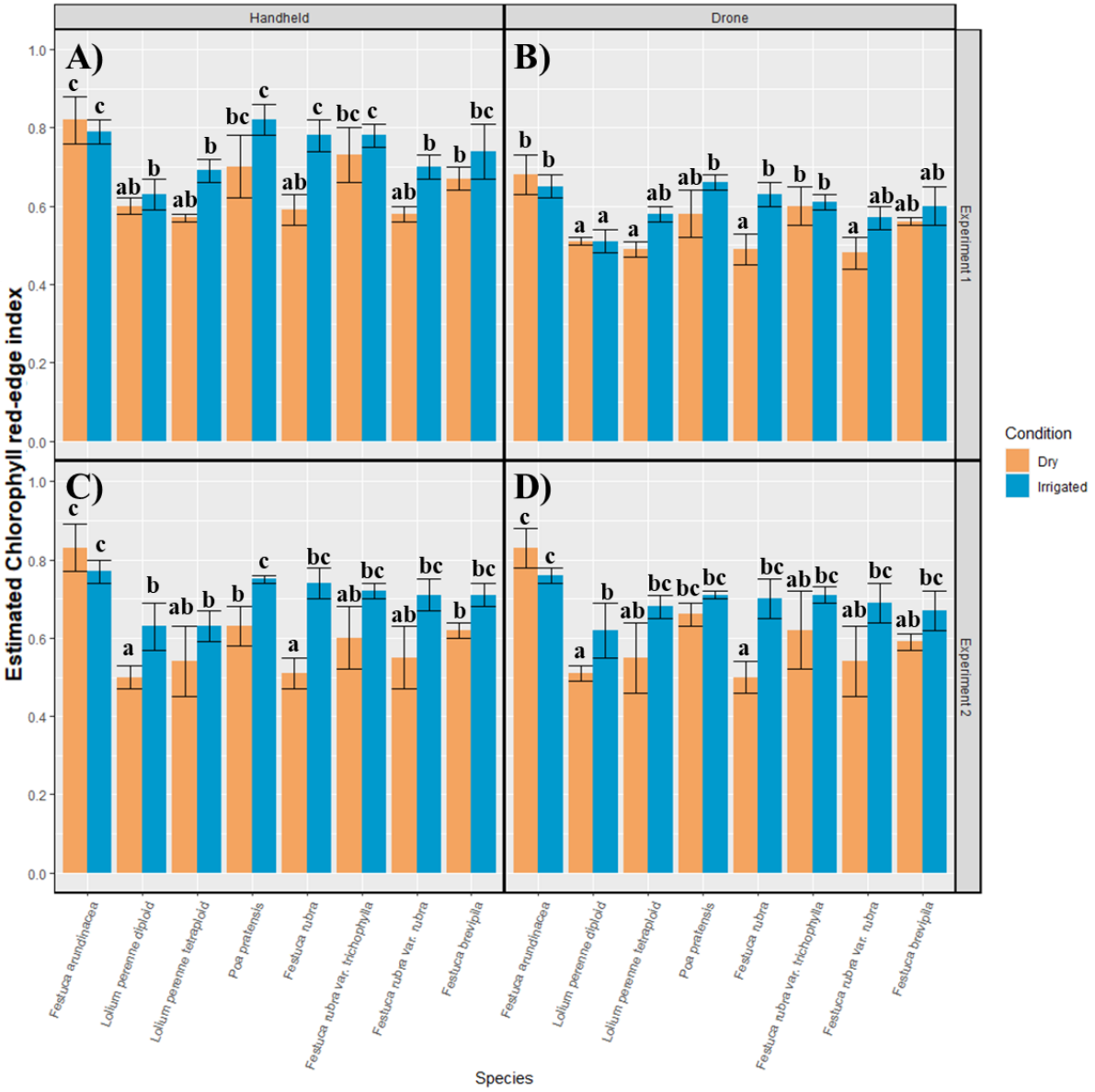

Figure 3.8: Estimated chlorophyll red-edge index of grass genotypes' dry (A, C) and irrigated (B, D) plots in two different 2022 experiments. Both the first experiment (A, B) and second (C, D) were scheduled in August 2022. Grass plots of 3 cm cutting height were imaged with either hand-held Tec5 camera or a hyperspectral camera attached to a drone, and denoted a diameter of 72.3 cm. The bars are averages and standard errors of 3 replicates/ genotype/ condition. Chlorophyll red-edge was calculated as $((R_{721}^{-1}) - (R_{782}^{-1})) * R_{762}$ where R refers to reflectance at specified wavelengths. Statistics was by two-way ANOVA with Tukey post-hoc where p-values of ≤ 0.05 are denoted by different alphabets. The genotypes were *Festuca arundinacea* (rietzwenkgras), *Lolium perenne* diploid (Engels raaigras diploid), *Lolium perenne* tetraploid (Engels raaigras tetraploid), *Poa pratensis* (veldbeemdgras), *Festuca rubra* (gewoon roodzwenkgras), *Festuca rubra trichophylla* (roodzwenkgras met fijne uitlopers), *Festuca rubra rubra* (roodzwenkgras met forse uitlopers), and *Festuca brevipila* (hardzwenkgras).

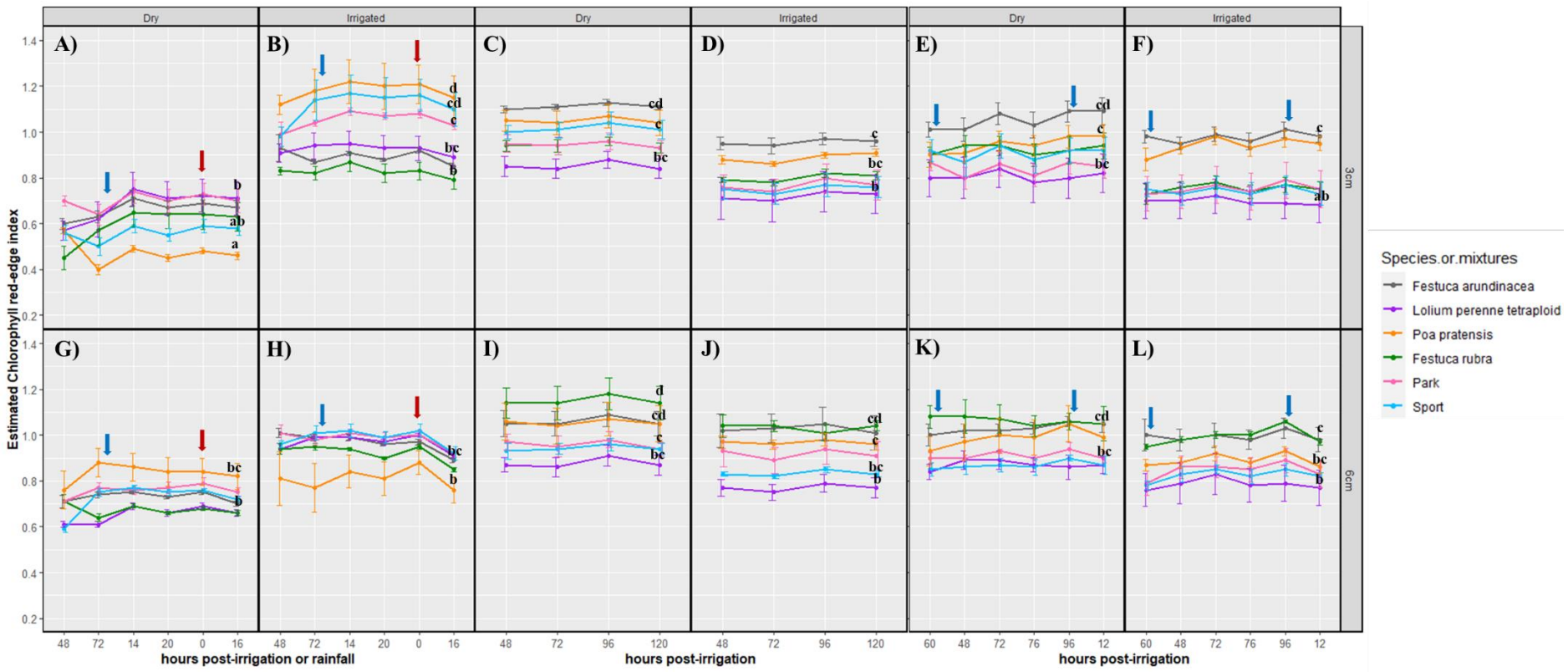

Figure 3.9: Estimated chlorophyll red-edge index of selected grass genotypes' dry (A, C, E, G, I, K) and irrigated (B, D, F, H, J, L) plots at definite timepoints in 2023. The first experiment (A, B, G, H), second (C, D, I, J) and third (E, F, K, L) were scheduled in June, August and September 2023 respectively. Scheduled irrigation, denoted as blue arrows, took place 72 hours after a dry spell in the first experiment, and after 60 hours and 96 hours post-dry spell measurements in the third experiment. Unprecedented rainfall, denoted with red arrows, also occurred during one timepoint measurement in experiment 1. Grass plots were imaged with a hand-held Tec5 device and denoted a diameter of 72.3 cm. The points are averages and standard errors of 3 replicates/ genotype/ condition/ cutting height at the timepoints post-irrigation or rainfall in the x-axis. Chlorophyll red-edge was calculated as $((R_{721}^{-1}) - (R_{782}^{-1})) * R_{762}$ where R refers to reflectance at specified wavelengths. Statistics was by two-way ANOVA with Tukey post-hoc where p-values of ≤ 0.05 are denoted by different alphabets. The genotypes were *Festuca arundinacea* (rietzwenkgras), *Lolium perenne* tetraploid (Engels raaigras tetraploid), *Poa pratensis* (veldbeemdgras), *Festuca rubra* (gewoon roodzwenkgras), park mixture composed of 35% *Lolium perenne* diploid: 50% *Poa pratensis*: 15% *Festuca rubra trichophylla*, and sport mixture consisting of 50% *Lolium perenne* diploid: 50% *Poa pratensis*.

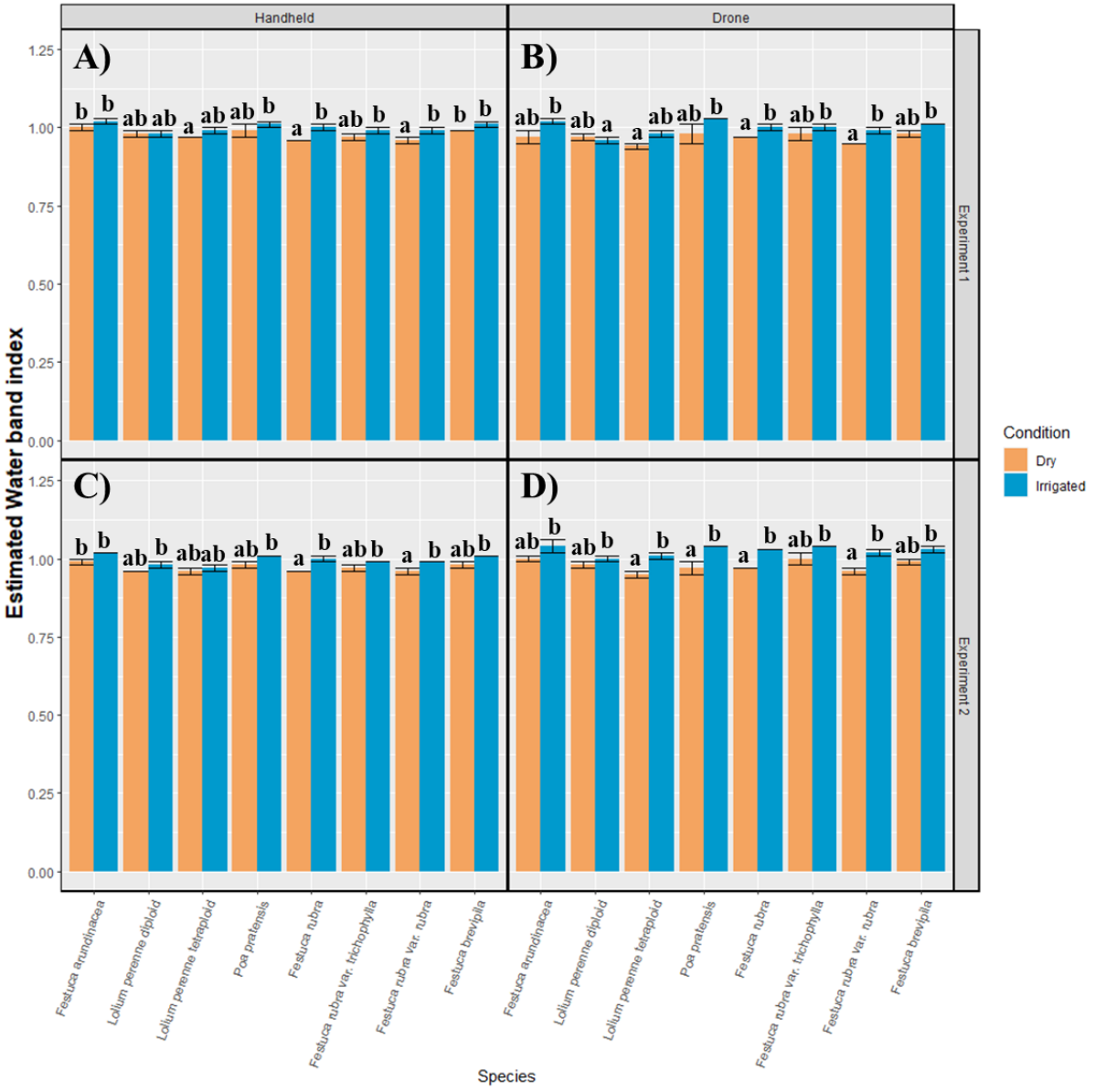

Figure 3.10: Estimated water band index of grass genotypes' dry (A, C) and irrigated (B, D) plots in two different 2022 experiments. Both the first experiment (A, B) and second (C, D) were scheduled in August 2022. Grass plots of 3 cm cutting height were imaged with either hand-held Tec5 camera or a hyperspectral camera attached to a drone, and denoted a diameter of 72.3 cm. The bars are averages and standard errors of 3 replicates/ genotype/ condition. Water band index was calculated as R_{900} / R_{971} where R refers to reflectance at specified wavelengths. Statistics was by two-way ANOVA with Tukey post-hoc where p-values of ≤ 0.05 are denoted by different alphabets. The genotypes were *Festuca arundinacea* (rietzwenkgras), *Lolium perenne* diploid (Engels raaigras diploid), *Lolium perenne* tetraploid (Engels raaigras tetraploid), *Poa pratensis* (veldbeemdgras), *Festuca rubra* (gewoon roodzwenkgras), *Festuca rubra trichophylla* (roodzwenkgras met fijne uitlopers), *Festuca rubra rubra* (roodzwenkgras met forse uitlopers), and *Festuca brevipila* (hardzwenkgras).

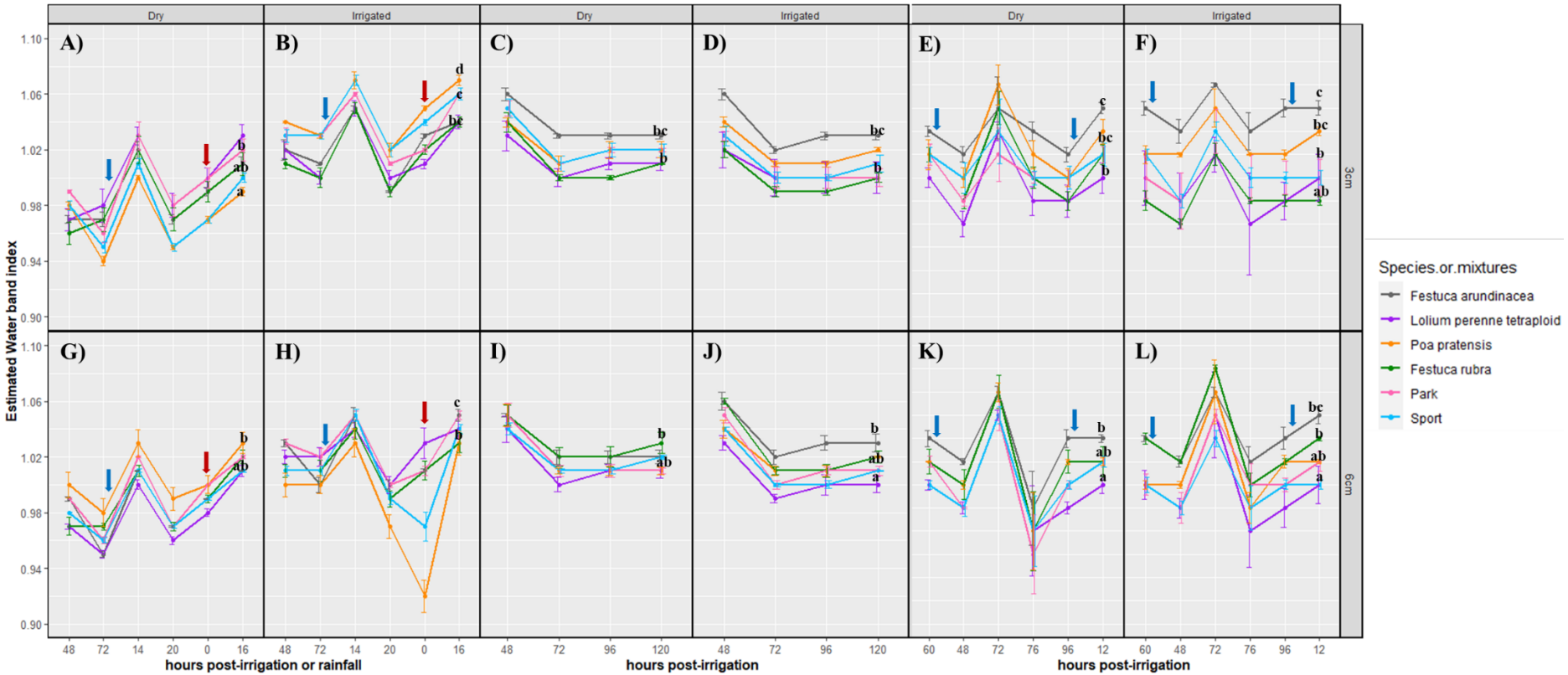

Figure 3.11: Estimated water band index of selected grass genotypes' dry (A, C, E, G, I, K) and irrigated (B, D, F, H, J, L) plots at definite timepoints in 2023. The first experiment (A, B, G, H), second (C, D, I, J) and third (E, F, K, L) were scheduled in June, August and September 2023 respectively. Scheduled irrigation, denoted as blue arrows, took place 72 hours after a dry spell in the first experiment, and after 60 hours and 96 hours post-dry spell measurements in the third experiment. Unprecedented rainfall, denoted with red arrows, also occurred during one timepoint measurement in experiment 1. Grass plots were imaged with a hand-held Tec5 device and denoted a diameter of 72.3 cm. The points are averages and standard errors of 3 replicates/ genotype/ condition/ cutting height at the timepoints post-irrigation or rainfall in the x-axis. Water band index was calculated as R_{900} / R_{971} where R refers to reflectance at specified wavelengths. Statistics was by two-way ANOVA with Tukey post-hoc where p-values of ≤ 0.05 are denoted by different alphabets. The genotypes were *Festuca arundinacea* (rietzwenkgras), *Lolium perenne* tetraploid (Engels raaigras tetraploid), *Poa pratensis* (veldbeemdgras), *Festuca rubra* (gewoon roodzwenkgras), park mixture composed of 35% *Lolium perenne* diploid: 50% *Poa pratensis*: 15% *Festuca rubra trichophylla*, and sport mixture consisting of 50% *Lolium perenne* diploid: 50% *Poa pratensis*.

3.5 PRI512 associates with real time measurements of soil moisture content but not temperature

Hyperspectral imaging data of all genotypes was correlated with on-ground measurements data from Work Package 2 'Climate and temperature'. These on-ground measurements were soil temperature and soil moisture content. Here, a correlation matrix and PCA was used to characterise all parameters (estimated hyperspectral indices and on-ground measurements) that explain our dataset.

There was variation among parameters in the correlation matrix of the 2022 experiments (Fig. 3.12A). Most of the hyperspectral indices showed significant positive correlation with each other (appear as black or indigo), except CTR2 and NDRE. NDRE and soil temperature had no significant correlation with any of the estimated or measured parameters. CTR2 on the other hand showed significant negative correlation (appear as pale yellow) with most hyperspectral indices but not with NDRE and both on-ground parameters. PRI512 significantly positively or negatively correlated with most of the parameters, including soil moisture content. The first two principal components, PCA1 and PCA2 are the most important explaining ~85% of variance in the whole 2022 dataset (Fig. 3.12B). All the parameters have significant representation within both PCA1 and PCA2 indicated by high square cosine values of > 0.5, and the best represented parameters were NDVI, CTR2, OSAVI, carotenoid, NDVI-red-edge, BNDVI, GNDVI and PRI512.

The 2023 correlation matrix was similar to observations in the 2022 experiments (Fig. 3.12A, C). Therefore, indicating the robustness of PRI512 since it showed strong positive or negative correlation with most parameters, including measured soil moisture content. Also similarly, the first two principal components explained ~82% of the variance within the dataset and well represented parameters by the two components were GNDVI, NDVI-red-edge, NDVI, CTR2 carotenoid, BNDVI, and PRI512, chlorophyll content, NDRE and moisture content (Fig. 3.12D).

Non-correlation between PRI512 and soil temperature in both experimental years may be linked to small variation in on-ground soil temperature (± 3°C) among all genotypes at each timepoint measurement, compared to other parameters that showed larger variation among the genotypes.

Overall, PRI512 is a good index for detecting and estimating drought and heat stress in turf grass monocultures and mixtures. Its correlation with the measured soil moisture content better supports this inference, indicating that this index can also be used as an alternative readout on soil moisture changes.

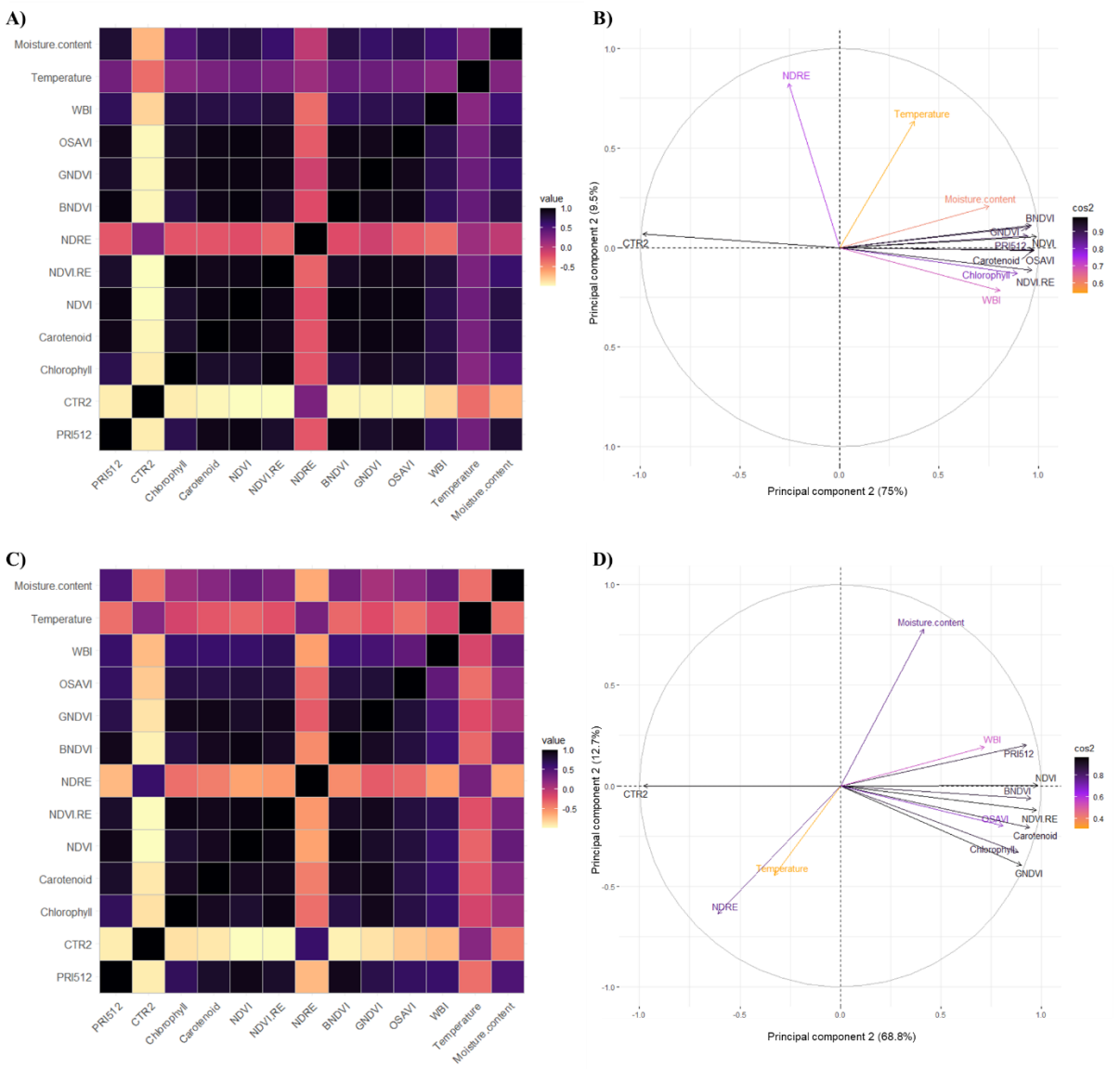

Figure 3.12: Explanation of the datasets with a correlation matrix (A) and a principal component analysis bi-plot (B) of the 2022 experiments; and another correlation matrix (C) and a principal component analysis bi-plot (D) of the 2023 experiments. The first eleven parameters denoted common hyperspectral indices as estimated PRI512 (photochemical reflectance index 512), CTR2 (Carter index 2), chlorophyll content, carotenoid content, NDVI (normalised difference vegetation index), NDVI-RE (red-edge), NDRE (normalized difference red edge index), BNDVI (blue NDVI), GNDVI (green NDVI), OSAVI (optimized soil-adjusted vegetation index) and WBI (water band index). Measured parameters, soil temperature and soil moisture content were also included in the correlation matrix. The biplot indicates the distribution of the parameters in PCA 1 and PCA 2. Significant positive correlations between parameters appear as black/ indigo (< 0.5) while significant negative correlation appear as pale yellow (< -0.5). All other colours indicate no significant correlation between any two parameters.

3.6 RNA sequencing results indicate a role of stress-related genes in crop responses

From the 2022 hyperspectral imaging results (Fig. 3.1-3.11), *F. rubra* and *L. perenne* tetraploid was identified as a drought (and heat) sensitive genotype while *F.arundinacea* had the opposite phenotype. Samples of these genotypes with contrasting hyperspectral index phenotypes were taken for mRNA sequencing to determine underlying genes that may be linked to the observed phenotypes. After data de-multiplexing, mRNA sequencing resulted in a total of hundreds of millions of raw sequencing reads (input reads) for *F.arundinacea*, *F. rubra*, and *L. perenne* (Table 3.1). Raw reads were further processed for trimming adapter sequences and used for de-novo transcriptome assembly per genotype.

Table 3.1: Statistics of de-novo transcriptome assembly.

De-Novo assembly	***Festuca arundinacea***	***Festuca rubra***	***Lolium perenne***
Input reads	157,144,430	178,389,696	120,102,296
Total assembled contigs	888,183	945,176	628,573
N50 contig size bp	397	390	418
Min contig size bp (setting)	200	200	200
Max contig size bp	8,237	10,111	8,898
Total de-novo assembly size bp	348,867,094	364,162,408	256,656,360

The PCA shows the distribution of samples collected from the dry and irrigated plots in the two 2022 experiments per genotype (Fig. 3.13). The first two PCAs explained ~40% of the variance observed among the samples per genotype. Differential gene expression (DE) analysis was performed to identify potential genes with at least a 2x fold change (double concentration) in the dry samples compared to its expression in their corresponding irrigated samples. There were 364 downregulated- and 173 upregulated genes in *F. arundinacea* while *L. perenne* had 295 downregulated- and 422 upregulated genes. There was a remarkably large difference (~ 6x) between downregulated (237 genes) and upregulated (1435 genes) genes in *F. rubra*. This may be linked to the less stringent settings for the FDR p-value for filtering the downregulated genes in this species. Zooming into the results for *F. rubra*, only one gene was upregulated in both 2022 experiments while there were 79 overlapping downregulated genes. Interestingly, the upregulated gene was a calcium binding protein KIC. A calcium signature is an initial response to osmotic stress including drought stress resulting in the induction of multiple calcium binding proteins (Kolukisaoglu 2004). A heat shock protein 3 (HSP3) was an interesting significantly downregulated gene while most of the other downregulated genes function in normal plant processes.

The differences between the drought sensitive *F. rubra* or *L. perenne*, and the resilient *F. arundinacea* can be linked to several significantly up- and down-regulated heat shock proteins (e.g., HSP3, HSP9, HSP15, HSP16, HSP90, HSP104, STI1) between the two genotypes, and dehydrins (e.g., DHN1, DHN3, DHN4, RAB15) that was strongly up-regulated in *F. rubra* only. HSPs are molecular chaperones involved in protein folding and transport and are induced by both heat and drought stress (Jiang and Huang 2002; Rahman et al. 2022). Molecular chaperones are proteins that interact with, repair or transport other proteins to perform their usual task (Hartl et al. 2011). Dehydrins on the other hand, are dehydration-protective proteins accumulated during drought stress and may contribute to drought tolerance or sensitivity of genotypes (Jiang and Huang 2002; Hu et al. 2010). Interestingly, pathogenesis- and microbial-related genes were significantly up-regulated indicating the presence of

pests and diseases at the time of sampling, and this is not unusual in such uncontrolled experiments. It should be noted that the RNA sequencing results give us first indications on genes of interest that should be further characterised with targeted molecular tools and used as markers to validate the hyperspectral index results and to identify drought resilient markers.

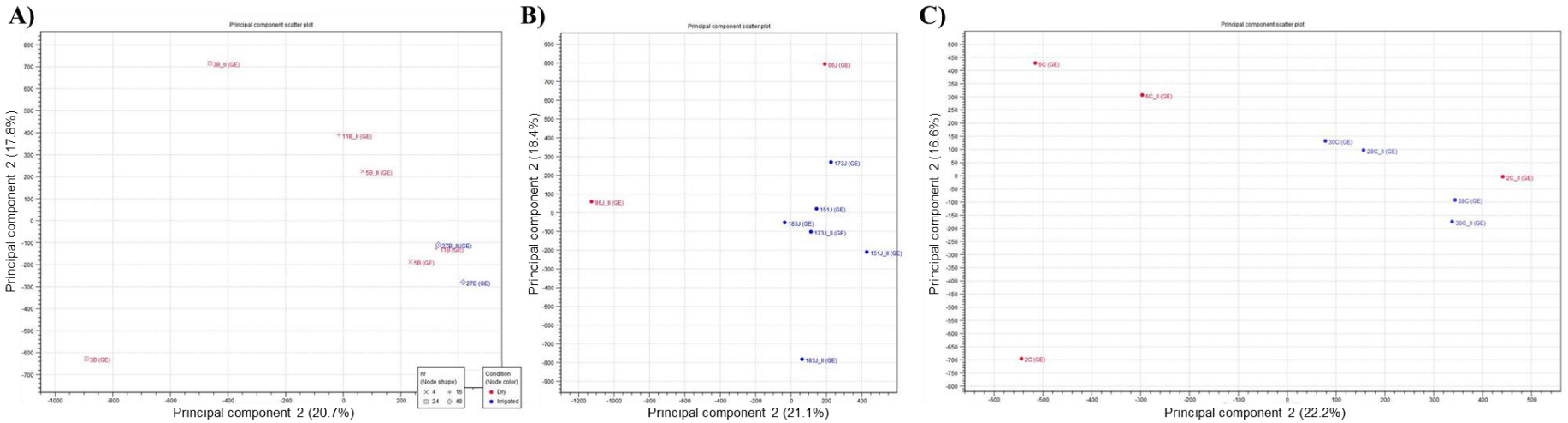

Figure 3.13: Principal component analysis results of all RNA sequencing data for *Festuca arundinacea* (A), *Festuca rubra* (B) and *Lolium perenne* (C). Samples from the dry plots are represented in red while those from the irrigated plots are in blue.

4. Discussion and Conclusions

Our main findings from the five turf grass experiments of late spring or summer 2022 and 2023 are summarised below.

1) The reflectance output from both hyperspectral cameras were mostly similar indicating that the imaging technique i.e., using either hand-held or drone-mounted cameras is possible, depending on consumer requirements.
2) Additionally, drones can measure large areas in a short time compared to the handheld cameras, that require more manpower and hours. On the other hand, the drone technique requires more technical training, than using the handheld hyperspectral cameras. Moreover, it may not be permitted in all aerial spaces.
3) Although similar trends were seen independent of the technique, bigger significant differences were observed with the drone measurements. Thus, indicating that the camera attached to the drone is a slightly more sensitive camera for imaging and stress detection.
4) Significant differences between dry and irrigated turf grass genotypes observed at the first 2022 timepoint were further enhanced in the second timepoint. This is linked to a longer dry period prior to hyperspectral imaging at the second timepoint, compared to the first timepoint.
5) The biggest differences in 2023 where only found in the first experiment (performed June 2023 during a heat wave). Responses between dry and irrigated plots of the genotypes where similar in the second and third experiment. This was because, although dry periods were observed prior to and during the measurements, drought and heat stress did not still occur in August and September 2023 when these experiments where scheduled.
6) For the 2023 experiments, the 3 cm cutting height plots showed larger variation among the genotypes compared to 6 cm cutting height plots. This observation may be due to a higher frequency of overlapping grass blades occurring on plots with the longer turf grass length and thus interfering with the reflectance measurements. Therefore, the grass height is an important factor influencing hyperspectral imaging and should be considered.
7) PRI512 and CTR2 values differentially varied among the genotypes in both 2022 and 2023 experiments indicating the robustness of these indices for detecting drought and heat stress in the genotypes. Both indices have been also established as indicators of short- and long-term drought and heat stress in cattle-grazed grassland (Hermanns et al. 2021).
8) Indices such as NDVI red-edge, chlorophyll red-edge and WBI showed that genotypes remained moderately green and healthy even when there was already indication of stress from the hyperspectral- and mRNA sequencing results. Thus, supporting the potential use of PRI512 and CTR2 as indices for detecting (early) drought and heat stress in turf grass. Therefore, these indices may give faster/ quicker information on the status of the grasses, than a human being can detect by eye.

9) PRI512 also significantly correlated with real-time sensor measurements of moisture content but not soil temperature. Again, supporting the robustness of this index and its use to also estimate changes in soil moisture content. Furthermore, using drone techniques give information on soil moisture content of large areas in short time compared to point measurements detected by sensors.
10) The results indicated that *Festuca rubra* (gewoon roodzwenkgras) and sport mixture are drought (and heat) sensitive genotypes while *Festuca arundinacea* (rietzwenkgras) and park mixture are resilient genotypes. Our observations on the turf grass are like recent findings that indicated *F. arundinacea* as a fast-growing drought-tolerant species (Taleb et al. 2023).
11) Interestingly, the main difference between park mixture and sport mixture is a 15% presence of the moderately resilient species *Festuca rubra trichophylla* instead of higher proportions of the sensitive species *Lolium perenne* diploid. This may explain some of the contrasting differential variation we have observed between these two mixtures although further molecular characterisation of both mixtures is needed to make stronger conclusions.
12) Sensitive species such as *F. rubra* may still be beneficial for cultivation since the species also shows quick recovery from the drought stress, although connecting this to suitable irrigation regimen still needs to be elucidated. An ideal climate-proof candidate may be genotypes that show little or no negative effects to drought and heat stress, and at the same time quickly recover from the stress upon irrigation, rainfall and lowering of temperature.
13) The differences between the drought sensitive and resilient genotypes can be linked to significant differential expression of several up- and down-regulated genes most notably, HSPs and dehydrins. The genes identified from the mRNA sequencing analysis still need further validation with targeted molecular tools.
14) In the experiments, only one variety per species was assessed. Thus, there is still need to test the responses of multiple, commonly cultivated varieties and give suggestions based on varieties rather than at species level.
15) Overall, these results are promising to show hyperspectral imaging as a potential method for adoption to estimate drought stress under field conditions, and could possibly be used as a (new) technique to select stress resilient genotypes

Work Package 2: Climate and temperature

Leon Mossink

Contribution Statement and Acknowledgement

Work package 2 was mainly supported by Jan Rinze van der Schoot of Open Teelten, Dr. Bert Heusinkveld of Meteorology and Air Quality, Prof. Paul Struik of Centre for Crop Systems Analysis, Prof. Bernd Leinauer of New Mexico State University, Inge van de Wiel of Centre for Crop Systems Aalysis, Ayodeji Deolu-Ajayi and Adrie van der Werf of Agrosystems research. Leon Mossink of Centre for Crop Systems Analysis was involved in all aspects of the project, including report writing and reviewing.

5. Introduction

Our climate is changing, causing frequent and extreme heat events and Urban Heat Island (UHI) effects in Western Europe (KNMI, 2023). Urban greening is one of the ways to minimize these negative heat effects on citizen health. However, whilst for trees a lot is known about cooling capacity, not much is known about the added value of turf grass in urban areas for their potential cooling effect. This remains especially unknown in Western European countries. Additionally, there is very limited research data on management of different grasses (monocultures and mixtures) and the implications for cooling. To get more insight on potential cooling effect of turf grass under different management strategies, the following research questions were composed:

1) What is the potential cooling effect of grass vegetation, compared to other surfaces?
2) How do grass management strategies (irrigation and mowing) affect the potential cooling effect of grass vegetation?

The first research question involves mapping the cooling effect of various turf grass vegetation compared to other terrains, possibly supplemented with additional measurements. Research question 2 focuses on investigating the effects of different management methods on the cooling effect of turf grass vegetation through field research. The focus of our research in WP2 on "grass vegetation" includes common turf grass species found gardens, parks, road verges, sports fields (e.g., golf, soccer), and biodiverse grasslands, and termed as practical situations. Both turf grass monocultures and mixtures have been examined in these practical situations and on experimental turf grass fields. In the case of "other terrains", our study considered paved surfaces such as tiles, bricks, concrete, and artificial turf.

6. Methodology

6.1 Experimental setup

The focus of the research on “turf grass vegetation” includes both monocultures and grass mixtures occurring in practical situations, on experimental turf grass fields, and on other terrains. Several experiments have been conducted from 2020 to 2023 (Table 6,1), and the results are presented in this report. Maps of the locations indicated in Table 6.1 are shown in Annex 2.

Table 6.1: Experiments performed in WP2 from 2020 to 2023

Year	Type of Research	Location	Type of Measurements
2020	Literature Review	-	-
2021	Turf grass vs. Paved Surfaces (Tiles)	Barenburg Wolfheze Experimental Fields	Surface temperature diurnal variation, meteorological data
2022	(Turf)Grass vs. Paved Surfaces (Parking Lot, Artificial Turf)	De Bongerd WUR Campus and practical park + parking lot	Surface temperature diurnal variation, meteorological data
2022, 2023	Turf grass irrigated and non-irrigated (3cm/6cm mowing height)	Nergena WUR Campus	24-hour measurements, 'hottest time of the day' measurements; DGCI and Canopy Cover %; joint measurements with WP1
2022, 2023	Biodiverse grass vs. short park grass, Concrete	Skatepark Zutphen	Surface temperature before and during drought periods
2023	Root Research	Nergena WUR Campus	Sampling

6.2 Literature Study

In 2020, a literature study was conducted with the aim of identifying knowledge gaps and searching for relevant background information regarding the (main) research questions within WP2. The literature study was carried out using databases such as Cab Abstracts, Scopus, and Google Scholar to search for relevant literature, and EndNote was used to organize, select, and manage literature related to specific topics and research questions. A total of over 9000 titles were screened. The abstracts of 600 titles were read, and 301 papers were ultimately included in the substantive research (Fig. 6.1). Main messages from selected papers of the literature study are found in Annex 3.

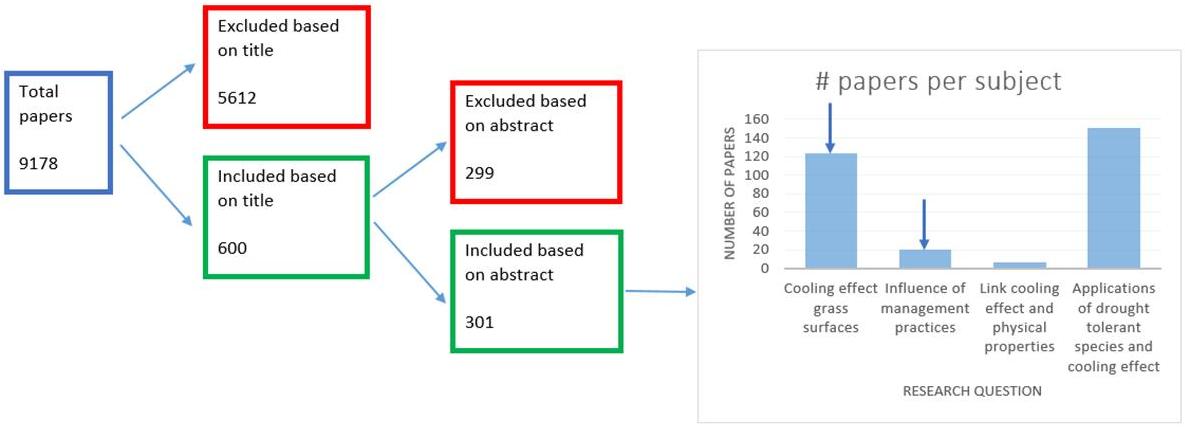

Figure 6.1: Selection procedure for including or excluding papers and reports in the substantive literature study.

6.3 Experimental Fields Barenburg Wolfheze

Field measurements were conducted in 2021 at the experimental field of Barenburg in Wolfheze. This location has several varieties of Poa pratensis (Veldbeemd) and Lolium perenne (Engels raaigras) planted as ongoing CGO trials. Half of these plots were irrigated, and the other half was non-irrigated (the idea was to cause water stress in these plots). The objective was to compare plots in these two different conditions with pavements of various colours. Measurements were carried out between 10 a.m. and 4 p.m. using a Davis 6163EU VP2 Plus weather station to record (micro)climate Additionally, I-Tec E IR sensors on tripods placed 1 m above ground and connected to a Campbell CR1000X logger with a log interval of 10 minutes was used to record surface temperature. A Fieldscout Handitrace TDR 350 soil moisture and soil temperature sensor and logger were also used to periodically (every hour) record volumetric soil moisture percentage and soil temperature. Measurements were conducted on September 7, 2021. There was no drought event during the entire 2021 summer, so the measurements became a comparison between all turf grass plots now without water stress, compared to different types of paved surfaces (observed as different coloured tiles). Two plots with Lolium perenne, two plots with Poa pratensis, and two differently coloured tiles (light grey and dark grey) were measured. A small part of the experimental setup is shown in Figure 6.2.

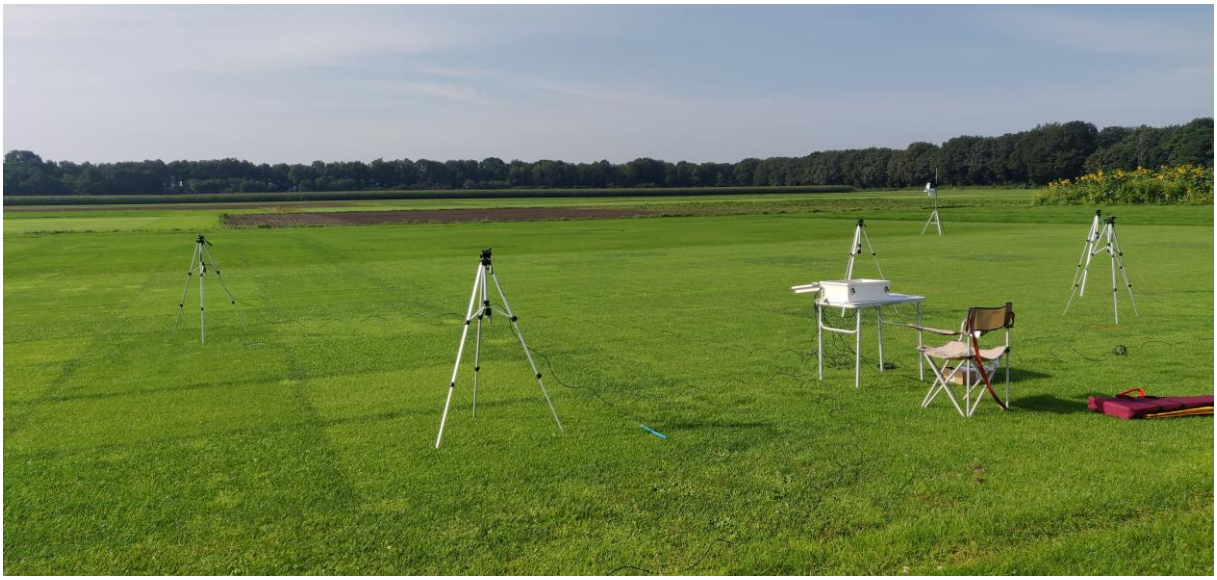

Figure 6.2: Experimental setup in Barenburg Wolfheze CGO turf grass field.

6.4 Nergena WUR Campus Experimental Field

In 2022 and 2023, 24-hour measurements were conducted on specified days before, during, and after warm and dry periods (Table 6.2). Measurements were taken for surface temperature of turf grass monocultures and mixtures, and paved/ tiled surfaces, as well as measurements on air temperature and other (micro)climate data. See Annex 1 for an overview of the turf grass field. Measurements of surface temperature, soil moisture percentage, and soil temperature using handheld sensors were also taken at different times of the day i.e., morning, early afternoon and late afternoon. All the measurements were taken on cloudless days to prevent temperature data disruption. Weekly photographs of all plots in the turf grass field were loaded into Turfanalyzer software to determine dark green colour index (DGCI) and canopy cover (percentage of ground area covered by the turf grass). Equipment specifications can be found in Annex 4. In 2022, there was runoff of irrigation water from a 3 cm cutting height treatment of the irrigation treatment to a section of plots in the 6 cm cutting height dry treatment. The 6 cm cutting height dry treatment data is therefore not included in the 2022 analysis.

Table 6.2: selection of experiments performed on Nergena experimental field between 2022 and 2023.

Date	Type of Measurements	Turf grass	Equipment	Comments
June 29, 2022	24-hour measurements	Lolium perenne tetraploid, Concrete	I-Tec IR sensors, Davis weather station	No drought yet
July 18, 2022	Morning, afternoon, late afternoon measurements	Festuca arundinacea, Lolium perenne tetraploid, Park Mixture, Sports Mixture	I-Tec IR sensors, Davis weather station, Fluke IR camera, Fieldscout TDR 350	No drought yet; significant temperature differences observed
July 19, 2022	Morning, afternoon, late afternoon measurements	Festuca arundinacea, Lolium perenne tetraploid, Park Mixture, Sports Mixture	I-Tec IR sensors, Davis weather station, Fluke IR camera, Fieldscout TDR 350	Hottest day of the year; surface temperature differences observed
August 9, 2022	Morning, afternoon, late afternoon measurements	Festuca arundinacea, Lolium perenne tetraploid, Park Mixture, Sports Mixture	I-Tec IR sensors, Davis weather station, Fluke IR camera, Fieldscout TDR 350	No drought yet; differences in surface temperature observed
August 23, 2022	Morning, afternoon, late afternoon measurements	Festuca arundinacea, Lolium perenne tetraploid, Park Mixture, Sports Mixture	I-Tec IR sensors, Davis weather station, Fluke IR camera, Fieldscout TDR 350	Drought started; significant temperature differences observed
June 14, 2023	Morning, afternoon, late afternoon measurements, and 24-hour measurements	Festuca arundinacea, Lolium perenne tetraploid, Park Mixture, Sports Mixture	I-Tec IR sensors, Davis weather station, Fluke IR camera, Fieldscout TDR 350	Drought started; significant temperature differences observed

Relative humidity (RH) and air temperature was not measured per individual plot on the Nergena experimental field because surface area of the plots was too small. The air temperature and RH were measured at two locations in the test field, namely in the middle of the 'dry or non-irrigated' part and in the middle of the 'irrigated' part. The PET value could be calculated with more certainty if measurements were taken on plots of 0.5 hectare each and with little wind. The differences between irrigation and no irrigation would probably be greater since the air temperature is likely to be lower with application of irrigation. The RH would then probably suddenly be higher before irrigation, which has a negative effect on the PET (higher heat stress), but a reduction in air temperature generally has a greater positive effect than the increase in RH that would take place at the same time.

In 2022 and 2023 measurements, DGCI and canopy cover % (amount of leaf material with chlorophyll per observed ground area % m^2/ m^2) observations were made. These observations took place weekly, starting when drought had not yet occurred and the grass was therefore still green, until several weeks after the first late summer rain had started. DGCI and Canopy cover % together can tell something about the amount of potential evaporation and therefore cooling capacity of a surface, because evapotranspiration can only take place through living plant material. The disadvantage is that only the top visually visible layer of the surface is included in the analysis, so there is no prediction of (living) leaf area per square meter (also known as Leaf Area Index: LAI) and therefore

cannot be made with these observations. The measurement period for 2022 was July 18 to October 12. The measurement period in 2023 was from May 17 to September 11. The measurements were taken with an imaging tub - a mortar tub that is placed upside down on the turf grass with a hole in the middle into which a camera fit exactly. 2 LED panels have been placed on the inside of the mortar tank (JGS LED panel 6500K). The camera used is a Canon Powershot G7X Mark III. For all observations, aperture was set to f3.2, shutter speed 1/60 and ISO value 800. Grayscale was set to custom (determined by using a colour fan on which the camera colours were subsequently calibrated). The settings were the same for all observations, as was the light; no outside light could enter the mortar tank and therefore not on the surface that was photographed. All images were analysed with Turfanalyzer software, with all data generated using the same analysis settings (see Appendix 4). The values for cover percentage do not exceed 95% because even under ideal conditions there is always some ground surface area visible in the observation made, or a small amount of shade from overlapping turf grass leaves.

6.5 Sports centre de Bongerd, Wageningen University Campus

Sports complex de Bongerd is located on the WUR campus. Measurements were taken on several days in 2021 and 2022 to compare the cooling capacity of grass, artificial grass and parking lot during warm, completely sunny days. Three complete (Davis) weather stations were used, Fluke and Testo IR cameras, and Fieldscout TDR soil moisture + soil temperature sensor/logger. Point measurements have been made, as well as daily measurements (Fig. 6.3). A park and parking lot at another location (next to Sports Center de Koekoek, Vaassen, municipality of Epe) were also included in the study as reference areas.

On September 6, 2021, measurements taken with complete weather station, IR thermal imaging camera, soil moisture and soil temperature was between 11.30 a.m. and 4 p.m., with measurements taken around 12 p.m. on the WUR campus, and then around 3 p.m. at a park and adjacent parking lot (Ireneveld/Koekoek Vaassen). From the collected data, the PET was calculated with RayMan Pro software (Matzarakis et al. 2007; Matzarakis et al. 2010; Matzarakis et al. 2018; Matzarakis et al. 2021; Fröhlich et al. 2019).

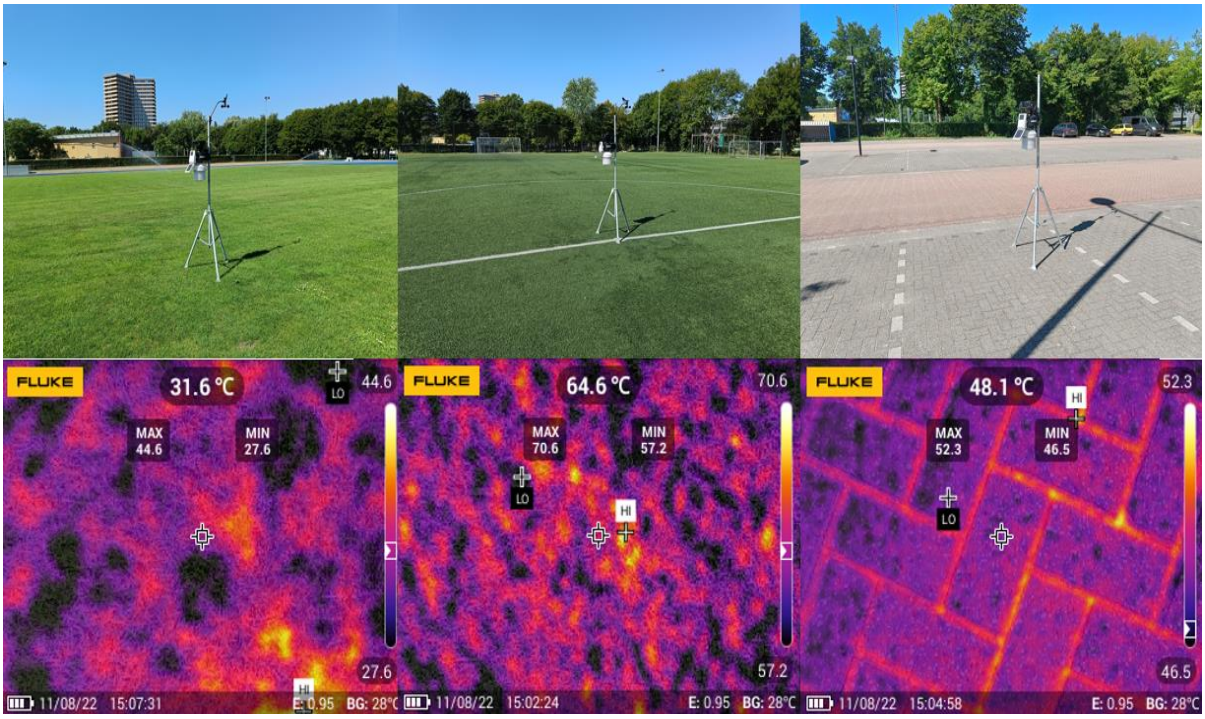

Figure 6.3: Weather station setup with surface temperature observations around 3:00 PM on August 11, 2022.

6.6 Skatepark Zutphen biodiverse turf grass fields

Measurements were carried out on several days on turf grass test fields measured in Work package 3 “Climate and Biodiversity”. These fields consisted of four different soil treatments and a control plot (tillers, row tiller, weed harrow). These fields also have different methods of sowing with biodiverse grass seed (full fields, partial sowing in rows). In addition, short park grass from the adjacent park was included in the measurements, as well as a concrete skate park located 15 m away from the biodiverse grass fields. A complete (Davis) weather station, I-Tec IR sensors, Fluke and Testo IR camera, Fieldscout TDR 350 soil moisture and soil temperature sensor and logger were used (Fig 6.4, 6.5).

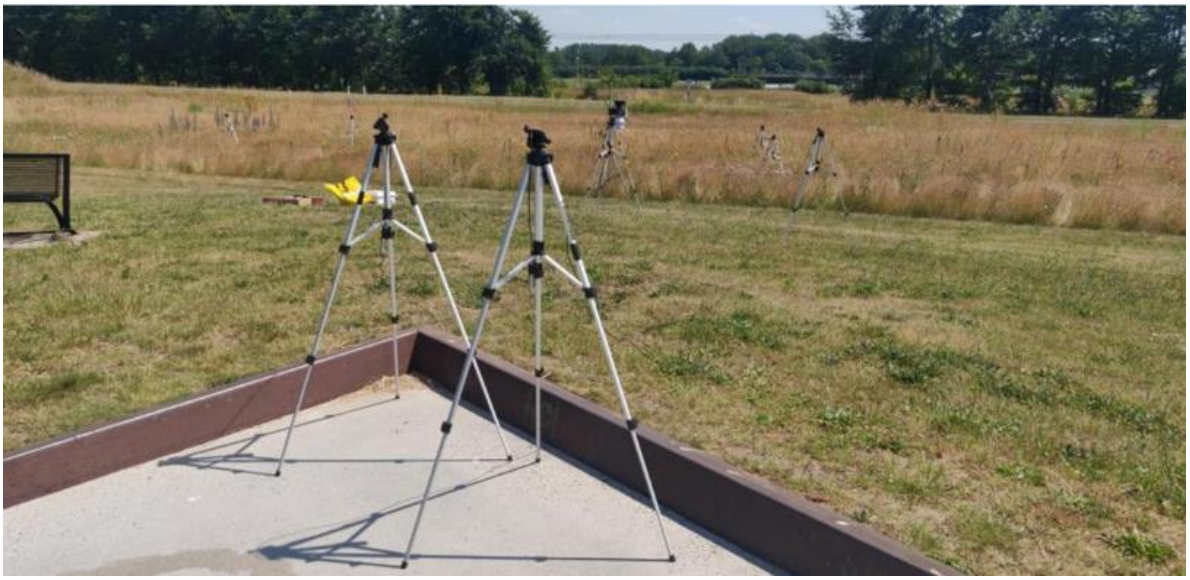

Figure 6.4: Measuring setup trial location skate park Zutphen.

Figure 6.5: Thermal camera image of broadleaf herbs and dried grass.

6.7 Root research on Nergena experimental site

At the beginning of 2023, a root investigation took place at the Nergena experimental turf grass field. Festuca arundinacea and Lolium perenne tetraploid were selected because these monocultures have been extensively investigated on climatic responses. Plots of these two genotypes under both dry and irrigated conditions were included in this root studies but only the 3 cm cutting height was considered, because the 6 cm cutting height was partly unusable due to irrigation in 2022. For each treatment, 3 plots per genotype per condition were included, where 3 technical replicates were taken at the following depths: stubble, 0-5cm depth, 5-10 cm, and 10-20 cm. In total, 3*3*2*2*4= 144 samples were collected for analysis. The samples were rinsed until only plant material remained, this was dried for > 48 hours at 70°C and then, the dry weight of the sample was determined. All dry weights are listed and statistically analysed using a statistical model output GLMM. The model is fitted to root biomass, dry weight per depth/ condition (dry or irrigated)/ turf grass genotype (tetraploid ryegrass or tall fescue), and a nested effect of plots and technical replicates included (1| Plot/Repeat). This resulted in possible simple models where the goal is to choose the smallest possible Akaike Information Criterion with as few degrees of freedom as possible. The top model was chosen with condition, soil depth, genotype, interaction condition: soil depth and interaction condition: genotype (Fig. 6.6).

```
Global model call: glmmTMB(formula = Drooggewicht ~ Diepte * Behandeling * Grassoort +
    (1 | Plot/Herhaling), data = datazs, na.action = "na.fail",
    ziformula = ~0, dispformula = ~1)
---
Model selection table
    cnd((Int)) dsp((Int)) cnd(Bhn) cnd(Dpt) cnd(Grs) cnd(Bhn:Dpt) cnd(Bhn:Grs) cnd(Dpt:Grs) cnd(Bhn:Dpt:Grs) df  logLik  AICc  delta
32      0.7330          +        +        +        +            +                                        11  56.143 -87.5   0.00
16      0.7020          +        +        +        +            +                                        10  53.879 -85.5   2.05
12      0.7265          +        +        +                     +                                         9  52.624 -85.4   2.12
64      0.7279          +        +        +        +            +            +                           13  56.609 -83.3   4.19
48      0.6970          +        +        +        +            +                        +                  12  54.345 -81.4   6.13
128     0.7403          +        +        +        +            +            +           +                + 15  57.197 -79.2   8.36
24      0.6573          +        +        +        +                         +                            9  49.112 -78.4   9.15
3       0.6385          +                 +                                                              6  45.424 -78.0   9.52
8       0.6264          +        +        +        +                                                     8  46.963 -76.5  11.06
4       0.6509          +        +        +                                                              7  45.709 -76.3  11.24
56      0.6523          +        +        +        +                         +           +                11  49.513 -74.3  13.26
39      0.6090          +                 +        +                                     +                9  47.013 -74.2  13.35
40      0.6213          +        +        +        +                                     +               10  47.348 -72.4  15.11
1       0.2795          +                                                                               4 -23.067  54.5 142.06
5       0.2550          +                          +                                                    5 -22.706  56.0 143.54
2       0.2918          +        +                                                                      5 -22.976  56.5 144.08
6       0.2673          +        +                 +                                                    6 -22.614  58.1 145.59
22      0.2983          +        +                 +                         +                          7 -22.030  59.2 146.71
7       0.6141          +                 +        +                                                    7
Models ranked by AICc(x)
Random terms (all models):
  cond(1 | Plot/Herhaling)

> summary(sel)
 Family: gaussian  ( identity )
Formula:          Drooggewicht ~ Behandeling + Diepte + Grassoort + Behandeling:Grassoort +      Diepte:Behandeling + (1 | Plot/Herhaling)
Data: datazs

     AIC      BIC   logLik deviance df.resid
   -90.3    -60.8     56.1   -112.3       97

Random effects:

Conditional model:
 Groups         Name        Variance  Std.Dev.
 Herhaling:Plot (Intercept) 3.648e-04 1.910e-02
 Plot           (Intercept) 6.978e-12 2.641e-06
 Residual                   2.034e-02 1.426e-01
Number of obs: 108, groups:  Herhaling:Plot, 36; Plot, 12

Dispersion estimate for gaussian family (sigma^2): 0.0203

Conditional model:
                                      Estimate Std. Error z value Pr(>|z|)
(Intercept)                            0.73297    0.03934  18.633  < 2e-16 ***
BehandelingNiet beregend              -0.23779    0.05563  -4.274 1.92e-05 ***
Diepte5-10 cm                         -0.65421    0.04754 -13.760  < 2e-16 ***
Diepte10-20 cm                        -0.64983    0.04754 -13.668  < 2e-16 ***
GrassoortTetra                        -0.01296    0.03985  -0.325 0.745020
BehandelingNiet beregend:GrassoortTetra  0.12378    0.05635   2.196 0.028059 *
BehandelingNiet beregend:Diepte5-10 cm   0.23559    0.06724   3.504 0.000458 ***
BehandelingNiet beregend:Diepte10-20 cm  0.21815    0.06724   3.245 0.001176 **
---
Signif. codes:  0 ‘***’ 0.001 ‘**’ 0.01 ‘*’ 0.05 ‘.’ 0.1 ‘ ’ 1
```

Figure: 6.6: Print of the model used in root research on Nergena experimental site.

7. Results

7.1 Literature study

Papers from the literature study were categorized per research question (Fig. 7.1). The type of research identified in the papers can be grouped into 4 main categories.

1) Measurements i.e., both in uncontrolled fields and in controlled environments, and it covers surface temperature, air temperature, and relative humidity.

2) Remote sensing of surface temperature differences (surface) over time, based on satellite imagery.

3) Model studies particularly using the ENVI-Met program.

4) Literature studies combining datasets from different papers.

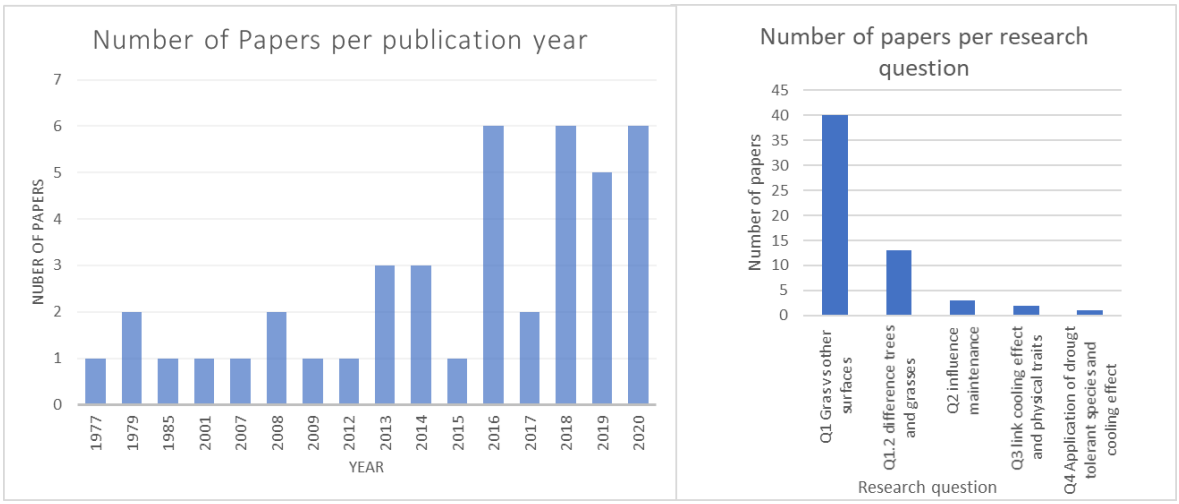

Figure 7.1: Number of analysed papers categorized per publishing year (left graph) and per research question (right graph).

The majority of the analysed papers are from the years 2013 – 2020 (Fig. 7.1). Research on (UHI) is relatively young, thus most fundamental knowledge-based papers are mainly from earlier decades, and those addressing UHI mitigation are mainly from the last decade 2010, and onwards. Most of the analysed papers involve studies conducted in the USA, China and Germany (80% is USA and China). The USA and China experience significant UHI issues, and many cities in these countries experience more extreme climates (warmer temperatures and drought events). Therefore, conducting research in the Dutch or Western European context is interesting due to differences from the former in climate, vegetation, and urbanisation. Additionally, the climate in the Netherlands is shifting more towards the climate of cities in warmer regions such as the USA and China.

The literature study yielded the following conclusions, summarized and categorized per sub-questions:

For the research question on cooling effect of grass vegetation, it was observed that the condition of the turf grass is crucial for the cooling effect. Shorter and drier turf grass have smaller leaf surface area and experience less water evapotranspiration, resulting in a reduced cooling effect (observed as elevated surface temperature and air temperature). Grass can however have a significant cooling effect on urban areas (e.g. Amani-Beni, 2018; Lee, 2016; Armson, 2012; Connors, 2012; Shashua-Bar, 2009).

The cooling effect of natural turf grass compared to stone and artificial turf also showed differences. Natural turf grasses are often have tens of degrees cooler surface temperature than paved surfaces and various types of artificial turf. The air temperature (at 150 cm height) for turf grass is also at least 1°C lower than for paved areas such as artificial turf (e.g. Jim, 2016). Irrigation provides only a few tens of minutes cooling for artificial turf. With natural turf grass, the effect lasts longer because water not only evaporates from the leaf surface but is also utilised from the soil through evapotranspiration. The method of irrigation can make a difference. When irrigation is performed during the day and in short periods, a larger proportion of the water evaporates directly from the surface and does not reach the root zone. Also, small amounts of irrigation water can heat up more quickly than a larger amount, leading to a temporary increase in soil surface temperature. Reducing the waterflow but with longer irrigation periods on the other hand leads to more soil moisture being available for evapotranspiration. Also, a small amount of irrigation water can heat up more quickly than a larger amount, leading to a temporary increase in soil surface temperature.

Trees and shrubs have a larger cooling effect during the day while turf grass fields have a greater cooling effect in the evening and night. Therefore, a combination of trees, shrubs and turf grass provides the biggest cooling effect. The cooling effect of turf grass fields in air temperature diffuses less deeply (up to about 10 meters) sidewarts outwards into built-up areas than green zones with grass and trees (up to about 60 meters) (Grilo, 2020).

Management practises can also affect the cooling effects of turf grass. Irrigation of turf grass leads to more evapotranspiration by the turf grass and thus, a greater cooling effect (Amani-Beni, 2018). The length of the grass influences the leaf surface area and with sufficient water availability. The difference between long and short grass was examined in this study.

External drivers affect cooling effect of turf grass. Certain turf grass species can cope better with external drivers such as high temperature and high vapor pressure deficit (VPD) (Sinclair, 2008).

7.2 Barenburg field measurement

Barenburg field measurements showed that ark grey tiles heated up quickly (Fig. 7.3). The tiles were warmer than turf grass (both for Poa pratensis and Lolium perenne) from ~11 a.m., while the light grey tiles only became warmer than the turf grass around 12 noon. At 1 p.m., the dark grey tiles were 41°C, compared to 36.3 °C for the grey tiles and an average of 31.6 °C for turf grass surfaces. At 2.40 p.m., the surface temperatures peaked. The dark grey tiles were 45.2 °C, the light grey tiles were 39.6 °C, and the turf grass averaged at 31.8 °C. Afterwards, the turf grass surfaces slowly cooled down, while the tiles remained at a stable warm temperature until the last timepoint measurements of 4 p.m. The conclusion is that tiles heated up quickly from noon and seem to reach a peak surface temperature late in the afternoon (3-4 p.m.). The colour difference between the tiles makes a difference, as seen in the contrast between the light grey and dark grey tiles.

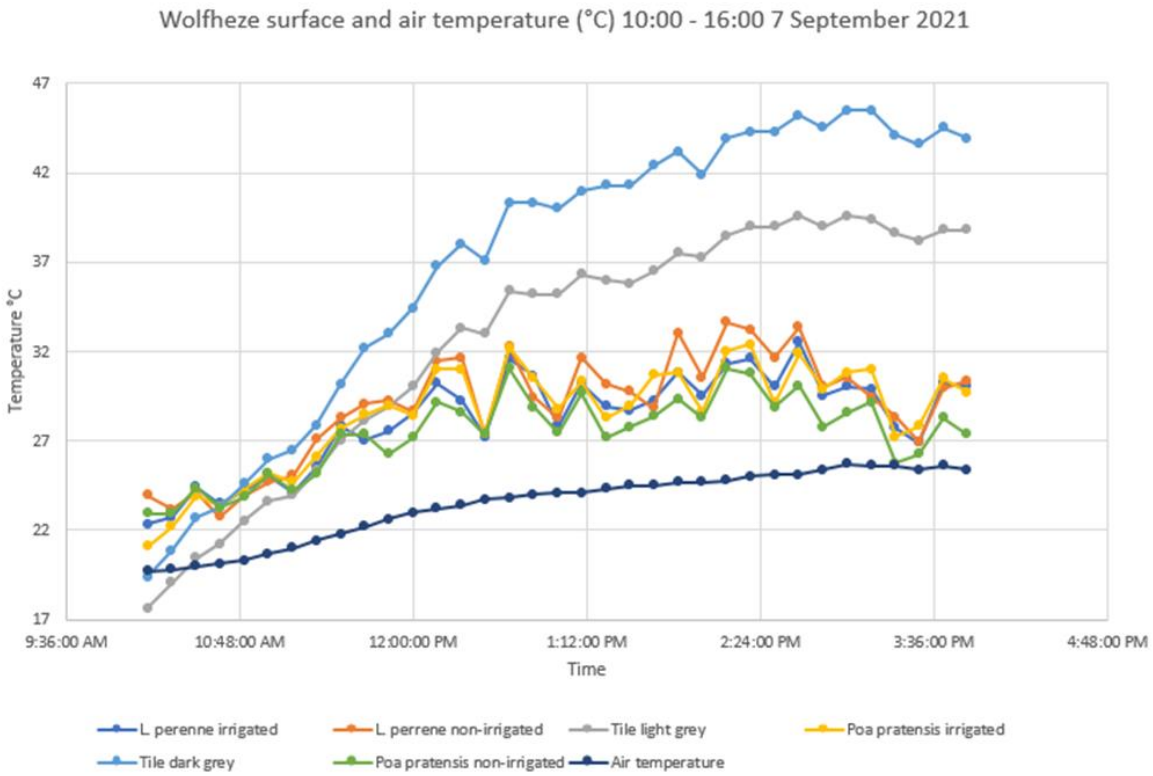

Figure 7.3: Measurement results at the Wolfheze experimental field on September 7, 2021. Measurement interval is 10 minutes. On the y-axis the measured surface temperature of all measured surface is displayed as well as the air temperature. On the x-axis the time during the measurement day is displayed. The line colours are explained in the legend below the graph. Each line resembles one plot.

7.3 Measurements in Nergena experimental site

The first timepoint (June 29, 2022) 24-hour measurements was performed on concrete, park mixture, sport mixtures and Lolium perenne tetraploid. At this timepoint, drought had not yet occurred, so significant differences was not observed among the genotypes but rather between concrete and all turfgrass for the 3 cm and 6 cm cutting height. Soil moisture percentage was ~ 20% VWC on all plots. In the morning (until 10 a.m.) all genotypes showed almost equal surface temperature (Fig. 7.4). From 11 a.m., differences between concrete surfaces and turf grass surfaces became apparent. At the hottest time of the day (~ 4 p.m.), the air temperature was 27°C, the concrete surface was between 43 to 45°C, while all turf grass surface temperature were lower between 30 to35°C. The concrete surface remained much warmer than the grass surfaces until late at night. At 9 p.m., the concrete surface was ~ 30°C while the turf grass was ~ 20°C. The concrete surface was about 23°C while the turf grass was around 15°C at 2 a.m. in the night. Only at 7:30 am, were all surfaces again similar because the turf grass slowly warmed up due to sunlight.

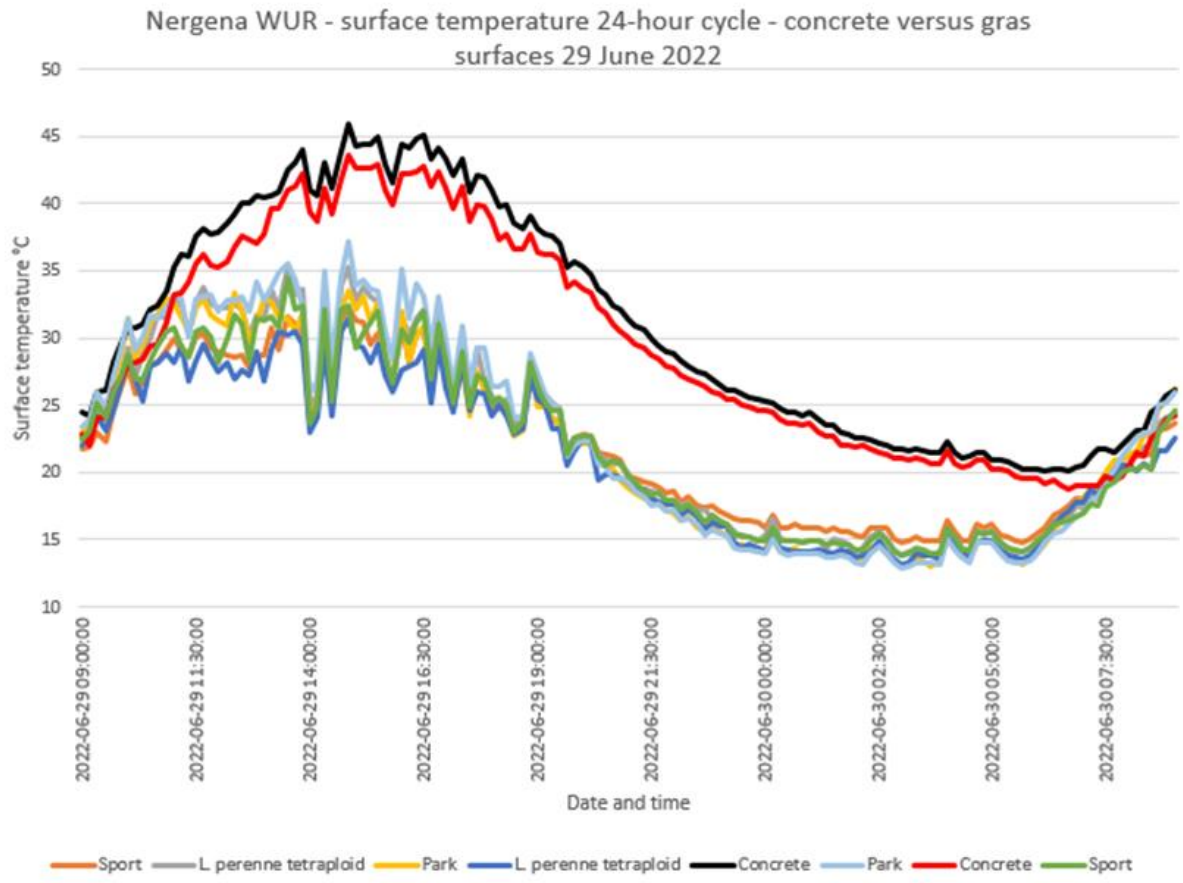

Figure 7.4: 24-hour cycle measurements on Nergena experimental turf grass field June 29, 2022. Measurement interval is 10 minutes. On the y-axis, the surface temperature of the measured surfaces is displayed. On the x-axis, the date and time of measurements are displayed. Each line resembles one plot.

July 19 was the hottest day in 2022 with a maximum measured air temperature of 36°C. In general, at an air temperature of 36°C, the surface temperature for all irrigated turf grass plots was ~30°C (Fig. 7.5). Where Festuca arundinacea turned out to be slightly cooler than the other grass surfaces (p-value < 0.05). Dry plots of turf grass (3cm cutting height) had an average of 37°C for Tall Fescue and 44°C for other turf grass genotypes, although the variation within a plot was large, so there were no significant differences. The measurements showed contrasts between the two conditions (irrigated vs dry) for some genotypes. tall fescue and Lolium perenne tetraploid had no significant differences between their dry and irrigated plots (p-values= 0.12 and 0.11 respectively), while 3cm park mixture and sport mixture showed significant differences between dry and irrigated conditions (p-value= 0.012 and 0.034 respectively). This could partly be explained by the fact that Festuca arundinacea and Lolium perenne tetraploid were on average cooler than Park and Sport mixtures. The variation within a plot was also quite large because the fields were in an initial phase of drought. The turf grass surfaces were barely dried out at this timepoint measurement but started to turn a strange yellowish-green colour in the plots under dry conditions. This contrasts with measurements taken on August 9, when almost all genotypes except Festuca arundinacea were largely yellow in colour, and therefore there was less variation within a plot (Fig. 7.7). Also look at figure 7.14 DGCI 2022, which shows that during this period of the year, the DGCI was still in the initial phase of transition from green to yellow for turf grass mixtures and monocultures, while this stabilized on August 9 (driest period of the year).

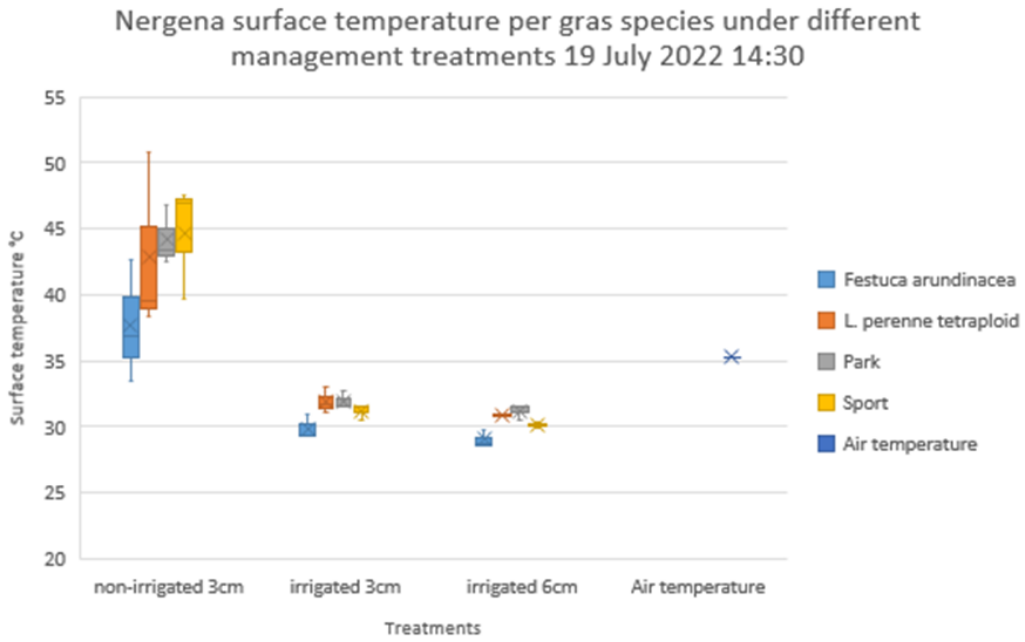

Figure 7.5: Surface temperatures for different turf grass surfaces (monocultures and mixtures) under different management in the Nergena experimental field WUR July 19, 2022, 2:30 PM. All measurement are performed around 14:30 p.m. On the y-axis the surface temperature of the measured plots and the air temperature is displayed. On the x-axis the treatments are displayed (plots that receive no irrigation throughout the measuring season May-September are referred to as 'non-irrigated'). Each box resembles a combination of three plots.

Under the microclimate conditions, irrigation during the measurements reduced heat stress level from 'extreme heat stress' to 'strong heat stress' (Fig. 7.6).

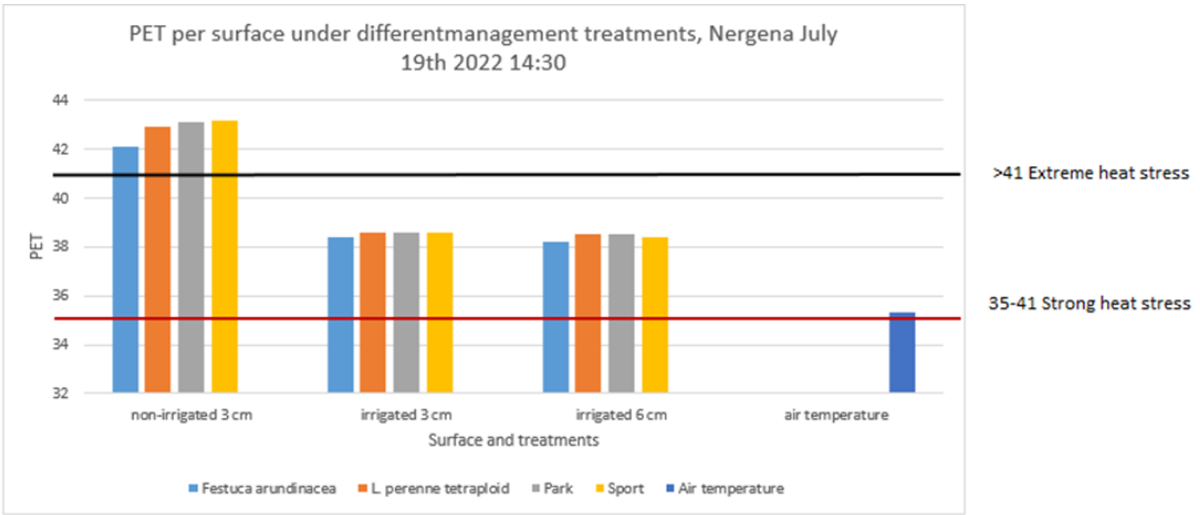

Figure 7.6: PET for different grass areas (monocultures and mixtures) under different management, Nergena experimental field WUR July 19, 2022, 2:30 PM. On the y-axis, the calculated PET for the measured plots is displayed as well as the air temperature in °C. On the x-axis the treatments are explained (dry plots are referred to as 'non-irrigated'). Each bar is and average of three plots within one treatment.

On August 9, 2022, air temperature was a maximum of 26°C and there was a large difference between irrigated and dry conditions because it was very dry and warm for weeks prior to the August 9 measurements. There was little variation among dry plots because turf grass in almost all these plots were yellow in colour, except plots containing tall fescue, that were slightly greener (Fig.7.7). Significant differences between irrigated and dry conditions for all surfaces was recorded (p-values ≤ 0.05). The irrigated surfaces had an average temperature of 27°C at 2.50 p.m., with no significant differences between 3 and 6 cm cutting height. Festuca arundinacea visually appears slightly less warm but had no significant temperature difference. In the dry condition, surface temperature of tall fescue (3cm cutting height only) was on average 35°C, while the other genotypes averaged between 42 to 45°C. This meant that the surface temperature of Festuca arundinacea was significantly cooler than that of other turf grass genotypes. This is supported with statistics where Festuca arundinacea vs. Lolium perenne tetraploid p-value= 0.003, Tall Fescue vs. park mixture p-value= <0.001), and Festuca arundinacea vs. sport mixture p-value= =0.09 due to the large variation within the sport mixture plots.

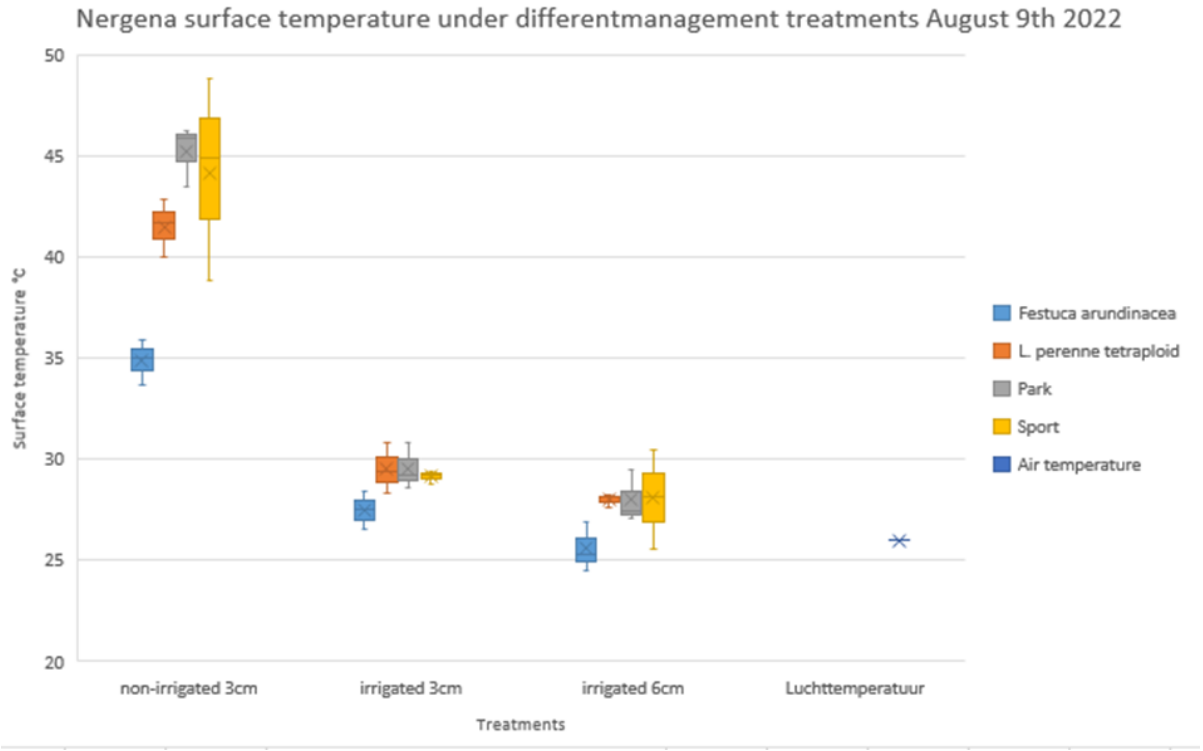

Figure 7.7: Surface temperatures for different grass surfaces (monocultures and mixtures) under different management, Nergena test field WUR August 9, 2022, 2:30 PM. On the y-axis the surface temperature of the measured plots and the air temperature is displayed. On the x-axis the treatments are displayed (dry plots are referred to as 'non-irrigated'). Each box resembles a combination of three plots.

Under the microclimate conditions during the measurements, all turf grass genotypes experienced 'moderate heat stress' (Fig. 7.8). The PET shows the same trend as seen in Figure 7.7.

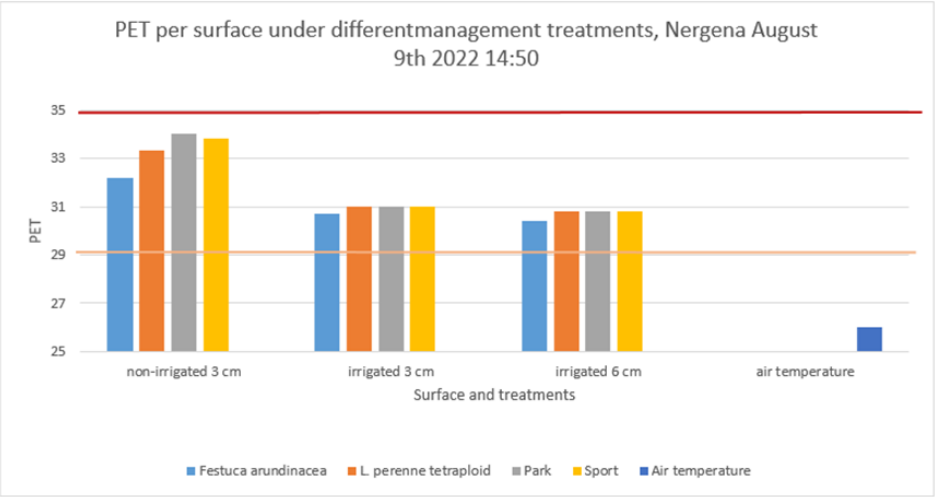

Figure 7.8: PET test field Nergena August 9, 2022. On the y-axis, the calculated PET for the measured plots is displayed as well as the air temperature in °C. On the x-axis the treatments are explained (dry plots are referred to as 'non-irrigated'). Each bar is and average of three plots within one treatment.

Surface temperatures for the 3 cm park and sport mixture under dry conditions are the same at the August 23, 2022, timepoint. The surface temperature peaks at 45°C on the dry plots, while for the irrigated 3cm plots it remains around 35°Cat an air temperature of 29°C (Fig. 7.9).

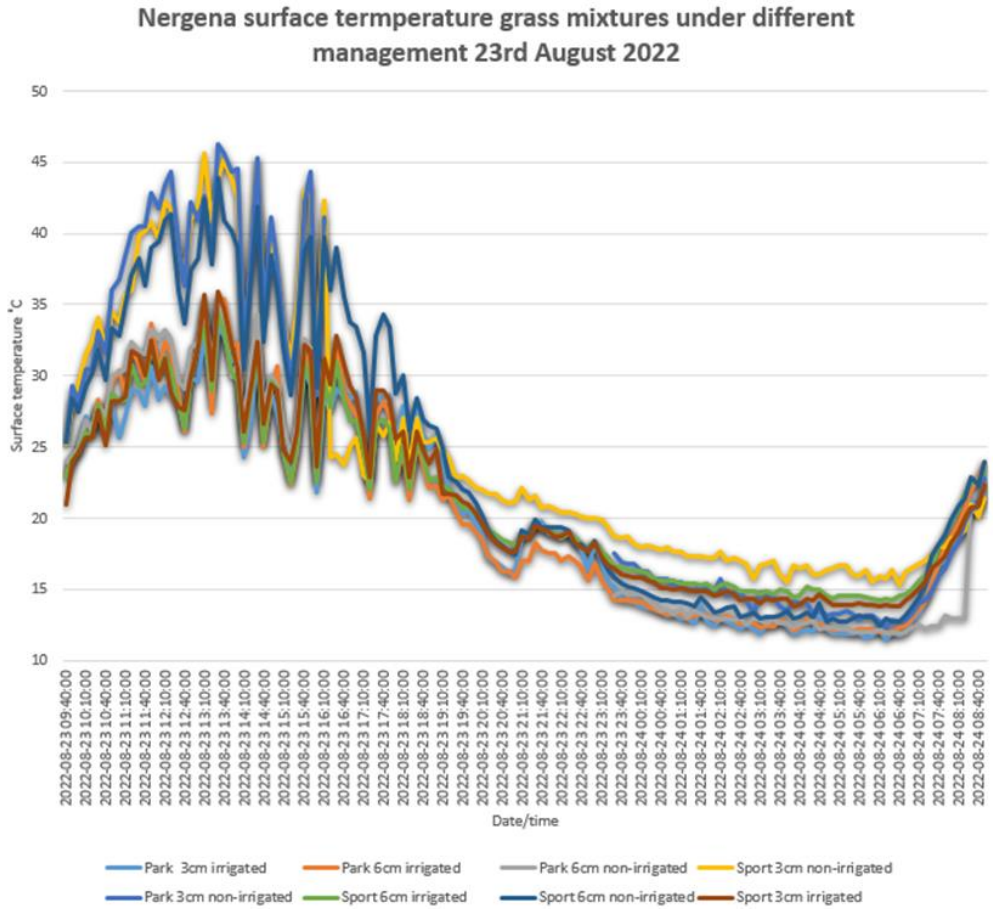

Figure 7.9: 24-hour cycle Nergena test field August 23, 2022. Measurement interval is 10 minutes. On the y-axis, the surface temperature of the measured surfaces is displayed. On the x-axis, the date and time of measurements are displayed. Each line resembles one plot.

On June 14, 2023, all 4 by 4 m sized plots in the experimental turf fields were measured between 1 and 4 p.m., and in a continuous 24-hour cycle on Festuca arundinacea, Lolium perenne tetraploid, park mixture and sport mixture at 3 and 6 cm cutting height and under both dry and irrigated conditions. Surface temperature of tall fescue in the dry conditions was significantly cooler than that of park mixture (p-value= 0.0065) and sport mixture (p-value= 0.0091), but not significantly cooler than Lolium perenne tetraploid with p-value= 0.06 (Fig. 7.10). Differences between mowing height within non-irrigation and irrigation treatments were not observed. Differences were observed between dry and irrigated conditions. In almost all cases, the surface temperature on irrigated plots (both 3 and 6cm cutting height) is significantly cooler than under dry conditions. Except when tall fescue under dry conditions is compared with park mixture in irrigated conditions. In these cases, p-value > 0.05, because tall fescue is on average the coolest in all cases and park mixture is the warmest on average in all cases. Tall fescue reached a maximum surface temperature of ~ 37°C degrees for both 3 and 6 cm cutting height under dry conditions in the 24-hour cycle and for Tp Ryegrass this was about 43°C (Fig. 7.11).

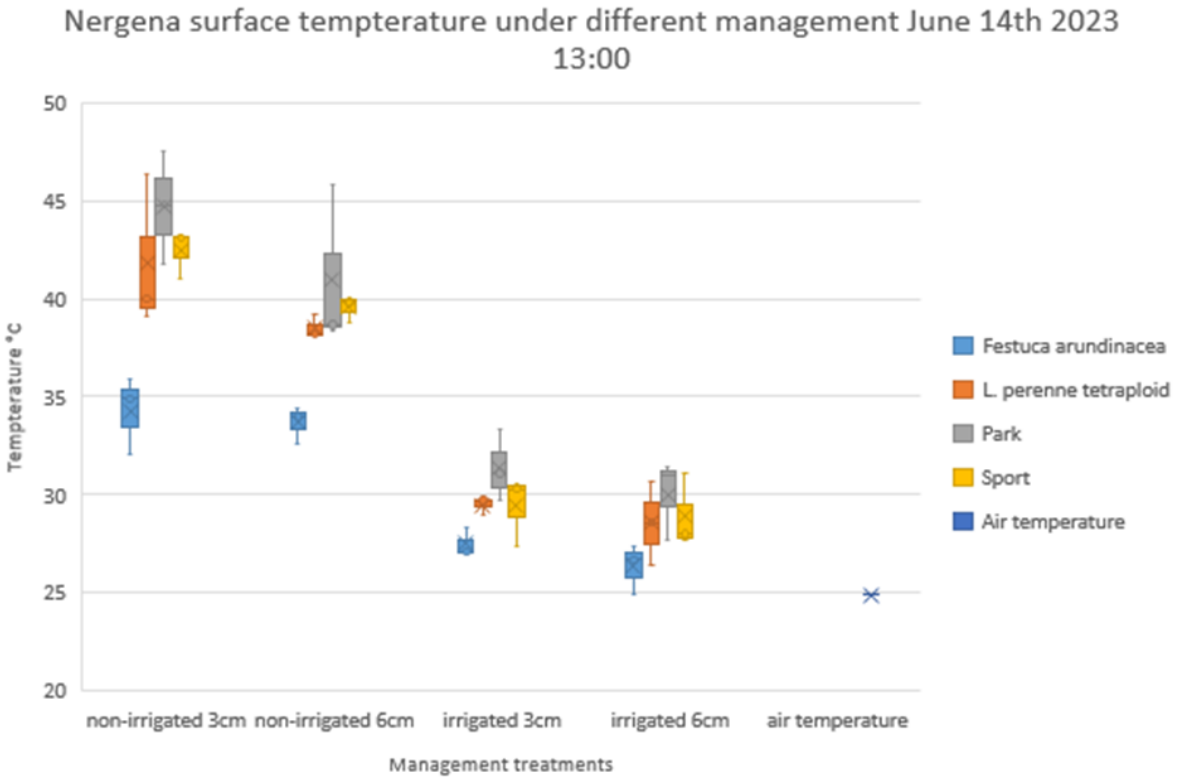

Figure 7.10: Nergena June 14, 2023, 1:00 PM - surface temperature of grass surfaces under different treatments. On the y-axis the surface temperature of the measured plots and the air temperature is displayed. On the x-axis the treatments are displayed (dry plots are referred to as 'non-irrigated'). Each box resembles a combination of three plots.

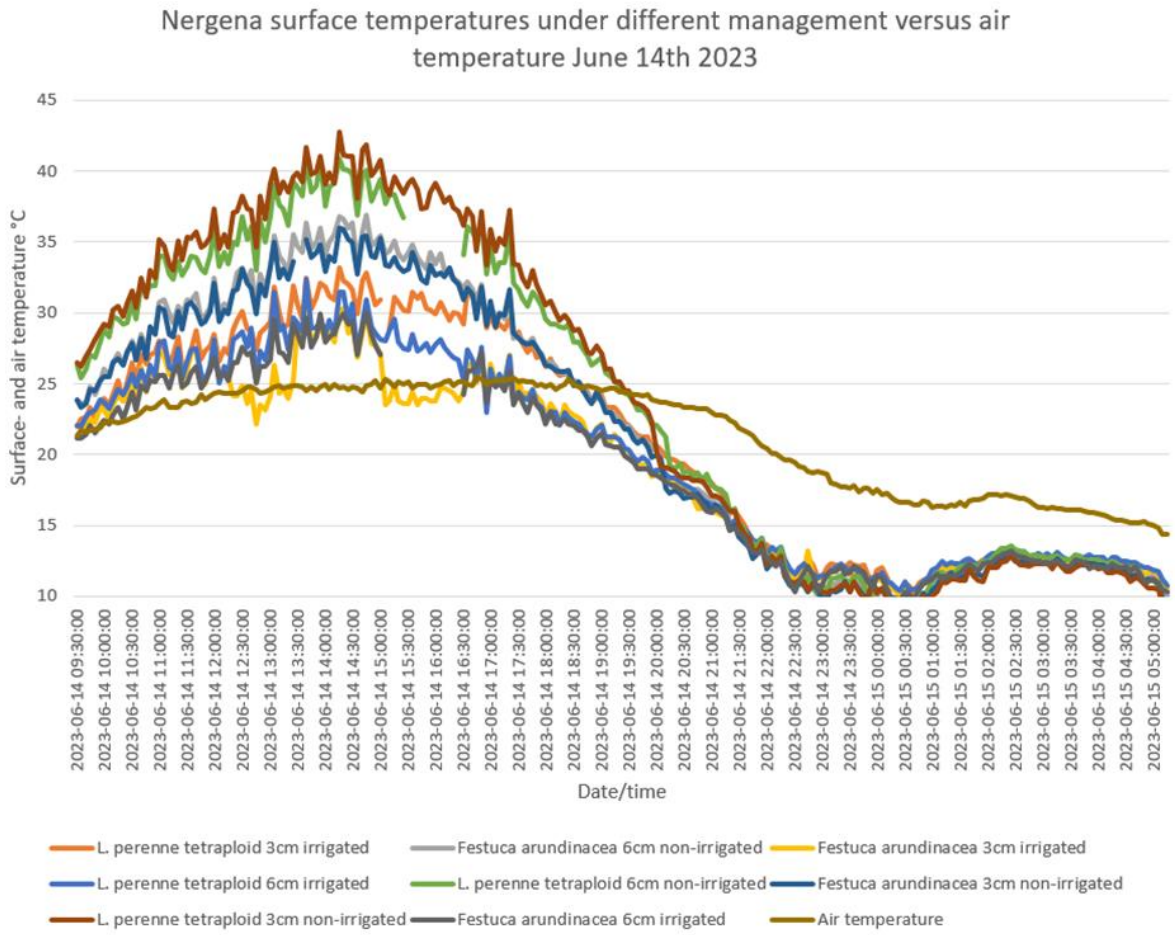

Figure 7.11: Nergena June 14, 2023 – 24-hour cycle surface temperature of grass surfaces under different treatments versus air temperature. On the y-axis, the surface temperature of the measured surfaces is displayed. On the x-axis, the date and time of measurements are displayed. Each line resembles one plot and line colours are explained in the legend below the graph.

7.4 DGCI and cover percentage

From May 17, 2023, the average DGCI starts to decrease for several genotypes with the 3 cm cutting height under dry condition (Fig. 7.12). Poa pratensis, becomes a lot less green and average DGCI dips slightly after June 14. On June 14, the combination of heat and drought was most extreme, as 0 mm of precipitation had fallen in the previous period of 33 days, and on the day itself it was +25°C. Festuca brevipila, sport mixture, park mixture and Lolium perenne diploid also show a downward trend until June 14, while Lolium perenne tetraploid and especially Festuca arundinacea, remained relatively green. After the precipitation (which started on June 17), the DGCI rebounded for all genotypes. For the 3 cm cutting height, irrigated plots were also less green in the period without rainfall (half May until half June) than in the period after the first precipitation occurred (mention date). For cover % 3cm cutting height dry treatment, Festuca arundinacea performed best. The cover % remained highest during the long period without rainfall (lowest value 68%). Poa pratensis dropped to 34% canopy cover % and for the other genotypes it was to around 50%. All 12 mixtures and 8 monocultures have been observed and analysed in the Turfanalyzer program, but only a selection with quite diverse species and mixtures has been included in the graphs below to ensure that the figures do not become too confusing. The 3 cm irrigated plots show that the canopy

cover % was stably high at the same level for all genotypes. Only in the dry period are some deviations visible, especially for Hard Fescue, which was lower than the genotypes for a period.

Figure 7.13 shows the 6 cm cutting height turf grass response and the patterns are consistent with Figure 7.12 Tall fescue scores highest under dry conditions, followed by tetraploid ryegrass. Poa pratensis dips lowest in DGCI and canopy cover %. Under irrigated conditions and with a cutting height of 6 cm, it is striking that Festuca brevipila shows a lower canopy cover % than the other genotypes when irrigated during the period without rainfall.

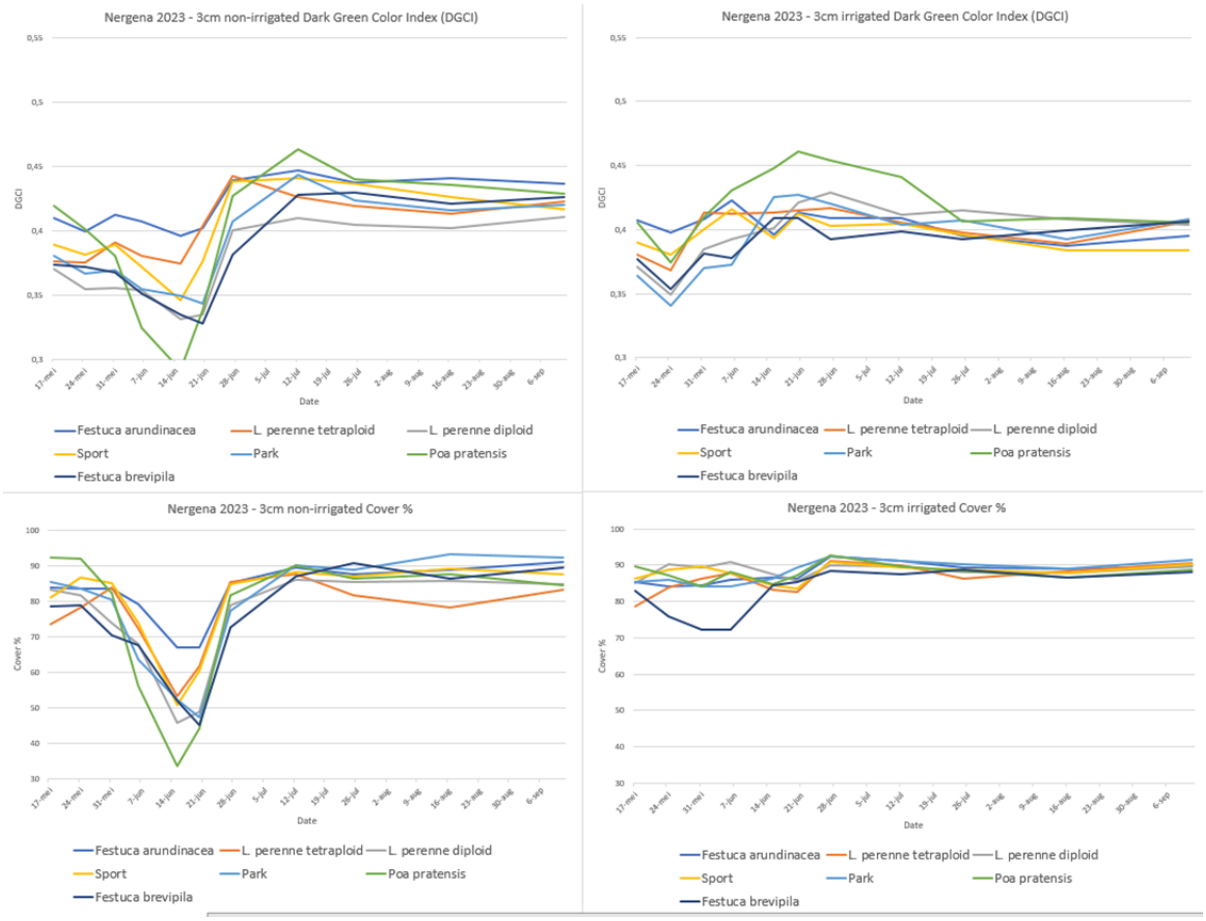

Figure 7.12: DGCI and Cover % 2023 3cm cutting height. On the y-axis, either Cover % or Dark Green Colour Index (DGCI) is displayed. On the x-axis, date of measurement is displayed. Measurements were performed once per week on average. Each line resembles a minimum of 3 plots and line colours are explained in the legend below the graph.

The year 2022 was dry for much longer and a lot warmer than 2023. Figures 7.14 and 7.15 therefore show a different progression over time than the previous Figures 7.12 and 7.13. The drought started in 2022 after July 25 and lasted until 8 September. Roughly halfway through this warm, dry period (after August 10) there was a short-wet period, which is also reflected in the graphs (Fig 7.14, 7.15). Poa pratensis also appears to have suffered most from the drought in 2022. Festuca arundinacea dipped around 69 soil cover %, while hard fescue also seemed to do well with a dip of up to 59%. The latter is striking because Festuca brevipila had an average low DGCI on the 3 cm cutting height. For DGCI, Festuca arundinacea showed the most greenness, followed by Lolium perenne tetraploid. The turf grass genotypes were revived during the short-wet period around mid-August, both in DGCI and in canopy cover %. It is striking that after the long dry and warm period there is a recovery in canopy cover % (although not completely), but that in terms of DGCI the genotypes no longer come close to the levels before the

dry, warm period. 7,15b shows an time-series of plot 1 with sport mixture. All 240 plots have been imaged in this way troughout the growing seasons 2022 and 2023.

Figure 7.13: DGCI and Cover % 2023 6cm cutting height. On the y-axis, either Cover % or Dark Green Colour Index (DGCI) is displayed. On the x-axis, date of measurement is displayed. Measurements were performed once per week on average. Each line resembles a minimum of 3 plots and line colours are explained in the legend below the graph.

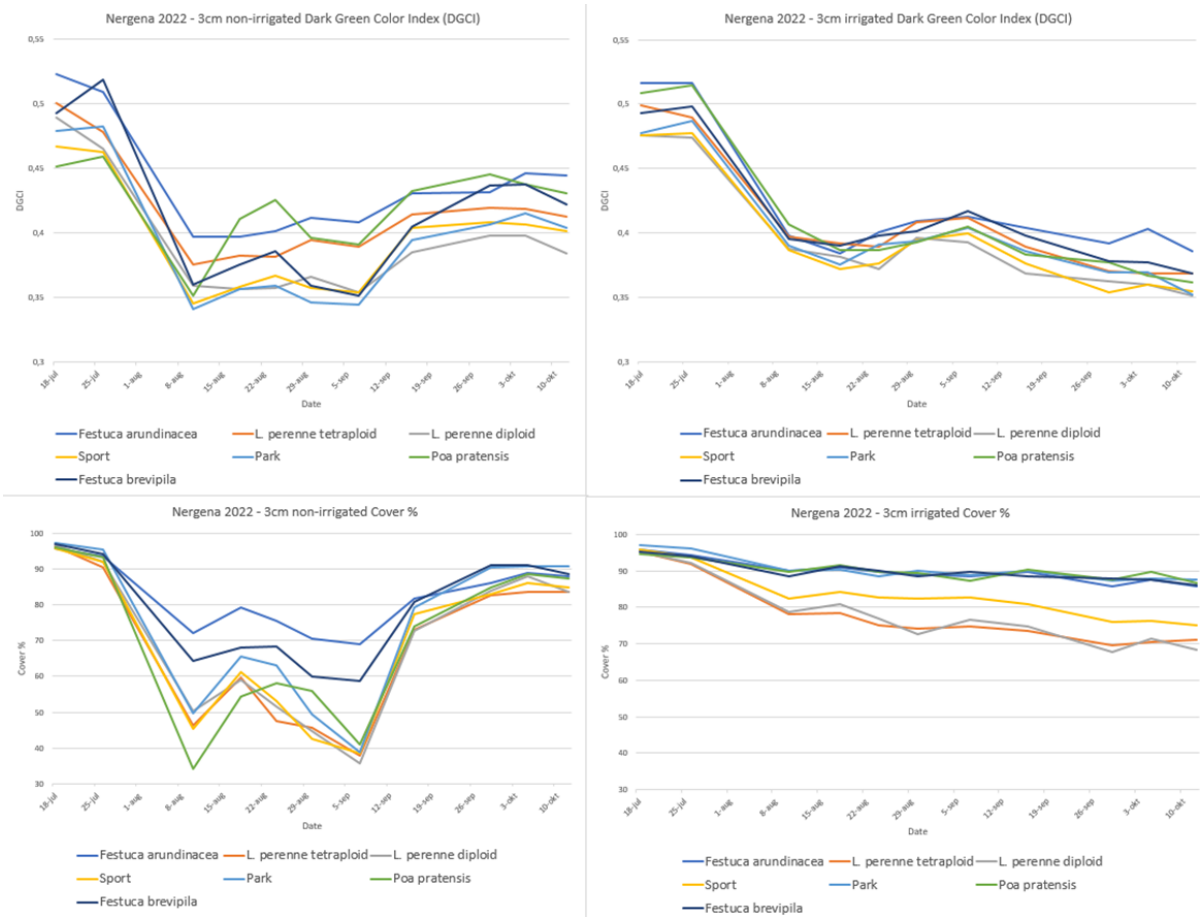

Figure 7.14: DGCI and Cover % 2022 3cm cutting height. On the y-axis, either Cover % or Dark Green Colour Index (DGCI) is displayed. On the x-axis, date of measurement is displayed. Measurements were performed once per week on average. Each line resembles a minimum of 3 plots and line colours are explained in the legend below the graph.

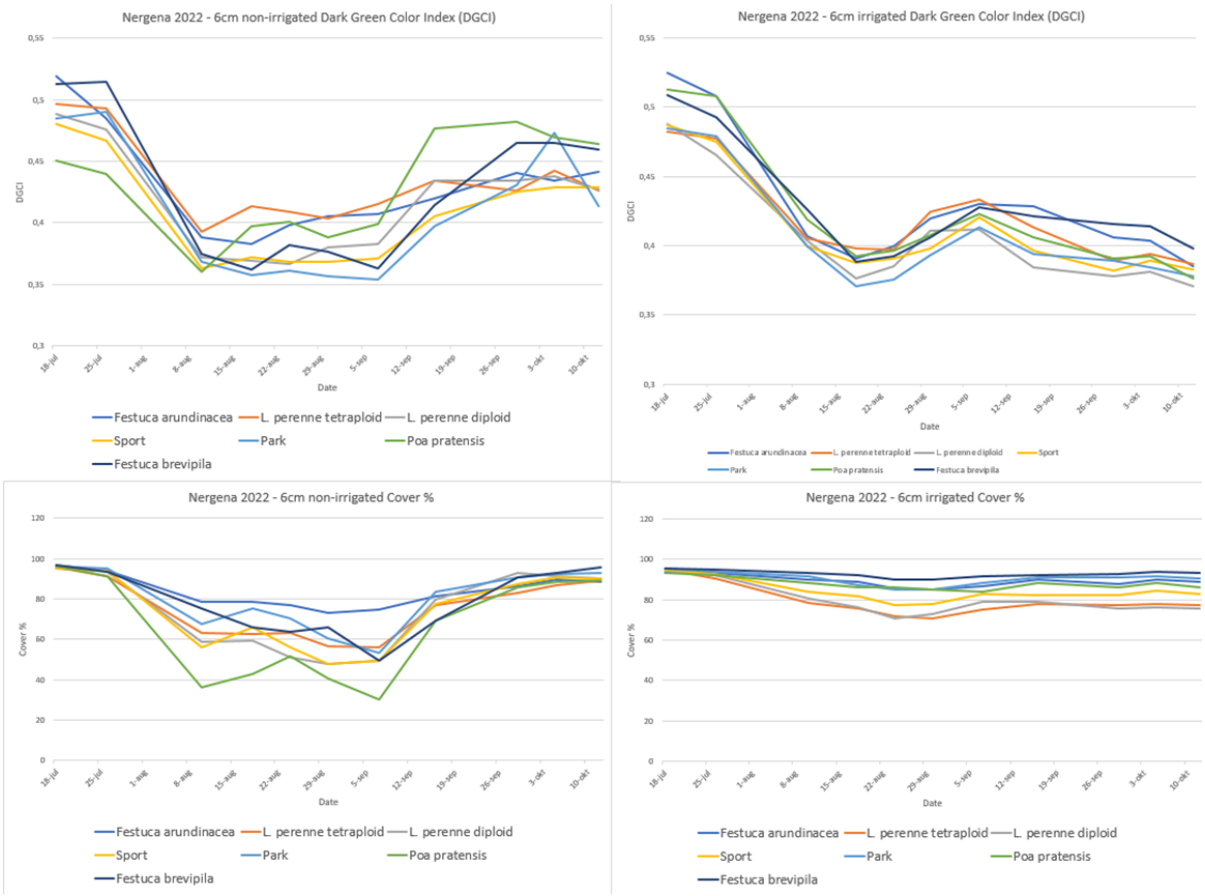

Figure 7.15: DGCI and Cover % 2022 6cm cutting height. On the y-axis, either Cover % or Dark Green Colour Index (DGCI) is displayed. On the x-axis, date of measurement is displayed. Measurements were performed once per week on average. Each line resembles a minimum of 3 plots and line colours are explained in the legend below the graph.

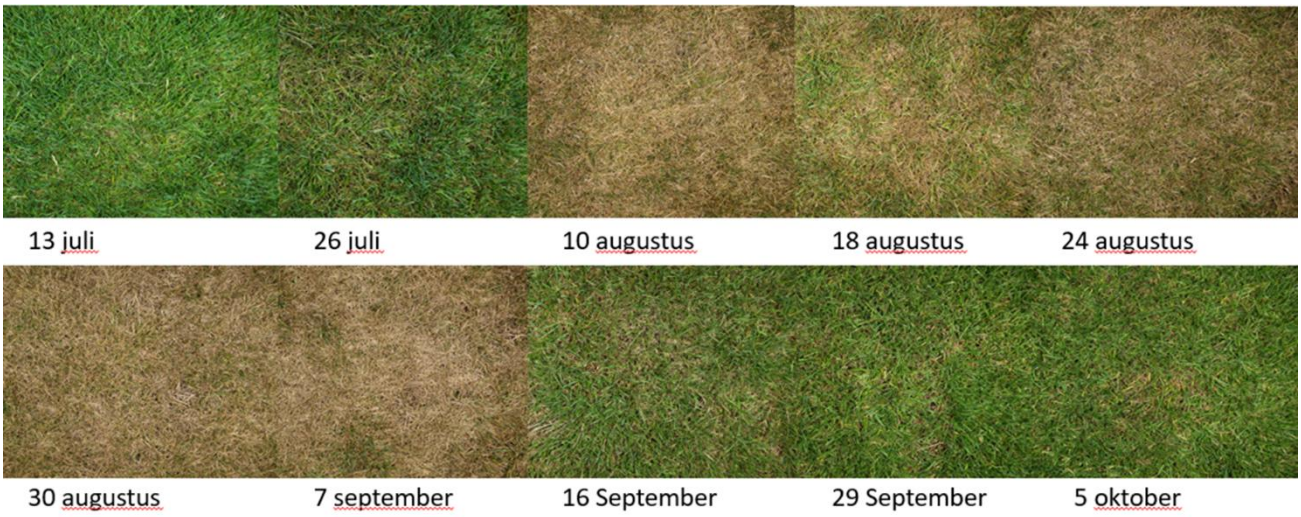

Figure 7.15b: Example of time series DGCI and Canopy cover imaging. Plot 1 sport mixture Nergena 13 July – 5 October 2022

7.5 Sports centre de Bongerd

On September 6th, 2021, measurements have been performed on sports centre the bongerd using a complete weather station, IR thermal imaging camera. Soil moisture and soil temperature readings have been taken as well. Measurements were taken between 11:30 AM and 4:00 PM, with measurements taken around 12:00 PM on the WUR campus, and then around 3:00 PM at a park and adjacent parking lot (Ireneveld/ Koekoek Vaassen). Figure 7.16 shows that the PET for artificial grass was on the borderline of 'moderate heat stress' and 'strong heat stress'. That was the highest PET measured on September 6. Remarkably, the lowest PET values were found for the parking lot at De Bongerd sports park and the lawn at the park, observed as 'low heat stress'. The parking lot has a low PET value due to the relatively high wind speed, while the surface temperature was also relatively low. The parking lot at the park on the other hand, scored 'moderate heat stress'.

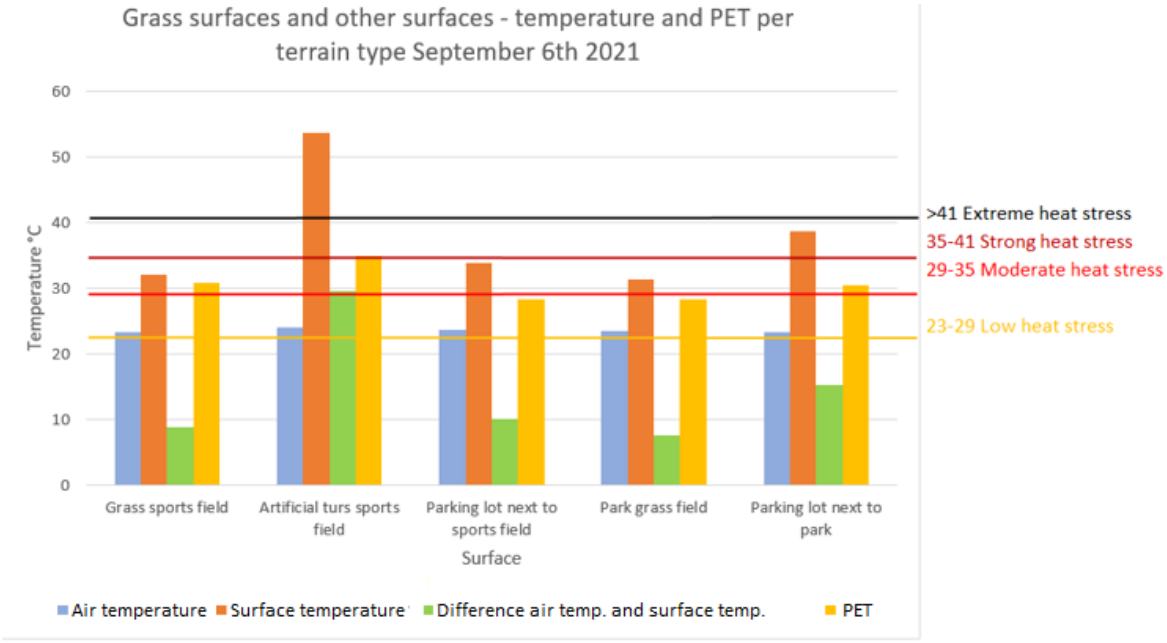

Figure 7.16: PET for different surfaces, September 6, 2021. On the y-axis, the calculated PET for the measured plots is displayed as well as the air temperature in °C. On the x-axis the measured surfaces are explained.

Measurements on sports field with irrigated turf grass, and dry areas, artificial grass field and parking lot were performed on August 11, 2022, between 9 a.m. and 4 p.m. The air temperature reached 31.8°C late in the afternoon (~ 3 p/m.) on paved surfaces (artificial grass and parking lot) while above the grass it remained at 30.5°C. As can be seen in Figure 7.18, the air temperature was structurally approximately 1°C higher on paved surfaces than above grass. At 9.30 a.m., the surface temperature for artificial grass was already 43°C while the surface of the parking lot was 30°C and the turf grass was 25°C. At 1 p.m., the artificial turf peaked at a surface temperature of 67°C, while the parking lot was 44°C and the grass was 35°C. Late in the afternoon (when the air temperature peaked) the surface of the artificial grass was 65°C, the parking lot was 48°C, the non-irrigated grass (with 5% VWC soil) was 39°Cand the irrigated grass (this grass had been irrigated the previous day and had a soil moisture percentage of 15% VWC) 32°C (Fig. 7.17).

From the collected data, the PET was calculated with RayMan Pro software (Matzarakis et al. 2007; Matzarakis et al. 2010; Matzarakis et al. 2018; Matzarakis et al. 2021; Fröhlich et al. 2019). At 9.30 a.m. the PET over grass was

in the 'low heat stress' range. The parking lot and the artificial grass were already experiencing 'moderate heat stress'. From 12 noon there was 'extreme heat stress' on artificial grass. The highest classification for PET. There was a moment of 'extreme heat stress' in the parking lot at 3.00 p.m., but there was 'strong heat stress' for most of the afternoon. The grass reached 'strong heat stress' in the afternoon. While irrigated turf grass often remained low in the 'strong heat stress' range, the turf grass under dry conditions was on average somewhat higher in the same range. There was never 'extreme heat stress' above the grass.

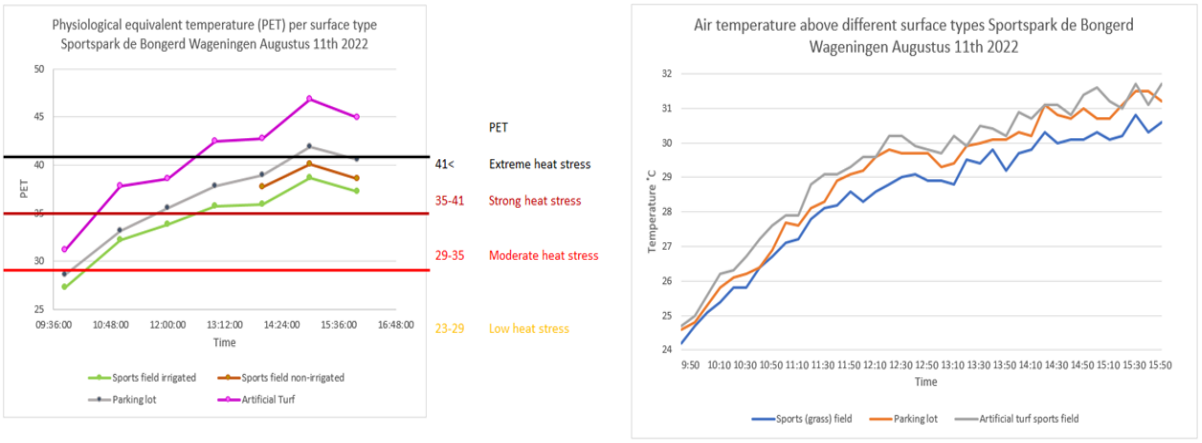

Figure 7.17: Calculated PET (left graph) and measured air temperature (right graph) above different surfaces of the De Bongerd sports complex, during different times on the day of August 11, 2022. On the y-axis, either calculated PET is displayed or measured air temperature. On the x-axis, time of day during the measurement day is displayed. In the legends below the graphs, measurement location/surface is explained.

7.6 Skatepark Zutphen biodiverse grass fields

On June 15, 2022, the air temperature was a maximum of 24.5°C degrees and the soil moisture content were around 8% on all plots. Both the biodiverse turf grass and park mixture were still mostly green in colour. The biodiverse turf grass was about 50 cm high while the short park grass was about 3 cm high. Measurements showed that biodiverse grass was on average cooler than park mixture (Fig. 7.18) and that the concrete on the skate park was not much warmer than the short park grass. The surface temperature of biodiverse grass is more difficult to measure than short grass, as longer grass moves more, and it is virtually impossible to maintain a fixed distance between sensors and canopy for all measurements.

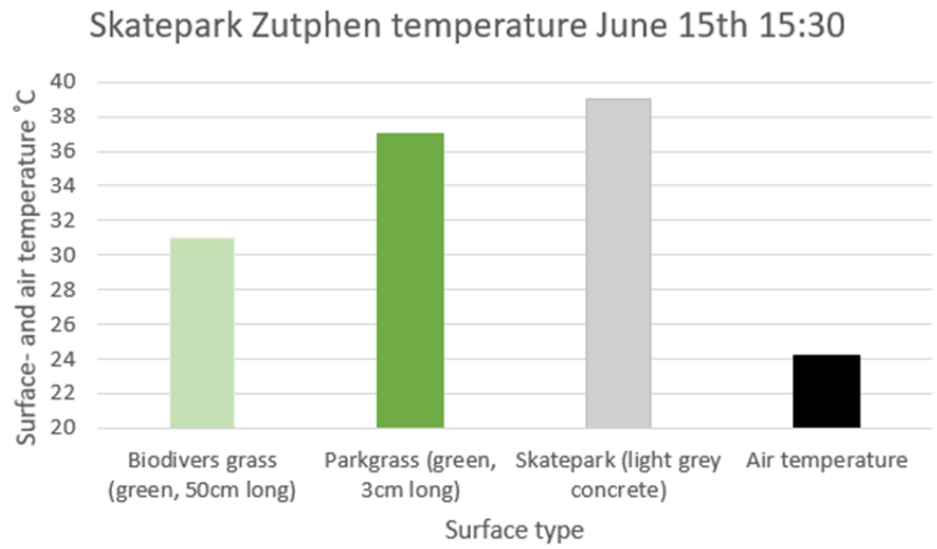

Figure 7.18: Surface temperature of various surfaces of Zutphen skate park June 15, 2022. On the y-axis, surface temperature of each measured surface is displayed as well as air temperature. On the x-axis, measured surface is explained.

On August 10, 2022, the air temperature was a maximum of 29.3°C and the soil moisture content was around 2 to 3% on all plots so it was a hot and very dry day. Both the biodiverse grass and the park grass were predominantly yellow in colour. Apart from broadleaf herbs, which were largely represented in some plots. The biodiverse grass was about 50 cm high while the park grass was about 3 cm high. Measurements showed that biodiverse grasses were much warmer than the measurements taken on June 15 (Fig. 7.18, 7.19). Interestingly, concrete was in many cases even cooler than the surface of desiccated grasses, although the surface temperature of the desiccated grasses was difficult to measure (Fig. 7.19). Broadleaf herbs could be between 20 to -30 °C cooler than dried grass, which was about 10 to 20 °C cooler than concrete.

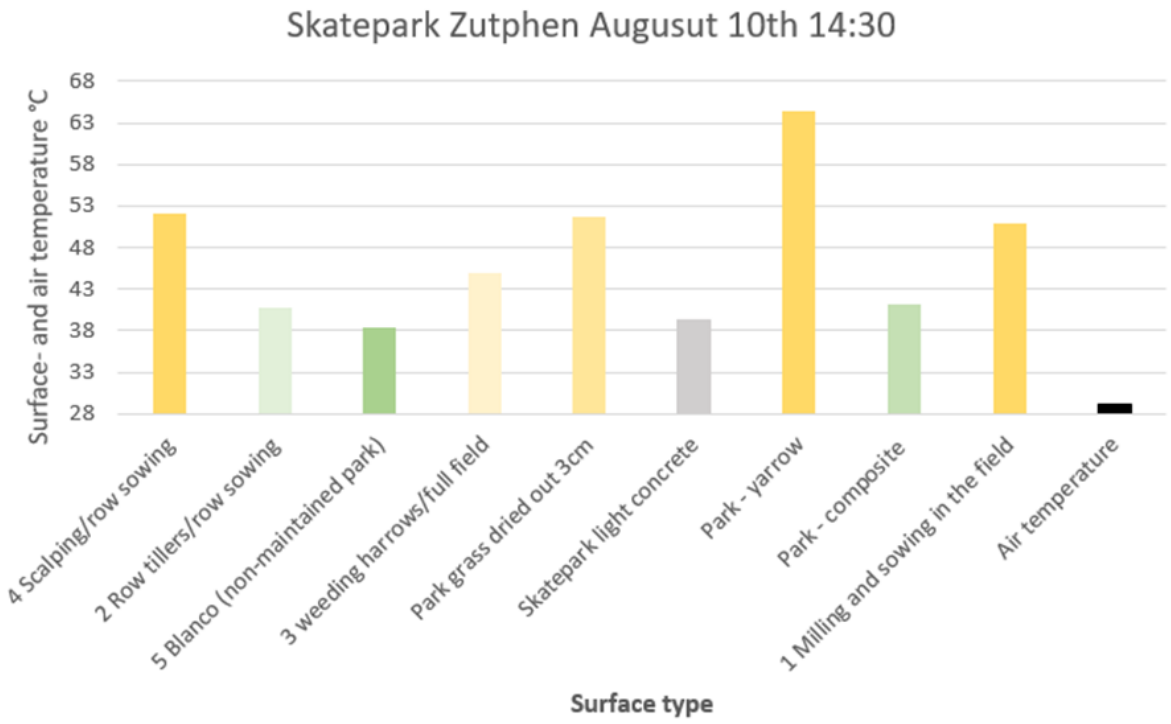

Figure 7.19: Surface temperatures of Zutphen skate park trial location August 10, 2022. On the y-axis, surface temperature of each measured surface is displayed as well as air temperature. On the x-axis, measured surface (including treatment if applicable) is explained.

7.7 Root research on Nergena experimental site

A simple model to understand the differences between the root system of the two genotypes was used and the results are summarised. Firstly, there is a difference in root biomass (total) between irrigated and dry conditions where less root biomass occurs the turf grass is irrigated, both in Lolium perenne tetraploid and in Festuca arundinacea.

Secondly, there is less root biomass in the deeper layers 5 – 10 cm and 10 – 20 cm than in the top layer 0 – 5 cm, both in irrigated and dry conditions and for and both genotypes. Another point is that Lolium perenne tetraploid has slightly less root biomass than Festuca arundinacea on average independent of the condition and soil depths. In addition, Lolium perenne tetraploid has slightly more root biomass than Festuca arundinacea under dry conditions only.

8. Discussion and Conclusions

Conclusions Nergena measurements

- Turf grass was consistently cooler than paved surfaces, especially during the hottest part of the day, and remained cool in the evening and night. For further research, it would be interesting to conduct research into different types of artificial grass (hybrid grass?) and paved surfaces such as grass tiles, to see what the differences are. Methodologically, more use can be made of remote sensing, as was also evident in the joint measurements with work package 1.
- Mowing height did not seem to have an influence on surface temperature, but irrigation had a structural influence on the surface temperature of grass. The difference increased as the colour difference between the irrigated and dry treatments increased due to a long-term soil moisture percentage of around 5%
- Dry grass could be between 5 and 25 degrees warmer than irrigated grass, while Festuca arundinacea and sometimes also Lolium perenne tetraploid was often significantly cooler than grass mixtures Sport and Park mixture.
- Within the irrigated treatments, Festuca arundinacea was in some cases cooler than other grass surfaces.
- For follow-up research, it is highly advisable to look at different cultivars within species, as drought and heat tolerance are properties for which further selection is and can be made. Perhaps the contribution to the cooling effect can be increased by using the same species, but with the most climate-resistant varieties. Remote sensing can also contribute to this research. A very useful addition for measuring the cooling effect of grass under different management would also be measuring current evaporation.

Conclusions DGCI and Cover %

- In **2023**, Poa pratensis became a lot less green after the drought started from mid-May and DGCI dips slightly after June 14. The combination of heat and drought was most extreme on June 14. Almost all species experienced a large drop in DGCI. Festuca arundinacea the drop was least apparent, followed by Lolium perenne tetraploid.
- After the first precipitation (which started on June 17), the DGCI rebounded for all surfaces quickly. With 3 cm of irrigation, the irrigated part was also less green in the dry period than in the period after the first precipitation had fallen again.
- For cover % at 3cm no irrigation, it can once again be seen that Festuca arundinacea performed best. The cover % remained highest during the long dry period (lowest value 68%). Poa pratensis dropped to 34% canopy cover % and the other species to around 50%. The 3cm irrigation graph shows that the canopy cover % was stably high at the same level for all species and mixtures. Only in the dry period are some deviations visible, especially for Festuca brevipila, which was lower than the other species and mixtures for a period.
- For the 6cm cutting height treatments, Festuca arundinacea scores highest when not irrigated, followed by Lolium perenne tetraploid. Poa pratensis dips lowest in DGCI and canopy cover %. When irrigated at

a cutting height of 6 cm, it is striking that Festuca brevipila shows a lower canopy cover % than the other species and mixtures when irrigated in the (extremely) dry period, although the difference is less significant than with the 3 cm irrigation treatment.

- In **2022**, Poa pratensis appears to have suffered most from the drought. Festuca arundinacea dipped around 69 canopy cover% in 2022, while Festuca brevipila also seemed to do well with a dip to 59%. The latter is striking because Festuca brevipila had a relatively low DGCI on average with the 3cm treatments. For DGCI, Festuca arundinacea showed the most greenness, followed by t Lolium perenne tetraploid. Poa pratensis bluegrass recovered greatly in 2022 during the short-wet period around mid-August, both in DGCI and in canopy cover %. It is striking that after the long dry and warm period there is a recovery in canopy cover % (although not completely), but that in terms of DGCI the species and mixtures no longer come close to the levels before the dry, warm period.
- In general, the monocultures of Festuca rubra, Poa pratensis and mixtures with r Festuca rubra and Poa pratensis appeared to be the most sensitive to persistent dry and warm periods in terms of DGCI and Canopy Cover %. Monocultures of Festuca arundinacea had on average the highest DGCI and Cover %. Mixtures with Festuca arundinacea and Lolium perenne tetraploid were also greener on average and had a relatively high Cover % in non-irrigated treatments.

Discussion measurements Nergena

- Statements made about the differences between grass species are based on 1 variety per species. Because there are 2 treatments (irrigation/no irrigation and 3cm/6cm mowing height), and this was done for 12 monocultures and 4 mixtures, there was no room to include multiple varieties per species in the research design. There are already 240 individual objects in the current field. With 3 varieties per species this would be 720. To be able to construct, maintain and continuously measure such several plots would also require three times the costs and time investment, which would not be realistic. For follow-up research, it is good to measure different varieties, such as CGO test fields of the partners where there are already different varieties per species. The condition is that there is also room to withhold irrigation from part of the plots (for example at the end of a test) so that a comparison of irrigation/no irrigation can be made.
- Greenness and surface temperature are good indicators of the degree of (potential) evaporation within a grass vegetation. However, it is much better (albeit more time-consuming) to also take actual evapotranspiration measurements on grass surfaces that are and are not irrigated. Measured surface temperature only says something directly about the top observed leaf layer and not about the leaf layers below it, which can also contribute to a cooling effect. Current evapotranspiration and CO2 exchange measurements are also very interesting to perform on grass surfaces with different cutting heights. In this way, data can be collected that shows more directly the extent to which the grass evaporates. Combined with CO2 exchange, photosynthetic capacity can also be monitored.

Possibilities for further research

- Research on multiple varieties within a species. To what extent is there variation between varieties when looking at the (potential) cooling effect?
- Research into current evaporation and CO2 exchange/photosynthesis capacity of grass surfaces under different treatments (irrigation/no irrigation, 3cm/6cm cutting height).

Conclusions measurements of De Bongerd sports complex WUR campus and park + parking lot

- Both air temperature and surface temperature appeared to be lower for grass surfaces than for paved surfaces. Both parameters are important drivers for the PET index. Because the air temperature and especially the surface temperature is higher on paved surfaces in the afternoon than on grass, the PET is also (much) higher on the measured paved surfaces. During the measurements it turned out that the more extreme the heat, the greater the difference between the surfaces.

Discussion measurements of De Bongerd sports complex WUR campus and park + parking lot

- There are many variants of artificial grass that differ in colour, height of the artificial grass blades, granules/no granules, etc. This also applies to the paved surface of parking lots, which also differ in color.
- The air temperature can also be influenced by trees or other objects around the site. Although the measured objects are not representative of all comparable objects, the measured objects are a rather normal reflection of what is seen as 'sports field', 'park', 'artificial grass field', 'parking lot'. It is possible to repeat the same experiment again at a different location with similar but slightly different surfaces. Possibilities for further research
- Research on hybrid artificial grass fields, parking lots with hybrid tiles (tiles with spaces in between where grass grows)

Conclusions measurements on biodiverse grasslands and comparison with paved surface, short mown park grass

- When there was green (evaporating) vegetation, biodiverse grass appeared to be cooler than other surfaces, although surface temperature of biodiverse grass is more difficult to measure with field measurements close to the canopy. During drought, the broadleaf and green herbs turned out to be a lot cooler than other, often yellow vegetation. The short park grass became very warm as it turned from green to yellow and became even warmer than the light concrete of the skate park.

Discussion measurements on biodiverse grasslands and compare with paved surface, short-mown park grass

- Although a high-resolution thermal camera can clearly see which individual species, vegetation compositions and vegetation states (parched or green) are cool or warm, it is difficult to make statements about an entire plot because the variation within a plot is very can be big. The variation within plots also appears to be extra-large in the transition from sufficient soil moisture to low soil moisture contents. This may be due to the wide variety of species, some of which can root (very) deeply and others not at all or less, so that the water that a plant needs to evaporate remains available for a long time for some species and not for others.
- To take surface temperature measurements on biodiverse grasslands, it is advisable to measure from a greater distance above the 'surface' than +/- 1 meter above ground level as is currently done. This is because there are height differences in vegetation within biodiverse grasslands and the canopy can move even with small amounts of wind, so measurements are not always the average of the same parts of leaf area within a plot. This makes time-series measurements over a day with multiple measurements at fixed points more difficult to compare.
- Measurements from higher above the plots such as drone imaging can provide a solution to these problems, because averages can then be calculated for an entire plot, making variation within plots less important, and reducing the problem of moving leaves.

Possibilities for further research

• Drone imaging surface temperature biodiverse grass plots in addition to manual measurements taken closer to the canopy.

Financial Source

This project (project number BO-60-003-002) was funded by a public-private partnership (PPP)/ publiek-private Samenwerking (PPS) between the Ministry of Agriculture, Nature and Food Quality (LNV: Ministerie van Landbouw, Natuur en Voedselkwaliteit), and a consortium of several parties from the grass seed breeding industry (Plantum and its members DLF, DSV zaden Nederland BV, Barenbrug and Limagrain), the Branchevereniging Sport en Cultuurtechniek (BSC) and the Nederlandse Golf Federatie (NGF). Implementation of the project performed by Wageningen Plant Research, Wageningen Environmental Research and Wageningen University.

References

Alhaithloul HAS (2019) Impact of Combined Heat and Drought Stress on the Potential Growth Responses of the Desert Grass Artemisia sieberi alba: Relation to Biochemical and Molecular Adaptation. Plants 8:416. https://doi.org/10.3390/plants8100416

Amani-Beni M, Zhang B, Xie G, Xu J (2018) Impact of urban park's tree, grass and waterbody on microclimate in hot summer days: A case study of Olympic Park in Beijing, China. Urban Forestry & Urban Greening. https://doi.org/10.1016/j.ufug.2018.03.016

Armson D, Stringer P, Ennos AR (2012) The effect of ree shade and grass on surface and globe temperatures in an urban area. Urban Forestry & Urban Greening. https://doi.org/10.1016/j.ufug.2012.05.002

Chandramaty I, Kitchley JL (2018) Study and analysis of efficient green cover types for mitigating the air temperature and urban heat island effect. International Journal of Global Warming. https://doi.org/10.1504/IJGW.2018.090182

Connors JP, Galetti CS, Chow WTL (2012) Landscape configuration and urban heat island effects: assessing the relationship between landscape characteristics and land surface temperature in Phoenix, Arizona. Landscape Ecology. https://doi.org/10.1007/s10980-012-9833-1

Fahad S, Bajwa AA, Nazir U, et al (2017) Crop production under drought and heat stress: Plant responses and management options. FrontPlant Sci 8:1147. https://doi.org/10.3389/fpls.2017.01147

Fröhlich D, Gangwisch M, Matzarakis A, (2019) Effect of radiation and wind on thermal comfort in urban environments - Application of the RayMan and SkyHelios model. Urban Climate 27, 1-7

Gatto E, Buccolieri R, Aarrevaara E, Ippolito F, Emmanuel R, Perronace L, Santiago JL (2020) Impact of Urban Vegetation on Outdoor Thermal Comfort: Comparison between a Mediterranean City (Lecce, Italy) and a Northern European City (Lahti, Finland). Forests. https://doi.org/10.3390/f11020228

Hartl FU, Bracher A, Hayer-Hartl M (2011) Molecular chaperones in protein folding and proteostasis. Nature 475:324–332

Hermanns F, Pohl F, Rebmann C, et al (2021) Inferring grassland drought stress with unsupervised learning from airborne hyperspectral VNIR imagery. Remote Sens (Basel) 13:1885. https://doi.org/10.3390/rs13101885

Hu L, Wang Z, Du H, Huang B (2010) Differential accumulation of dehydrins in response to water stress for hybrid and common bermudagrass genotypes differing in drought tolerance. J Plant Physiol 167:103–109. https://doi.org/10.1016/j.jplph.2009.07.008

Jiang Y, Huang B (2002) Protein alterations in tall fescue in response to drought stress and abscisic acid. Crop Sci 42:202–207. https://doi.org/10.2135/cropsci2002.2020

Jim CY (2016) Solar–terrestrial radiant-energy regimes and temperature anomalies of natural and artificial turfs. Applied Energy. https://doi.org/10.1016/j.apenergy.2016.04.072\

KNMI, 2023

Kolukisaoglu U (2004) Calcium Sensors and Their Interacting Protein Kinases: Genomics of the Arabidopsis and Rice CBL-CIPK Signaling Networks. Plant Physiol 134:43–58. https://doi.org/10.1104/pp.103.033068

Lee S, Park S, Woo J, Lee D, Baik J (2016) Impacts of in-canyon vegetation and canyon aspect ratio on the thermal environment of street canyons: numerical investigation using a coupled WRF-VUCM model. Journal of the Royal Metereological Society. https://doi.org/10.1002/qj.2847

Matzarakis, A., Rutz, F., Mayer, H., 2007: Modelling Radiation fluxes in simple and complex environments - Application of the RayMan model. International Journal of Biometeorology 51, 323-334

Matzarakis, A., Rutz, F., Mayer, H., 2010: Modelling Radiation fluxes in simple and complex environments - Basics of the RayMan model. International Journal of Biometeorology 54, 131-139

Matzarakis, A., Fröhlich, D. 2018: Influence of urban green on human thermal bioclimate - application of thermal indices and micro-scale models. Acta Horticul. 1215, 1-9. Doi: 10.17660/Acta Hortic.2018.215.1

Matzarakis, A., Gangwisch, M., Fröhlich, D., 2021: RayMan and SkyHelios Model. In: Palme, M., Salvati,A. (eds) Urban Microclimate Modelling for Comfort and Energy Studies. Springer, Cham., 339-361

Rahman MA, Woo JH, Song Y, et al (2022) Heat Shock Proteins and Antioxidant Genes Involved in Heat Combined with Drought Stress Responses in Perennial Rye Grass. Life 12:1426. https://doi.org/10.3390/life12091426

Shariatipour N, Heidari B, Shams Z, Richards C (2022) Assessing the potential of native ecotypes of Poa pratensis L. for forage yield and phytochemical compositions under water deficit conditions. Sci Rep 12:1121. https://doi.org/10.1038/s41598-022-05024-1

Shashua-Bar L, Pearlmutter D, Erell E (2009) The cooling efficiency of urban landscape strategies in a hot dry climate. Landscape and Urban Planning. https://doi.org/10.1016/j.landurbplan.2009.04.005

Taleb MH, Majidi MM, Pirnajmedin F, Maibody SAMM (2023) Plant functional trait responses to cope with drought in seven cool-season grasses. Sci Rep 13:5285. https://doi.org/10.1038/s41598-023-31923-y

Théau J, Lauzier-Hudon É, Aubé L, Devillers N (2021) Estimation of forage biomass and vegetation cover in grasslands using UAV imagery. PLoS One 16:e0245784. https://doi.org/10.1371/journal.pone.0245784

Zhang A, Hu S, Zhang X, et al (2021) A handheld grassland vegetation monitoring system based on multispectral imaging. Agriculture 11:1262. https://doi.org/10.3390/agriculture11121262

Annex 1: Main experimental turf grass field

The main experimental turf grass field was located on the Wageningen University and Research campus. The field was made up of individual big 4 x4 m plots or small 2 x 2 m plots. Plots either contained turf grass monocultures or in some cases, mixtures of turf grasses.

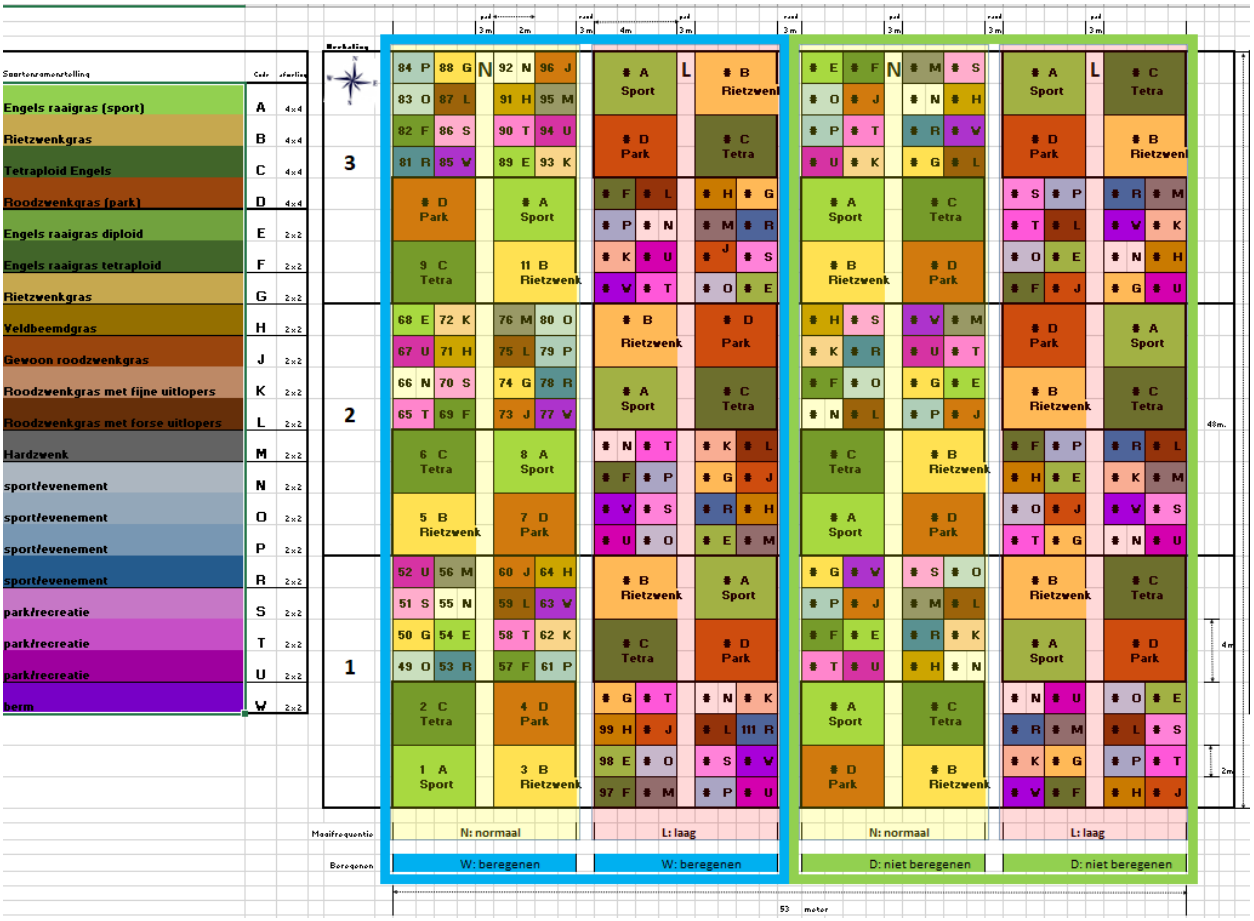

Map of turf grass field located in UNIFARM greenhouse Nergena, Wageningen University and Research.

Composition of individual turf grass plots based on codes A to W.

Big plots (4 x 4 m)	**Variety**	**Vesuvius**	**Fabian**	**Baraline**	**Dakisha**	**EuroCarina**	**Barpearl**	**Laverda**	**Hardtop**
Monocultures	**Code**	**Lp di**	**Lp te**	**Fa**	**Pp**	**Frc**	**Frt**	**Frr**	**Fo**
***Lolium perenne* diploid**	A	50			50				
Festuca arundinacea	B			100					
***Lolium perenne* tetraploid**	C		100						
Festuca rubra	D	20			20	30	30		
Small plots (2 x 2 m)									
1. Monocultures	**Code**	**Lp di**	**Lp te**	**Fa**	**Pp**	**Frc**	**Frt**	**Frr**	**Fo**
***Lolium perenne* diploid**	E	100							
***Lolium perenne* tetraploid**	F		100						
Rietzwenkgras	G			100					
Poa pratensis	H				100				
Festuca rubra	J					100			
***Festuca rubra* trichophylla**	K						100		
***Festuca rubra* rubra**	L							100	
Hardzwenk	M								100
2. Mixtures	**Code**	**Lp di**	**Lp te**	**Fa**	**Pp**	**Frc**	**Frt**	**Frr**	**Fo**
sport mixture	N	50			50				
sport mixture	O		50		50				
sport mixture	P	50		50					
sport mixture	R			50	50				
park mixture	S	35			50		15		
park mixture	T	20		25	25	10	10	10	
park mixture	U	20			20	20	20	20	
berm	W					20	10	20	50

Annex 2: Other testing sites

Map of Sports centre de Bongerd WUR Campus, and Sportscentre de Koekoek Vaassen, with measurement locations highlighted with red numbers.

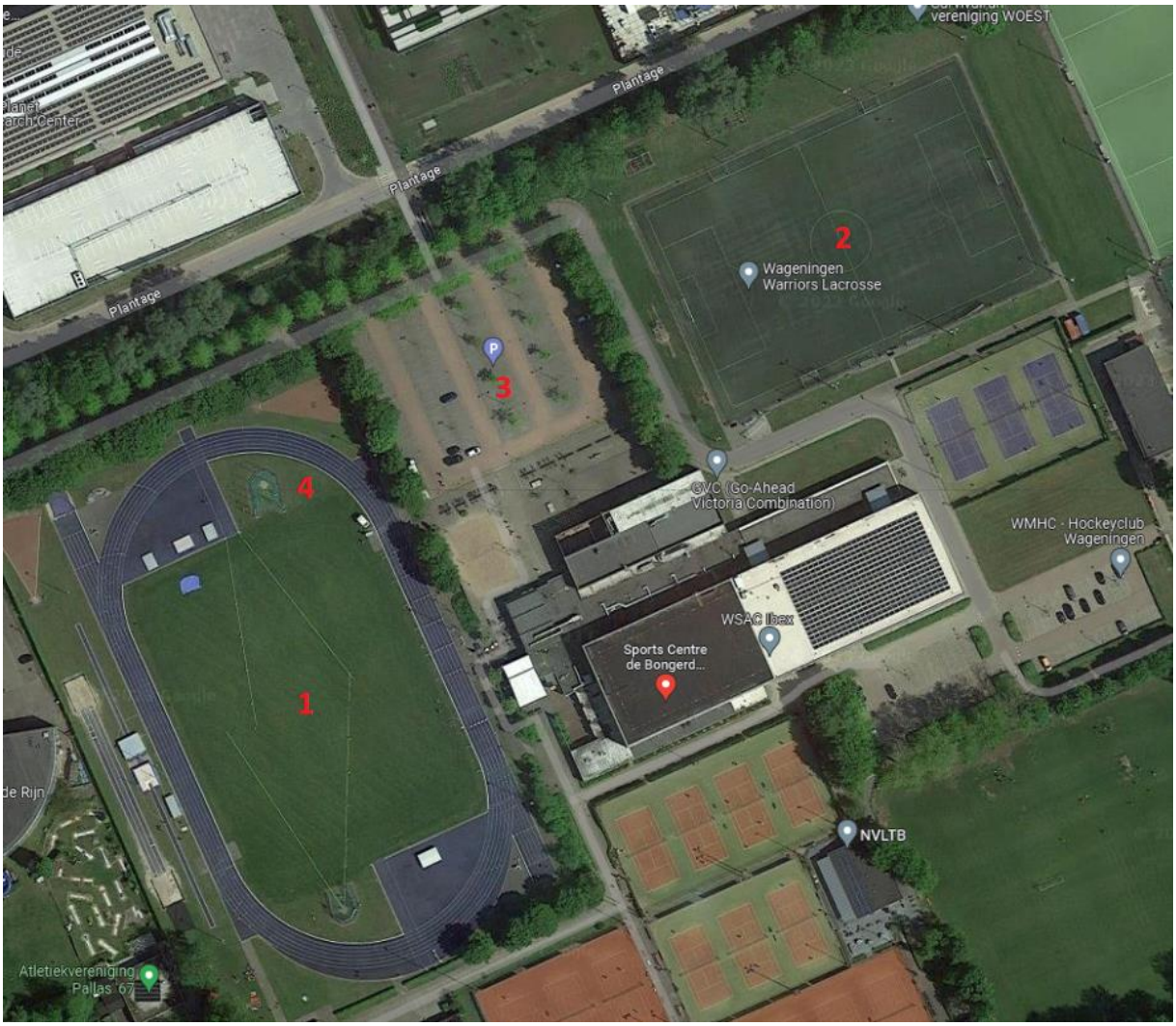

Sports centre de Bongerd

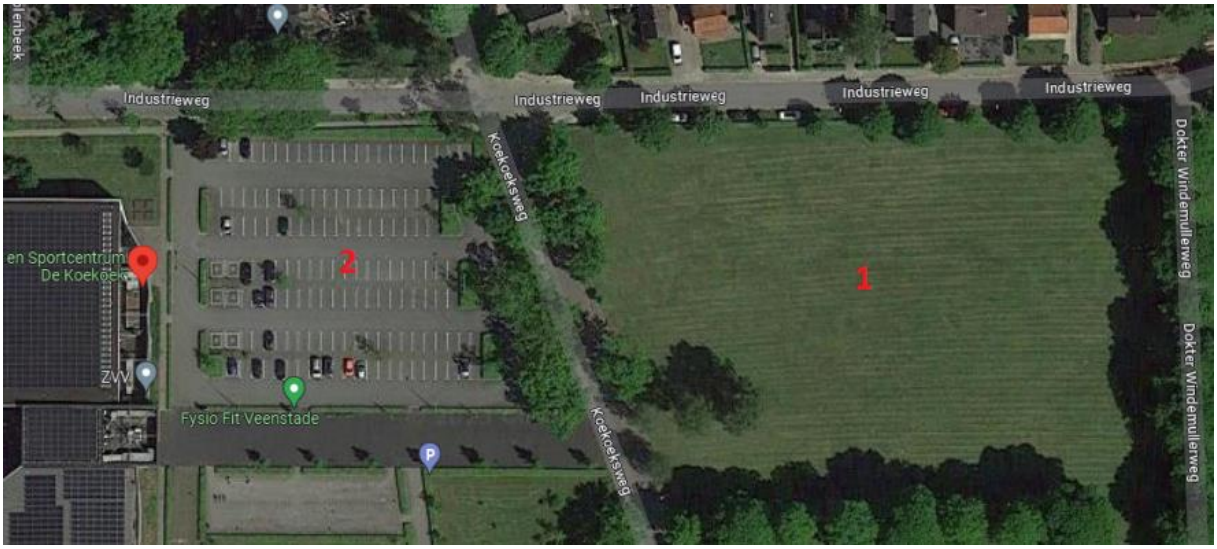

Sportscentre de Koekoek

Annex 3: Literature review

Main messages from 2020 literature study. The author surname/ last name and publication year are in the first two columns of the table below.

Author	Year	Main message
O'Neil	1979	The calibrated consumptive use coefficients for the Blaney-Criddle and SCS formula's for estimating evapotranspiration in production grasses, differed considerably from the current experiments. Measured values from the current experiment are higher.
Feldhake	1985	The evapotranspiration and canopy temperature for grass preconditioned to different shading levels are equal to grass preconditioned to full PAR when testing under full PAR.
Bell	1999	No significant variation was found between plots receiving morning shade and afternoon shade or between plots in 80% and 100% shade.
Sifers	2001	There were significant differences in root depth and root biomass between the different cultivars
Thomas	1977	Later cutting reduced leaf extension rates and leaf lengths in later seasons. Leaf appearance rates were reduced for only about 1 month after cutting.
Yu	2020	more attention should be paid to quantify the contributions of local background climate and landscape characteristics to the cooling effect (threshold-size) of blue-green space.
Yao	2020	Urban green space, especially forest contributes significantly to mitigating UHI in an urban block. UHI is mitigated most in summer months.
Su	2020	vegetation cooling is generally stronger during the daytime periods, in warm seasons, at low latitude zones, for forest lands and at leaf growth stage, while vegetation warming usually occurs in the opposite context.
Grilo	2020	green spaces with reduced areas can regulate microclimate, alleviating temperature by 1–3 °C and increasing moisture by 2–8%, on average. Green spaces with a higher density of trees were more efficient in delivering the cooling effect. Green spaces influenced temperature and relative humidity up to 60 m away from the parks' limits.
Gatto	2020	In summer, for both locations thermal comfort is improved by presence of green space. This accounts for both grass and tree vegetation.
Zhang	2019	An increase of park tree coverage and a decrease of sky view factor could reduce evening air temperature by around 2 °C and 2.5 °C respectively.
Wang	2019	Increase in tree density and Leaf Area Index (LAI) significantly decreases land surface temperature and Park Cool Island effect.
Sodoudi	2018	The spatial configuration and the vegetation type of green areas are both affecting the efficiency of the green areas' cooling effect. Most cooling in the afternoon and by big trees.
Chandramathy	2018	Higher land surface temperature in built up areas compared to different types of green cover.
Amani-Beni	2018	Grass irrigation management can have a positive effect on cooling effect of grass surfaces, irrigated grass can have similar cooling effects with small water bodies.

Amani-Beni	2018	Urban park's cluster trees with short ground vegetation generated higher cooling effect than single trees, grass and waterbodies.
Fung	2017	Woodland strip has a stronger cooling effect and creates more thermally comfortable environments than Rough and concrete plots.
Vahmani	2016	Transforming lawns to drought-tolerant vegetation resulted in daytime warming of up to 1.9°C, largely due to decreases in irrigation that shifted surface energy partitioning toward higher sensible and lower latent heat flux. During nighttime, however, adopting drought-tolerant vegetation caused mean cooling of 3.2°C, due to changes in soil thermodynamic properties and heat exchange dynamics between the surface and subsurface.
Lee	2016	On a hot summer day, averaged over 10-16CET, trees over grassland lead to a mitigation effect up to 2.7K for Ta, 39.1K for Tmrt and 17.4K for PET. In comparison, the effect of grasslands can be up to 3.4K for Ta, 7.5K for Tmrt and 4.9K for PET.
Yan-Dong	2015	as the percent tree cover increased by 10 %, the air temperature decreased by 0.26 °C during daytime, while as the percent lawn cover increased by 10 %, the air temperature decreased by 0.56 °C during nighttime.
Litvak	2014	Shading of turfgrass by trees decreases total evapotranspiration, as turfgrass evapotranspiration is highly sensitive to radiation. Turf with trees total evapotranspiration is lower than evapotranspiration of only turf.
Shashua-Bar	2009	Grasses reduce radiant loads, while differences in air temperature are small compared to trees.
Kong	2014	UCI intensity was affected by areas of forest vegetation and its spatial arrangements, as well as by the composition of the cool island and its neighbouring thermal environment.
Keresztesova	2013	Remarkable differences between different surface composition and cooling effect have been observed.
Armson	2012	Grass reduced maximum surface temperatures by up to 24 ◦C, similar to model predictions, while tree shade reduced them by up to 19 ◦C. In contrast, surface composition had little effect upon globe temperatures, whereas shading reduced them by up to 5–7 ◦C. These results show that both grass and trees can effectively cool surfaces and so can provide regional cooling, helping reduce the urban heat island in hot weather. In contrast grass has little effect upon local air or globe temperatures, so should have little effect on human comfort, whereas tree shade can provide effective local cooling.
Yu	2018	High relative humidity restricts cooling by urban green vegetation. Increased wind speed enhances the tree-covered cooling effect while weakening the grass-covered UGVs' in Mediterranean climate cities to achieve the most effective cooling with the smallest sized tree-covered UGV
Wang	2018	a park area threshold of 1.34 to 17 hectares provides the best PCI effect, that park shape (perimeter/area), Leaf Area Index (LAI), density, tree cover, water cover, and impervious surface cover have significant correlation with PCI development.
Balling	2008	Greater sensitivity to atmospheric conditions occurred in land use situations with large lots, many pools, a high proportion of irrigated mesic landscaping, and a high proportion of high-income residents.
Connors	2013	proportional area of grass explains much of the variation in mesic temperatures.
Jenrette	2007	significant potential air and surface temperature reductions between representative and proposed vegetation scenarios: 1) a Park Cool Island effect that extended to non-vegetated surfaces; 2) a net cooling of air underneath or around canopied vegetation ranging from 0.9 °C to 1.9 °C during the

		warmest time of the day; and 3) potential reductions in surface temperatures from 0.8 °C to 8.4 °C in areas underneath or around vegetation.
Declet-Barreto	2013	increasing vegetation in parks can mitigate local effects of the UHI by creating localized PCIs where extreme temperatures are lowered, sometimes significantly.
Sinclair	2008	cool-season grass Festuca arundinacea growth does not decrease but increases with higher temperatures (18,5 - 27 degrees), with stable VPD (1,2 kPa). With stable T and increasing VPD growth rates decline. Growth appears to in response to a maximum transpiration rate. When temperatures are higher in future, but VPD remains equal, growth rates can be stimulated rather than decreased in temperate climate zones.
Aram	2019	the highest cooling effect distance and cooling effect intensity are for large urban parks with an area of more than 10 ha; however, in addition to the area, the natural elements and qualities of the urban green spaces, as well as climate characteristics, highly inform the urban green space cooling effect.
Jim	2016	Intense incoming shortwave and longwave radiation absorbed readily by Artificial Turf materials raised turf surface temperature to 70.2C and substrate 69.3C, in comparison with <40C at Natural Turf.
Klemm	2015	10% tree crown cover within a street canyon lowered street averaged Tmrt about 1K. In contrast, our results did not show an influence of street greenery on street averaged T. both physical and psychological aspects of thermal comfort must be considered in urban design processes.

Annex 4: Equipment and software

Specifications on equipment and software**.** The main equipment used for measurements in field trials are listed below.

1. Davis 6163EU VP2 plus weather station: air temperature, relative humidity, incoming sunlight, UV, wind direction and speed, air pressure and precipitation amount. Including fan in radiation shield containing T/RH sensor. This results in very pure measurement of temperature and humidity. Weather station is suitable to participate in KNMI WOW Project. Logs every 5 minutes or every 10 minutes.

2. I-Tec E compact infrared sensors: Accuracy +/- 1 degree, repeatability +/- 0.5 degrees. Infrared spectral band 8um to 14um. Measuring surface at 1 meter sensor height Ø62mm = 192 cm^2.

3. Campbell CR1000X with programmed log interval of every 5 or every 10 minutes.

4. Fieldscout Handitrace TDR350: Accuracy VWC 3.0%, temperature +/- 1 degrees.

5. Fluke PTi120 Pocket Thermal Imager; Resolution 120*90 Pixels; Heat sensitivity 60 mK; accuracy +/- 2 degrees; Infrared spectral band 8um to 14um; Default emissivity setting 0.95.

6. Testo 865s Thermal camera: Resolution 320*240 pixels (SuperResolution setting). Heat sensitivity 100 mK; Thermal sensitivity 0.1 degrees, accuracy +/- 2 degrees. Infrared spectral band 7.5um to 14um; Default emissivity setting 0.95.

7. Imaging tub: a mortar tub that is placed upside down on the grass with a hole in the middle into which a camera fit exactly. 2 LED panels have been placed on the inside of the mortar tank (JGS LED panel 6500K). The camera used is a Canon Powershot G7X Mark III. For all observations, aperture was set to f3.2, shutter speed 1/60 and ISO value 800. Grayscale was set to custom (determined by using a colour fan on which the camera colours were subsequently calibrated).

8. Specialized Software: Turfanalyzer software: Settings (see relevant data file) and RayMan Pro: Settings (see relevant data file).

Corresponding address for this report:
P.O. Box 16
6700 AA Wageningen
The Netherlands
T +31 (0)317 48 07 00
wur.eu/plant-research

Report WPR-OT 1083